博士論文

# Role of Selenoprotein P Regulatory System in the Malignant Transformation of Glioblastoma (グリオブラストーマ悪性化におけるセレノプロテイン P 発現制御系の役割)

令和 5 年度

東北大学大学院薬学研究科

生命薬科学専攻

鄭 希 Zheng Xi

**Abbreviation**

2-ME: 2-Mercaptoethanol

BPB: bromophenol blue

BSA: bovine serum albumin

CBB: Coomassie brilliant blue

cDNA: complementary DNA

DMEM: Dulbecco's Modified Eagle's Medium

DMSO: dimethyl sulfoxide

DNA: deoxyribonucleic acid

EDTA: ethylenediaminetetraacetic acid

GBM: glioblastoma

KD: knock down

mRNA: messenger ribonucleic acid

PAGE: polyacrylamide gel electrophoresis

PCR: polymerase chain reaction

PI: Propidium Iodide

PVDF: polyvinylidene difluoride

RNA: ribonucleic acid

ROS: reactive oxygen species

RPMI1640: Roswell Park Memorial Institute 1640 medium

RT: reverse transcription

SDS: sodium dodecyl sulfate

siRNA: small interfering ribonucleic acid

TEMED: N,N,N',N'-Tetramethyl ethylenediamine

TMZ: Temozolomide

TTBS: tween 20 tris-buffered saline

Tris: 2-amino-2-hydroxymethyl-1,3-propanediol

Tween 20: Polyoxyethylene Sorbitan Monolaurate

WB: Western Blotting

SeP: Selenoprotein P

GAPDH: glyceraldehyde 3-phosphate dehydrogenase

GPx: Glutathione peroxidase

ApoER2: Apolipoprotein E receptor 2

LDL: Low Density Lipoprotein

CCDC152 coiled coil domain-containing protein 152

# Contents

# Introduction

## 1. Glioblastoma

Brain tumors are a deadly disease, with malignant and non-malignant subtypes consisting of more than 100 histologically distinct subtypes of central nervous system (CNS) tumors. Their epidemiology, clinical characteristics, treatment methods, and prognosis vary widely. Due to the complexity of their anatomical location and biological characteristics, they are difficult to treat[1]. In the past few decades, the incidence and 5-year survival rate of malignant brain tumors have not changed significantly[1,2].Gliomas are the most common primary tumors of the brain. They typically arise from glial cells or precursor cells and develop into astrocytomas, oligodendrogliomas, epithelioma, or oligodendrocytes tumors[3]. According to the classification of the World Health Organization (WHO), gliomas are divided into four grades, among which grade 1 and 2 gliomas are low-grade gliomas (LGG), and grade 3 and 4 gliomas are high-grade gliomas (HGG)[4]. Typically, the higher the grade, the worse the prognosis. The 10-year survival rate for low-grade glioma is 47%, with a median survival time of 11.6 years[5]. While the median overall survival time for grade 4 gliomas is 15 months[6].

Glioblastoma (GBM) is a grade 4 glioma and one of the most aggressive and fast-growing brain tumors[7]. GBM accounts for 82% of malignant glioma cases, and has an incidence rate of 3.23 per 100,000 population[8]. GBM can lead to neurologic symptoms including weakness, visual and sensory changes, mood changes, memory or executive function, language disorder, and headaches, among others [9].

The current standard of care for glioma is surgical resection followed by radiotherapy and temozolomide chemotherapy by temozolomide (TMZ) [10], however median survival rate after treatment is only around 14.6 months [10,11]. Thus, there is an urgent need to develop a new therapeutic strategy for GBM.

## 2. Ferroptosis

Ferroptosis was first described in 2012 and is characterized by iron-dependent lipid peroxidation and the generation of free radicals that occur directly before cell disintegration and cell death [12,13]. Recently, ferroptosis received much attention in the cancer research field [14,15], and interestingly it was reported that ferroptosis is also the underlying mechanism of action of TMZ[16]. TMZ is DNA-alkylating (methylating) agent and its susceptibility is regulated by O6-methylguanine methyltransferase (MGMT) expression, which plays repairer of DNA methylation [17]. A recent study suggested that many novel independent mechanisms play important role in TMZ resistance, e.g., autophagy[10,18], however, its contribution to ferroptosis-resistance is little known.

Ferroptosis reflects an antagonism between prerequisites for ferroptosis execution and ferroptosis-defense. The factors that promote ferroptosis are polyunsaturated fatty acid-containing phospholipid (PUFA-PL) synthesis and peroxidation, iron metabolism, and mitochondrial metabolism. Ferroptosis-regulatory systems mainly include the glutathione peroxidase 4 (GPX4)–reduced glutathione (GSH) system, the ferroptosis suppressor protein-1 (FSP1)–ubiquinol ($CoQH_2$) system, the dihydroorotate dehydrogenase (DHODH)–CoQH2 system, and the GTP cyclohydroxylase-1 (GCH1)–tetrahydrobiopterin (BH4) system[19]. When cellular activities promoting ferroptosis exceed the detoxification capacity provided by ferroptosis-regulatory system,

lethal accumulation of lipid peroxides on the cell membrane leads to subsequent membrane rupture and ferroptosis[20].

Since reduction of the lipid peroxidation process is related to chemotherapy sensitivity, inhibition of this process would be beneficial to overcome treatment resistance [21]. Glutathione peroxidase 4 (GPX4), a selenium-containing enzyme, plays reduction of lipid peroxidation [22]. GPX4 is the only GPX that converts phospholipid (PL) hydroperoxides to PL alcohols, and genetic or pharmacological inhibition of GPX4 induces uncontrolled lipid peroxidation and triggers ferroptosis under many in vitro and in vivo condition[23]. GSH is a cofactor used by GPX4. GSH and GSH-related enzymes are the most important antioxidant defense systems in the body, protecting cells from reactive oxygen species (ROS), radiation therapy and chemotherapy[24]. Compared with normal cells, the tumor cells produce more ROS[25]. GSH is a tripeptide composed of glycine, glutamic acid and cysteine, of which cysteine is the most important precursor[26]. Solute carrier family 7 member 11 (SLC7A11, also known as xCT) is the transport subunit of the xc system. Most cells obtain intracellular cysteine mainly through its uptake of cystine (the oxidized dimer form of cysteine)[27]. Removing cystine from the culture medium or blocking SLC7A11-mediated cystine transport with Erastin or other FINs induces potent ferroptosis in many cancer cell lines[28]. The SLC7A11-GSH-GPX4 axis is believed to constitute a major cellular system that regulates ferroptosis[19]. The regulatory mechanism of GPX4 expression in cancer cells has been studied; however, the underlying mechanism is complicated due to the unique regulation of its translation system, and thus it remains poorly elucidated.

## 3. Selenoproteins

Selenium is an essential trace element involved in many physiological processes, such as energy metabolism, immune function, antioxidant defense, and neuronal cell survival [29,30]. The incorporated selenium is metabolized to selenocysteine through a *de novo* metabolic pathway, in which proteins such as selenocysteine lyase, SEPHS2, PSTK, SPS2, and SEPSECS are involved [31,32]. The selenocysteine residue synthesized on tRNASec is translated in the presence of a stable loop structure called the selenocysteine-insertion sequence (SECIS) in the 3'-untranslated region of selenoprotein mRNA [33]. The human genome encodes 25 selenoproteins, including five types of GPX and three types of thioredoxin reductase (TXNRD). Both GPX4 and TXNRD1 are reported to contribute cancer proliferation and resistance to ferroptosise[34]. The regulatory mechanism of selenoproteins at the protein level is known to be highly dependent on selenium supply, as well as on mRNA levels because reduction of selenocysteine-tRNASec causes the codon corresponding to selenocysteine (termination codon UGA) to be recognized as a termination codon, resulting in mRNA degradation, translation arrest, and read-through [34,35]. Therefore, more attention should be given to whether comprehensive and large-scale analyses such as RNA-sequencing precisely reflect the variation of selenoproteins at the protein level.

Our research group previously reported that treatment with selenoprotein P (SeP; SELENOP, encoded by the *SELENOP* gene) siRNA resulted in a ferroptosis-like cell death in insulinoma MIN6 cells [36], and a recent study also indicated that neuroblastoma, a neuronal tumor, requires SeP as a selenium source to confer resistance against ferroptosis through GPX4 expression [37]. SeP is a selenium-containing extracellular protein that is mainly secreted from hepatocytes into plasma and incorporated into peripheral tissues [38]. In the central nervous system,

SeP expression is observed in several cell types, including neurons and ependymal cells [39]. Notably, the expression of SeP is relatively high in astrocytes [40], however the physiological/pathophysiological role of SeP expression in astrocytes and the central nervous system is not fully elucidated. SeP is a unique selenoprotein that contains 10 Sec residues per polypeptide, whereas other selenoproteins usually have only one [41]. This feature endows SeP with the distinct function of delivering Se to cells/tissues. Whole-body SeP knockout causes a reduction of selenium levels in the brain [42], while conditional gene knockout of SeP in the liver does not [43], suggesting that SeP production in the central nervous system plays a role in brain selenium retention.

4. ApoER2, a SeP receptor

Apolipoprotein E receptor 2 (ApoER2) belongs to the low-density lipoprotein receptor (LDLR) family, a type I transmembrane receptor that is highly homologous to its eponymous member[44]. ApoER2 is a protein that interacts with a variety of ligands. For example, reelin is one of the major ligands for ApoER2, which plays an important role in embryonic neuronal migration and postnatal long duration enhancement[45]. SeP is recognized by ApoER2 (LRP8), incorporated into cells, and degraded by lysosomes to produce selenocysteine [46,47]. SeP synthesized in the brain is incorporated into other brain cells and used to synthesize selenoproteins, which help maintain Se concentrations in the brain [40,48]. This system is called the “SeP cycle”, which is a cycling-selenium storage system used to retain selenoprotein levels in cells. The similar phenotype between SELENOP and ApoER2 KO mice implies that ApoER2 is a significant mediator of the SeP cycle [46,49]. Recently, a preferential selenium transport pathway involving SeP and high-affinity ApoER2 in a Sec lyase–independent manner

has been discovered [50]. While SeP is crucial for selenium metabolism, excess SeP production is associated with several diseases such as type 2 diabetes, dementia, and pulmonary hypertension [51]. Recent evidence suggests the implication of excess SeP in cancer [52,53]. Additionally, studies have shown that ApoER2 participates in APC/CDC20 complex formation during mitosis, and it promote cytokinesis abscission[54]. In conclusion SeP/ApoER2 may play an important role in selenium/selenoprotein regulation in the brain or in GBM. However, its understanding is limited.

5. Long non-coding RNA CCDC152, a regulator SeP expression

Less than 2% of the human genome contains genes that code for proteins yet about 90 % of the genome is transcribed into RNA[55]. Most of the non-protein coding parts of the human genome were originally considered junk DNA. However, later studies surprisingly revealed that most nucleotides that do not encode proteins are detectably transcribed[56]. Non-coding RNA can be broadly classified based on their size: small non-coding RNA represent non-coding transcripts less than 200 nucleotides in length, such as miRNA, siRNA, and piRNA. Non-coding transcripts longer than 200 nucleotides are called long non-coding RNA (lncRNA) [57]. More than 100,000 lncRNA have been discovered in the human genome, and new lncRNAs are rapidly being discovered and characterized. lncRNA are generally master regulators of gene expression and exert their functions through transcriptional, post-transcriptional and epigenetic gene regulation mechanisms[14]. Although there is considerable evidence that lncRNA function primarily as functional RNA molecules, small open reading frames do exist in lncRNA and, in some cases, may yield short functional peptides[58] .

Increasing evidence shows that during the occurrence and development of cancer, lncRNA act as oncogenes or tumor suppressors, regulating tumor progression. lncRNA play important functional roles in regulating the transcription and translation of metabolism-related genes, acting as decoys, scaffolds, and competing endogenous RNA (ceRNA), ultimately leading to metabolic reprogramming in cancer[59]. They can regulate tumor cells proliferation, differentiation, invasion, and metastasis metabolic reprogramming of cancer cells[60,61].

CCDC152 is a non-coding RNA called the coiled coil domain-containing protein 152, which is located in the antisense region of the SELENOP gene in the genome, and its sequence partially overlaps with the antisense of SeP mRNA[62]. Previous studies in our laboratory found that CCDC152 RNA specifically interacts with SeP mRNA and inhibits its binding to SECIS-binding protein 2, resulting in reduced ribosome binding. CCDC152 acts as a long non-coding RNA to reduce SeP protein levels through translational rather than transcriptional inhibition[62]. This is a study in the liver, the organ where most SeP synthesis occurs, and the role of CCDC152 for cancer is unknown. A multi-omics information study on the prognosis of osteosarcoma showed that high expression of CCDC152 is associated with lower risk and may be a protective factor[63]. Comparing RNA sequencing data of colorectal cancer liver metastases (CRC-LM) relative to primary CRC revealed upregulation of SeP and downregulation of CCDC152[64]. Although there have been some studies on CCDC152, we still know very little about it. The role of CCDC152 in glioblastoma is unknown.

## 6. Purpose of the study

In summary, the final goal is to contribute to the treatment of glioblastoma. To address that the present study aims to investigate the role and mechanisms of the SeP/ApoER2 pathway in glioblastoma, as well as the factors that regulate them（CCDC15）. The study will contribute to better understand the disease process of glioblastoma and find new therapeutic target.

## Materials and Methods

### Biological samples

Glioblastoma cell line, T98G , YKG1 A172 cells were obtained from Institute of Development, Aging and Cancer, Tohoku University, U87 and U251 cells were obtained from JCRB cell bank.

Patient-derived cell studies were approved by the ethics committee of the faculty of medicine at Tohoku University (Approved No. 2023-1-321), and the primary GBM cells were provided by Dr Masayuki Kanamori's group.

Human Tumor Sections Brain tissue sections from 22 cases were donated by Dr. Masayuki Kanamori, Department of Neurosurgery, Tohoku University Hospital, and immunohistological staining was performed.

F344/NJcl-rnu/rnu rat purchased from CREA Japan was used for experiment.

### Antibody

Anti β-actin (sigma, clone AC-15)

Anti GAPDH (015-25473 Wako pure chemical)

Anti hSeP (BD1BD1 antibody was prepared by a special immunology laboratory using full-length SeP as antigen, and its specificity has been confirmed[65].)

Anti TrxR1 (Cell Signaling Technology)

Anti GPx1 (abcum, ab108427)

Anti GPx4 (abcum, ab125066)

Anti LC-3A/B (cell signaling technology, 12741S)

Anti p62 (cell signaling technology,511S)

Anti mouse, peroxidase conjugated antibody (Dako, 20051789)

Anti rabbit, peroxidase conjugated antibody (Dako, 20073563)

Anti rat, peroxidase conjugated antibody (Dako,00063346)

Goat Anti-Rat IgG H&L (Alexa Fluor® 594) (ab150160)

Goat Anti-Mouse IgG H&L (Alexa Fluor® 488) (ab150113)

**Equipment**

Deuterium-depleted water (Millipore)

Block incubator (Astec)

Absorbance plate reader (Molecular Device)

Centrifuge MX-200 (Tomy Precision)

Electrophoresis apparatus NB-5010 (Nippon Eidoh)

Power pac 200 power supply (Bio-Rad)

Confocal laser scanning microscope FL-1000 (Olympus)

BLOCK INCUBATOR: B1-515A, ASTEC

CO2 incubator: SCA - 165DRS, ASTEC

CytoFLEX: BECKMAN COULTER

Nanodrop: Thermo SCIENTIFIC

Thermal Cycler Dice® Real Time System Single Software: TP870/TP850, Takara

Western Blotting Detector: WSE-6100 LuminoGraph I, ATTO

Wet type transfer device: 1701935JB01, BIO-RAD

Plate radar: Spectra Max iD5, Molecular devices

Vortex mixer: AUTOMATIC Mixer, YAZAWA

Rotator: MTR-103, AS ONE

Centrifuge: Model 5800, KUBOTA

**Reagents**

2-Mercaptoethanol (Nakalai)

Ammonium Peroxodisulfate (Nakalai)

Acrylamide (Nakalai)

Bromophenol Blue (Wako)

Dimethyl Sulfoxide (Nakalai)

Ethanol (Nakalai)

Glycerol (Wako)

Immobilon Western (Millipore)

Lipofectamine RNAiMAX (Invitrogen)

Methanol (Nakalai)

Methyl chloride (Wako)

N,N-Methylenebisacrylamide (Wako)

N,N,N,N-tetramethylethylenediamine (Wako)

Opti-MEM (Invitrogen)

Sodium chloride (Nacalai)

Sodium Dodecyl Sulfate (Nakalai)

Sodium Fluoride (Nakalai)

Tris-aminomethane (Nakalai)

Triton X-100 (Nakalai)

Tween 20 (Nacalai)

Bovine serum albumin (Nakalai)

Chemi-Lumi One Ultra (Nakalai)

KPL Peroxidase Substrate Solution (TheraCare)

ISOGEN II(NIPPON GENE)

Lysotracker Green DND-26( Invitrogen)

Skim milk (Morinaga Milk Industry)

RSL3 (Houston, USA),

Selenite (Kyoto, Japan)

Bafilomycin A1(10-2026、Focus Biomolecules)

Imidazole (19004-22、nacalai tesque)

Ni-NTA Agarose (141-09764、Wako)

AlamarBlue (2356802、invitrogen)

PVDF membrane: IPVH304F0、Millipore

Instant citrate buffer (20x concentrated solution): RM102-C, LSI Medience Co., Ltd.

Instant antigen retrieval solution H (20x concentrated solution): RM102-H, LSI Medience Co., Ltd.

Nichirei Histo Fine Kit: Used from SAB PO(R)

Methanol: 21915-93, nacalai tesque

Hydrogen peroxide: 7722-84-1, Wako

BSA: 01863-48, nacalai tesque

CytoFLEX Sheath Fluid: B51503, BECKMAN COULTER

PI solution: 25535-16-4, SIGMA ALDRICH

Ethanol: 14713-95, nacalai tesque

**Buffer**

30% Acrylamide: 29g of acrylamide and 1g of methylene bisacrylamide were dissolved in deionized water at 37°C and fixed to 100ml and filtered.

1.0 mol/L Tris-HCl solution at pH 8.0: Tris 12.1g was added to deionized water, dissolved in deionized water and fixed to 100 ml, and concentrated hydrochloric acid adjusted the pH to 8.0.

1.0 mol/L Tris-HCl solution at pH 6.8: Tris 12.1g was added to deionized water, dissolved in deionized water and then fixed to 100ml, and concentrated hydrochloric acid was used to adjust the pH to 6.8.

1.5 mol/L Tris-HCl solution at pH 8.8: Tris 18.2g, dissolved in deionized water and fixed to 100ml, concentrated hydrochloric acid to adjust pH to 8.8.

10% SDS solution: SDS powder 10g, add deionized water and heat to dissolve, fixed volume to 100ml, dilute hydrochloric acid to adjust the pH to 7.2.

10% ammonium persulfate solution: 0.5g ammonium persulfate, add deionized water to dissolve, fixed volume to 5ml, -20℃ storage.

TBST (10×) solution: 44g of NaCl, 100ml of 1M Tris-HCl solution at pH 8.0 and 5ml of Tween-20, dissolved with deionized water and fixed to 500ml.

Electrophoresis buffer (10×): Tris 15.2g, glycine 94g and SDS 5.0g were dissolved in deionized water and volume set to 500ml.

Transmembrane buffer: Glycine 2.9g, Tris 5.8g and SDS 0.37g were dissolved in deionized water and fixed to 600ml, 200ml methanol was added.

Ni-NTA Equilibration Buffer: 50 mM $NaH_2PO4\text{-}2H_2O$, 300 mM NaCl, 10 mM Imidazole (pH8.0)

Ni-NTA Wash Buffer: 50 mM $NaH_2PO_4\text{-}2H_2O$, 300 mM NaCl, 20 mM Imidazole (pH8.0)

Ni-NTA Elution Buffer: 50 mM $NaH_2PO_4\text{-}2H_2O$, 300 mM NaCl, 250 mM Imidazole (pH8.0)

**Kit**

DC protein assay kit（Bio-Rad）

PrimeScript RT Reagent kit（TAKARA）

Power SYBR Green PCR Master Mix（Thermo Fisher）

RNA Premium Kit 50 prets (FG-81050、Fast Gene)

**Medium**

DMEM (high glucose)（Nacalai）

RPMI 1640（Nacalai）

EMEM （ATCC）

Fetal bovine serum（Sigma）

Sodium hydrogen carbonate(Nacalai)

Penicillin-streptomycin(Invitrogen)

10×D-PBS（-）（Wako）

Trypsin（Becton）

**Plasmid**

Plasmid CCDC152Δ3’ , CCDC152Δ5,’were given by Prof. Mita form Doshisha University Faculty of Life Science and Medical Sciences Department of Medical and Life Systems.

**siRNA for KD**

siSeP

#1 F: 5’-GCAUAUUCCUGUUUAUCAA-3’
R: 5’-UUGAUAAACAGGAAUAUGC-3’

#2 F: 5’-GCAUAUUCCUGUUUAUCAA-3’
R: 5’-UUGAUAAACAGGAAUAUGC-3’

#3 F: 5’-GCAUACUGCAGGCAUCUAA-3’
R: 5‘-UUAGAUGCCUGCAGUAUGC-3’

siApoER2

#1 F: 5’-CGCUGAUCUCCUCCACUGA-3’
R: 5’-UCAGUGGAGGAGAUCAGCG-3’

#2 F: 5’-GUGACCUCUCCUACCGUAA-3’
R: 5’-UUACGGUAGGAGAGGUCAC-3’

#3 F: 5’-GACCUACUGACCAAGAACU-3’
R: 5’-AGUUCUUGGUCAGUAGGUC-3’

siCCDC152

#1 F: 5’-ACAAGGAGAUUGCAAUUCUUCGUAA-3’
R: 5’-UUACGAAGAAUUGCAAUCUCCUUGU-3’

#2 F: 5’-GCUACAACAGACCAUUGAA-3’
R: 5’-UUCAAUGGUCUGUUGUAGC-3’

**qPCR prier**

SeP

F: 5’-CCCCCAGCCTGGAGCATAAG-3’

R: 5’-TGCACAGGTATCAGCTGGCTT-3’

ApoER2

F: 5’-GTTGCCACCAATCGCATCT-3’

R: 5’-TCGGGTCACTGGCCTTGT-3’

CCDC152#1（for 5’）

F: 5’-GGGGAACTAGGAGCAACAGC-3’

R: 5’-AGACCTCCTTTGCTTGCATT-3’

CCDC152#2（for overlap sequence with SeP）

F: 5’-AGATGTCGACAATGGCAGCA-3’

R: 5’-CAGGCCTTCATCACCACCAT-3’

CCDC152#3（for 3’）

F: 5’-TGTGTCAACGGTGCATCTTA-3’

R: 5’-TCAGCTGACAGCCTTATGGT-3’

GPX1

F: 5’-CAGTCGGTGTATGCCTTCTCG-3’

R: 5’-GAGGGACGCCACATTCTCG-3’

GPX4

F: 5’-GAGGCAAGACCGAAGTAAACTAC-3’

R: 5’-CCGAACTGGTTACACGGGAA-3’

TrxR1

F: 5’-GAGGCAAGACCGAAGTAAACTAC-3’

R: 5’-CCGAACTGGTTACACGGGAA-3’

GAPDH

F: 5’-GCACCGTCAAGGCTGAGAAC-3’

R: 5’-TGGTGAAGACGCCAGTGGA-3’

## Method

**Data analysis for RNA sequence of GBM patients.** TCGA RNA-seq data of GBM patients were analyzed by GEPIA2 platform.

http://gepia2.cancer-pku.cn/#index

## Immunostaining

### Immunostaining of SeP (BD1) in human brain tumor tissue by LSAB method

Human brain tumor tissue sections were deparaffinized using xylene, and then the xylene was removed with ethanol and washed with distilled water. Endogenous peroxidase was inactivated with methanol containing 0.3% hydrogen peroxide, and antigen retrieval was performed using instant citrate buffer in an autoclave (121°C, 5 min). The sections were washed with distilled water and then three times with 0.01 MPBS, and blocking solution from Histofine Kit (Nichirei) was placed on the sections and incubated at room temperature for 30 minutes. The blocking solution was removed from the sections, and the BD1 antibody was adjusted to 42.5 μg/mL with antibody diluent (0.5% BSA/PBS/0.05% $NaN_3$), placed on the sections, and incubated overnight at 4°C.

The sections were then washed three times with 0.01 MPBS, biotin-labeled anti-rat IgG adjusted to 20 μg/mL with antibody diluent was placed on the sections, incubated for 30 minutes at room temperature, and washed again three times with 0.01 MPBS. HRP-labeled streptavidin from the Histofine kit was applied to the sections and incubated at room temperature for 30 minutes. After washing three times with 0.01 MPBS, DAB reaction was performed for 30 minutes. After washing with distilled water, hematoxylin nuclear staining was performed, and after washing with distilled water, dehydration with

ethanol and clearing with xylene were performed, followed by mounting and observation under a microscope.

<Evaluation method>

As a positive control, we used human liver tissue in which SeP is constantly expressed. When compared to liver tissue, the same level of color development is considered "positive expression," weak color development is "weak expression positive," and color development stronger than liver tissue is considered "positive expression." was defined as "strongly positive expression".

**Cell culture**

Cells were cultured indicated medium supplemented with 10% fetal bovine serum and 1% penicillin streptomycin in 5% $CO_2$, at 37°C. T98G was cultured with RPMI 1640 medium. YKG1, A172, U87 and U251 cells were cultured in DMEM high glucose medium. Patient-derived cell studies were approved by the ethics committee of the faculty of medicine at Tohoku University (Approved No. 2023-1-321). We obtained informed consent from the patient for the culture of patient-derived primary cells. The tumor cells were isolated from a GBM patient at Tohoku university hospital and cultured using EMEM supplemented with 10% fetal bovine serum and 1% penicillin-streptomycin. Cells were maintained in 10 cm dishes and passaged when cells were approximately 80% confluent. Cells used for experiments were washed with 1×PBS, incubated with 1 mL of 0.25% trypsin at 37°C and 5% $CO_2$, detached from the dish, centrifuged (1,000 rpm, 2 min) with the respective culture medium to remove the supernatant, resuspended in the medium again, and

counted using a blood cell counter The supernatant was then resuspended in medium and counted using a hemocytometer.

**Transfection**

**Knockdown:** Gene-specific and negative control siRNAs were purchased from Sigma (MO, USA). Lipofectamine™ RNAiMAX Transfection Reagent (Thermo Scientific, MA, USA) was used to transfect siRNA into cells (10 nM siRNA and 1μl Lipofectamine/ml), and the cells were harvested for subsequent treatments after 48 hours of transfection.

**Over-expression:** Plasmids were transfected into cells (1 μg plasmid and 1 μl Lipofectamine 2000/ml) using Lipofectamine™ 2000 Transfection Reagent (Thermo Scientific, MA, USA), and the cells were harvested 24 h after transfection for subsequent processing.

**RNA extraction and quantitative PCR**

After treatment, the cell culture medium was discarded, cells were washed with PBS, and ISOGEN II (NIPPON GENE, Tokyo, Japan), an RNA extraction reagent, was added. RNA was purified following the manufacturer's instructions, concentration was determined by NanoDrop (Thermo), and reverse transcription was performed using a PrimeScript RT Reagen Kit (Takara Bio Inc, Shiga, Japan). The reagent Power SYBR™ Green PCR Master Mix (Thermo Fisher Scientific, USA) and a thermal cycler (CFX Connect™, Bio-Rad, CA, USA) were used for quantitative PCR (qPCR).

**Cell viability**

After transfection of SeP or negative control siRNA for 24 hours, the culture medium was replaced and treated with RLS3 and selenite for an additional 24 hours. After that, medium were changed with 10% alamarBlue™ Cell Viability Reagent (Thermo Fisher Scientific), 90% complete DMEM and further incubated for 2 hr. After the incubation, a microplate reader (SpectraMax iD5, Molecular Device, MA, USA) was used to detect the fluorescence intensity at Ex 544/Em 585 nm. The data are shown as a ratio, with the control as 1.

**Cell counting**

Cells in culture were detached with 2.5% trypsin, medium was added, centrifuged, the supernatant was removed, and the cells were resuspended in the medium. After creating the cell suspension, trypan blue and the cell suspension were mixed at a ratio of 1:1, and the mixture was injected into a hemocytometer and counted. Based on this counting result, the required number of cells was adjusted and used for each experiment.

**Western blotting**

Cellular proteins were extracted with RIPA lysis buffer (50 mmol/L Tris-HCl Buffer pH 7.6, 150 mmol/L NaCl, 1% Nonidet P40 Substitute, 0.5% Sodium Deoxycholate, 0.1% SDS). Protein concentration was determined by DC protein assay reagents according to the manufacturer's instructions (Bio-Rad). Then, sample loading buffer was added and an aliquot of proteins were denatured at 95°C for 10 minutes, separated by SDS polyacrylamide gel electrophoresis, and transferred to PVDF membranes. Blocking was performed with 5% skim milk for 1 hour. The membrane was rinsed with TBST and cut

around the target protein molecular weight to suppress antibody volume, then incubated with indicated primary antibodies. After washing with TBST, the membrane was incubated with a secondary antibody for one hour at room temperature. Finally, protein bands were detected using an ImmunoStar LD kit (FUJIFILM Wako Pure Chemical Corporation, Japan) and Luminograph (ATTO, Tokyo, Japan).

**Generation of U87 cells constitutively expressing SeP**

<Preparation of lentivirus>

HEK293T cells were seeded in a 6-well plate at a concentration of $8 \times 10^5$ cells/1.8 mL/well, and 24 hours later, virus transfection mixture (Opti-MEM: 190 μL, psPAX2: 1.5 μg, pMD2.G: 0.84 μg, transfer plasmid: 2.34 μg, Polyethylenimine: 10 μg) was added in 200 μL. After 18 hours, the mixture was replaced with fresh DMEM containing 10%, and culture was continued for 72 hours. The medium was then collected, passed through a 0.45 μg/mL filter, and the resulting solution was treated as a virus solution.

<Preparation of virus-infected cells>

YKG1 cells were seeded in a 12-well plate at a concentration of $1 \times 10^5$ cells/0.1 mL/well, and immediately 0.1, 0.3, and 0.9 mL of the above virus solution was added. After culturing for 48 hours, Puromycin was added at a concentration of 1.5 μg/mL, and the culture was continued for an additional 48 hours. The obtained cells were collected and used as SeP constitutively expressing cells.

**Flow cytometry**

Cells were detached by addition of trypsin solution, washed once with 1×PBS(-), and suspended in 300 μL of 1×PBS(-). Then, 700 μL of 99.9% ethanol cooled at -20°C was added and incubated at -20°C for 2 hours. The cells were then centrifuged (1,000 rpm, 4°C, 2 min) to remove supernatant, and then suspended in 1×PBS(-) mixed with BSA to 1% and incubated at 37°C for 30 min. Finally, PI solution (final concentration 5 μg/mL) was added to the above cell suspension and mixed well to make cell samples.

Using CytoFLEX, fluorescence intensity was measured for 10,000 cells with PE-A on the horizontal axis and count on the vertical axis. The number of cells forming a peak was measured from the difference in fluorescence intensity and used for quantification.

**Crude purification and enrichment of SeP from culture supernatant**

SeP released from cultured GBM cells is so small that it is impossible to detect SeP simply by electrophoresis of the culture medium as usual. Therefore, we purified and concentrated SeP in the supernatant of the medium collected after 24 hours using Ni-Beads and used it as a sample.

<Collection of medium>

Cells were seeded into 6-well plates at $2.0 \times 10^5$ cells/2 mL/well, incubated for 48 hours, replaced with 1 mL of medium, and the medium supernatant was collected 24 hours later and used as a sample.

<Equilibration of Ni-beads>

Twenty μL of well-suspended Ni beads were used per mL of supernatant medium. First, Ni beads were transferred to a 1.5 mL tube and centrifuged at 500 × g for 5 minutes. The supernatant was removed so as not to absorb the beads, to which 10 times the volume of equilibration buffer was added, and the beads were thoroughly suspended in a vortex mixer. The beads were then centrifuged at 500 × g for 5 minutes, and the supernatant was removed so as not to suck in the beads.

<Addition of sample>

The culture medium supernatant was added to the equilibrated beads, and the beads were inverted and mixed at room temperature for 60 minutes using a rotator. The beads were then centrifuged at 500 × g for 5 minutes, and the supernatant was removed to avoid aspiration of the beads.

<Washing>

The beads were then centrifuged at 500 × g for 5 minutes, and the supernatant was removed so that the beads would not be sucked in.

<Elution of proteins>

After washing, an equal volume of elution buffer was added to the washed beads, and the beads were inverted and mixed using a rotator for 10 minutes at room temperature, then centrifuged at 500 × g for 5 minutes, and the supernatant was transferred to a new 1.5 mL tube to avoid sucking in the beads. This operation was repeated three times to make the cell supernatant sample.

**Lysotracker**

Cells were seeded on 8-well chamber slides (2,000 cell/well). siRNA was treated for 48 hrs and the medium was changed (with 75 nM lysotracker). Thirty min later the cells were visualized under a confocal microscope.

**Animal experiment**

**Cell conditioning is performed according to the following protocol**

U87 luciferase cells were introduced into siCON/siApoER2 two days before use. transfection methods are described in Transfection. Cells were recovered 48h after transfection with siRNA. Set the centrifuge to 4°C and start cooling. Tribucin is heated in a water bath. Collect flasked cells in 15 ml tubes according to the passaging protocol. Centrifuge at 200g, 4°C, 5min and remove supernatant. Tap to loosen the pellet, add 10ml of chilled 1xPBS and suspend/wash without pipetting. Centrifuge at 200g, 4°C, 5min and remove the supernatant without aspirating the pellet. Transfer the entire volume to a 0.6 ml tube hesambule. Centrifuge at 200g, 4°C, 5min and remove the supernatant without aspirating the pellet. Perform cell count (200x dilution)， The cell concentration was $10^5$/μl (Count error is ±10%, and if additional concentration adjustment is necessary, do it. All operations should be performed on ice).

**Preparation for animal experiments**

Wipe the table, etc. to be used for transplantation thoroughly with ethanol in advance Surgical instruments are sterilized before use

The rat is placed in an anesthesia box and anesthesia is induced with 20% isoflurane. Once the rat is asleep, Ketaral and Celactal are injected into the right thigh. Return the mouse to the anesthesia box and wait for the anesthesia to completely take effect. In the meantime, the treatment table is set up. Set the temperature board at 36°C and keep it warm. Place a piece of Styrofoam under the temperature board for height adjustment. When the body movements have disappeared, transfer the mouse to the stereo table. Hook the anterior teeth of the mouse to the anesthesia mask. Lower the isoflurane from 2.0% to 1.5%. Head immobilization is performed. At this time, the head should be level with the ground and immobile. Hamilton syringe on stereo table. Shave head hair with electric clippers. Disinfect with ethanol. Make a 15 cm incision in the scalp with a cooper. The periosteum is peeled off with a cotton swab to expose the Bregma. Move the Hamilton syringe once to the position of Bregma, then move it to the right lateral 25 mm and 0.5 mm anteriorly to confirm the position of the punctum. Confirm the puncture position and slowly turn the 18-gauge needle to puncture. Prepare the Hamilton syringe. Wipe the needle tip with 70% ethanol; after thoroughly washing the inside with PBS, fill with cell suspension. Before filling the syringe with cells, gently pipette and agitate the syringe. Slowly advance the needle tip 35 mm from the surface of the brain and return it 05 mm (creation of a pocket). Inject cells at a speed of 20ul/30min（the injection volume is 2ul）. After injection, the needle is left in place for 2 min. and the needle is returned and the surface of the head is wiped with a cotton swab. After the procedure, return to a new, warmed cage and wait for the anesthesia to subside. Neomycin 2mg/ml in drinking water for rats. After 32 days, Cycluc1 1.4 mg/kg was injected intraperitoneally and fluorescence intensity was measured 10 min after injected.

BLI was performed using IVIS Spectrum with open emission filter. Image generated by Living Image 4.3 software (PerkinElmer)

**Statistical analysis.** Each experiment was repeated at least three times independently, and the experimental data were expressed in the form of mean ± standard deviation. GraphPad Prism 9 was used to analyze the experimental results. The comparison between two groups was carried out by *t*-test, and the comparison between multiple groups was carried out by Dunnett's test or Tukey's HSD analysis. $P \leq 0.05$ means it is statistically significant.

**Ethical approval.** All experiments were performed in accordance with the relevant guidelines and regulations.

Results 1. SeP/ApoER2 pathway mediates GBM malignization and its mechanisms

1.1 Relationship between glioblastoma and SeP expression

In order to validate the expression of SeP in glioblastoma, we analyzed the human cancer database TCGA using the GEPIA2 analysis platform to investigate the expression of SeP in GBM tissue. The results are shown in the figure, comparing gene expression in normal tissue (N) and seeded tumor tissue (T), we found that SeP were increased in glioblastoma (GBM) and low grade glioma (LGG) tumors (Figure 1A). To verify SeP protein levels in actual patient specimens, we performed immunostaining using an established monoclonal antibody to SeP on tissue sections provided by Dr. Kanamori at Tohoku University Hospital to confirm SeP expression in brain tumor tissues from patients, and we found that SeP proteins were highly expressed in tissue sections from patients with high-grade brain tumors (Fig. 1B). These results suggest that not only SeP mRNA but also protein expression is increased under actual pathologic conditions.

SeP and the expression of the selenoprotein GPX, which is affected by SeP, may be correlated with the prognosis of glioblastoma. We searched the relationship between prognosis of glioblastoma and found that SeP and GPX4 is correlated with prognosis of GBM. The results showed that patients of GBM with high expression of SeP and GPX4 had a worse prognosis (Figure 2A). Patients with glioma can be classified as primary and recurrent, and tumor grading may increase in recurrent patients. Next, 18 patient samples were analyzed to test whether SeP protein expression correlates with prognosis. Immunostaining of onset and recurrent sample pairs from 18 glioma patients (Figure 2B), indicated that patients with SeP expression as weak positivity or

less at the time of onset who turned strongly positive at the time of recurrence had elevated malignancy of tumors. Patients with low SeP expression at the time of cancer initiation and strong positivity at the time of recurrence had a very poor prognosis. These results suggest that the expression of SeP protein levels may be associated with the grading and prognosis of patients with recurrent GBM.

The above results suggest that both SeP mRNA and protein expression are elevated in GBM tissues of patients and could be associated with worse prognosis.

1.2 Relationship between SeP and medication resistance

Temozolomide (TMZ) is the main drug for the treatment of gliomas. Its main mechanism of action is to inhibit cell proliferation by disrupting DNA strands, and it has also been reported to cause ferroptosis in GBM. In addition, TMZ resistance is regulated by MGMT mutations, which are frequently seen in GBM, and increased susceptibility to ferroptosis has been reported in TMZ-resistant GBM[66]. Therefore, we suggest that ferroptosis may be a new target for the treatment of GBM. On the other hand, selenium provided by SeP increases the expression of GPX, a ferroptosis inhibitor, which may be one of the mechanisms of GBM deterioration. In several types of cells, SeP expression plays a crucial role in cellular selenium metabolism and antioxidant defense via the preservation of glutathione peroxidases [41,53]. To verify the role of SeP in ferroptosis resistance in GBM, we selected T98G, which has the highest expression of SeP (Fig. 3A), in three GBM cell lines T98G, YKG1, and A172 held at the Institute of Development, Aging and Cancer, Tohoku University, and examined the expression of other antioxidant selenoproteins. T98G expressed the most SeP mRNA

among the three cells also had the highest expression of GPX (Fig. 3B). Therefore, we considered that T98G could be used as a GBM strain with high SeP expression.

We investigated the role of SeP expression in ferroptosis sensitivity in T98G. At first the knockdown efficiency of SeP was confirmed by qPCR (Fig. 4A), and the concentration of RSL3, an anti-cancer drug known to induce ferroptosis, was examined in negative control siRNA treated cells (Fig. 4B). From these results, we set the maximal RSL3 concentration that did not affect cell viability as 10 nM. Next, we examined cell viability following RSL3 treatment, and found that the effects of RSL3 were enhanced by SeP knockdown (Fig. 4C). These results indicate that SeP expression may confer protection against ferroptosis in glioblastoma cells.

1.3 SeP expression is responsible for maintaining GPx4 expression at the protein level in cultured GBM.

It has been reported that the ferroptosis regulatory system (GPX4) and anti-oxidative enzymes (GPX1) contribute to anti-cancer drug resistance [67,68]. We hypothesized that SeP expression in GBM would upregulate anti-oxidative selenoproteins and thereby promote ferroptosis resistance. To address this issue, we examined protein and mRNA levels of GPX4 and GPX1 in SeP siRNA-treated cells. The results shown in Fig. 4 indicate that although the three different siRNAs against SeP showed the same phenotype, siRNA #3 was the most efficient and thus was used as the representative siRNA in the following experiments. The results indicated that protein levels of GPX1 and GPX4 decreased significantly accompanied by SeP knockdown (Fig. 5A and B), while mRNA levels did not change (Fig. 5C). This suggests that SeP expression is involved in maintaining GPX protein levels, at least in cultured cells.

1.4 Selenium supplementation increases ferroptosis resistance in SeP siRNA-treated GBM.

It has been suggested that selenium supply increases selenoprotein levels at both transcriptional and translational levels. Therefore, we hypothesized that suppression of SeP expression in GBM would induce a decrease in GPX expression and increase susceptibility to ferroptosis via selenium depletion, and examined whether the above could be restored by the addition of selenite as a selenium donor.

Protein expression of GPX, which was reduced by the inhibition of SeP, was restored to the same level as the control after treatment with 5-20 nM of selenite (Fig. 6A). The increased susceptibility to ferroptosis induced by SeP knockdown was also restored to the same level as the control after addition of 10 nM selenite (Fig. 6B). These results suggest that basal SeP expression contributes to the maintenance of GPX protein expression and promotes ferroptosis resistance through the supply and retention of selenium.

1.5 Knockdown of ApoER2 reduces intracellular GPX

SeP is taken up into the cell by its receptor ApoER2. It is thought that ApoER2 may also affect the expression of selenoproteins such as GPX by influencing the SeP cycle. We examined the expression of these proteins after knocking down ApoER2. The results showed that all siRNAs from 1 to 3 significantly reduced the amount of ApoER2 proteins (Fig 7A). Meanwhile, the protein amount of GPX1 was also significantly reduced (Fig 7A), and the results showed that SeP/ApoER2 pathway affected the expression of antioxidant protein GPX in GBM cells. In the condition we also evaluated

the sensitivity against ferroptosis, however it was hardly changed may be because GPX4 levels were unchanged (data not shown). Thus, these results suggest that SeP and ApoER2 are both involved in maintaining of GPX levels, at least GPX1, and SeP is a major factor for contribute SeP cycle, rather than ApoER2. Again, it may be thought that GPX4 expression is more easily retained in cells and a partial decrease in selenium supply via ApoER2 inhibition does not result in decreased expression of GPX4 and increased susceptibility to ferroptosis.

1.6 Effect of SeP siRNA on ferroptosis resistance in patient-derived primary GBM.

To examine whether SeP in GBM maintains GPX expression through its own selenium supply, we examined the expression of SeP in primary GBM cells cultured from patient-isolated tissue and found that the expression of SeP in GAY12 was particularly high (Fig 8A). Then treated GAY12 cell with SeP siRNA. SeP mRNA levels were markedly reduced by SeP siRNA treatment (Fig 8B). In this condition, cellular morphology was not affected (Fig 8C). Ferroptosis sensitivity of the control siRNA-treated cells was also verified, and we found that the cells were sensitive to treatment with >15 nM RSL3 (Fig. 9A). Thus, we treated control and SeP siRNA-transfected cells with 15 nM RSL3 and examined cell viability. As with T98G, SeP inhibition decreased GPX4 expression (Fig 8C), which led to a significant increase in ferroptosis sensitivity (Fig. 9B), but addition of 10 nM selenite recovered both GPX levels and cell viability (Figs 9B and 9C). These results indicate that SeP plays a crucial role in maintaining GPX expression and ferroptosis resistance in GBM through selenium retention via cycling selenium storage. Possible mechanism is shown in Fig 10.

1.7 Effect of the SeP on cell proliferation of GBM

Although above studies indicate that the SeP/ApoER2 pathway acquires ferroptosis resistance in GBM cells by promoting selenium utilization, cancer malignancy is evaluated by multiple factors e.g., including cell growth and invasion. Interestingly, SeP not only provides selenium but also acts as a ligand involved in cell proliferation. In studies of colorectal cancer, SeP has been reported to bind to LRP5/6, a SeP receptor that is a homologous protein to ApoER2 and downstream activates WNT signaling to promote tumor growth[69]. Therefore, we hypothesized that SeP has the potential to act as a ligand and provide selenium in such a way as to promote cell proliferation in GBM. To verify the effect of SeP on the proliferation of GBM cells, we verified the proliferation rate of GBM cell lines and cells extracted from patients. Among the three cell lines, SeP and GPX highly-expressed T98G (Fig. 3A, B) showed the fastest proliferation (data not shown). SeP expression of GAY12 was highest in cells extracted from patients(Fig. 11A) and GAY2 proliferated fastest in patient cells (Fig. 11B).

Next, to verify the role of SeP in cell proliferation, we used the SeP highly expressed GBM cell line T98G, and we inhibited SeP expression in this cell line with siRNA (Fig. 12A). The results confirmed the KD of SeP lead to the decrease of cell proliferation (Fig. 12B). In contrast, we virally transfected U87, another cell line of GBM is low basal expression of SeP compared with T98G (data not shown). Thus, we used this cell line as like lower-expression SeP model of GBM. Transfection of SeP plasmid and over expression of SeP was confirmed by qPCR (Fig 13A), and at the protein level (Fig 13B). In the condition, proliferation was significantly increased by induction of SeP (Figure 13C). Interestingly, addition of selenite failed to affect proliferation of A172(Figure

13D), T98G and YKG1(data not shown) cells, this indicates selenium supplementation is not involved in proliferation. This is the difference phenotype compared with ferroptosis resistance found the above. Taken together with the knockdown experiments, these results suggest that SeP could be involved in cell proliferation of GBM as the ligand.

1.8 Effect of ApoER2 on proliferation GBM

Next, the effects of the SeP receptor ApoER2 were investigated. In a previous study in our lab, knockdown of ApoER2 in T98G resulted in decreased cell proliferation. Although there are multiple signaling pathways known to be downstream of ApoER2, RNA-seq analyses performed in our lab showed that the pathways involved in cell cycle and mitosis were the most altered as a result. Based on these results, we performed flow cytometry to confirm cell cycle fluctuations in ApoER2-kD T98G. An increase in the number of multinucleated cells was observed compared to control cells (unpublished observation by Hikari Sugiura). This situation is thought to reflect the state of cell arrest at the end of mitosis and the M phase. It is possible that ApoER2 promotes cell proliferation by enhancing the end phase of cytokinesis. Interestingly, by inhibiting the expression of SeP, the expression of ApoER2 was also reduced (Fig. 14A, B). This indicates SeP is not only a ligand but a regulator of the expression of receptor. In addition, to verify the role of ApoER2 in GBM proliferation in vivo, the luciferase steady-state expressing GBM cell line U87 was transplanted into the brains of immunodeficient nude rat, and a significant difference in body weight was observed between the two groups of rats on day 32 (Figure 15A). The proliferation of GBM was observed by bioluminescence, and the fluorescence intensity of GBM cells knocked

down with ApoER2 was significantly reduced compared with the control group (Figure 15B and C). The results showed that GBM with suppressed ApoER2 expression could hardly proliferate in rat brain. This suggests that ApoER2 is essential for the proliferation of GBM in the brain even at the animal level.

Discussion 1.

The present study reveals that 1. SeP is highly expressed in GBM, 2. this contributes to ferroptosis resistance by maintaining GPX expression at the protein level through selenium supplementation to GBM via formation of cycling selenium storage, and 3. SeP and ApoER2 could be involved in proliferation of GBM, and this is independent of selenium supplementation. Our findings identify SeP as a candidate therapeutic target for drug resistant-GBM (Fig 16).

Current cancer treatments do not effectively overcome resistance to chemotherapy drugs, and many studies have shown that induction of ferroptosis may be a novel cancer treatment strategy [70]. TMZ is currently the main drug used for treatment of GBM, however the prognosis of GBM patients remains poor, mainly due to TMZ resistance [66]. Immunohistochemical analysis of primary and recurrent GBM sample pairs from 24 patients receiving standard adjuvant chemotherapy and radiotherapy showed that recurrent tumors had increased vulnerability to oxidative stress and ferroptosis, and that GBM cells were more susceptible to ferroptosis than microglial cells [71]. In other words, TMZ-resistant cells were more likely to induce ferroptosis [16,72], and enhancing ferroptosis sensitivity could enhance the toxicity of temozolomide [73]. Thus, ferroptosis is a promising target to improve cancer immunotherapy in GBM. Studies have shown that elevated SeP levels are not only a consequence, but also contributes to the progression of certain diseases [53].Therefore, if expression of SeP in the brain can be suppressed, drug and treatment resistance of GBM might be overcome.

In GBM prognosis, p53 mutations and the expression of O6-methylguanine DNA methyltransferase (MGMT) gene are important for its treatment. MGMT-promoter methylation (negative regulation of MGMT) and other molecular abnormalities and imaging findings have made it possible to predict prognosis and treatment response in some cases, but accurate evaluation is still difficult. In this study, we validated the expression of SeP in various GBM cell-line which p53 is mutated and MGMT expression is regulated both positively and negatively. The results showed relatively high SeP expression in p53 mutated T98G and U251 (Fig. S1). The highest SeP expression was observed in primary GBM cells with negative p53, suggesting that p53 and SeP may be related in some way. At least, since the suppression of SeP expression did not affect the expression of MDM2 or MDM4, which are p53 regulators (Fig. S2), there is no involvement in this respect, and further detailed verification is needed. MGMT expression of T98G is positive while negative in U251[74,75]. However, even in such cells, suppression of SeP expression reduced GPX expression and increased RSL3 sensitivity as well as T98G cells (Fig. S3A-C). Taken together with the results from primary cells with high SeP expression, the data from at least three cell types suggest that cells with high SeP expression are commonly involved in conferring ferroptosis resistance through selenium retention at least regardless of the expression of MGMT.

Nonsense-mediated RNA decay (NMD) is often thought to be the contributing factor to the selenium-dependent regulation of selenoprotein mRNA[76,77]. Selenocysteine is an analog of cysteine, with selenium in place of sulfur, and is encoded by the termination codon UGA [78]. Insertion of selenocysteine into proteins requires a specific cis-acting stem-loop control element called SECIS, which is located in the 3'-untranslated region of the eukaryotic selenoprotein mRNAs, allowing translational read-through of the

UGA termination codon [34]. Although the amount of mRNA for many selenoproteins is not dependent on selenium concentration, translation of selenoproteins can be aborted at the UGA codon, resulting in incomplete and non-functional proteins [35]. Since selenoprotein variation in tumors may not be fully detected by approaches such as RNA-Sequence analysis, it is important to evaluate proteomics and protein activity as well.

Numerous studies have reported that GPX4 contributes to ferroptosis resistance via inhibition of lipid peroxidation [79]. On the other hand, although GPX1 has not been reported to be involved in ferroptosis, is thought to contribute to worsening prognosis, tumor growth, and treatment resistance in several cancers, including breast and bladder cancer, via its antioxidative activity [80-82]. Therefore, GPX family members may contribute to the malignant transformation and progression of GBM in a complex manner.

The effect of SeP knockdown on cellular selenium contents should be measured, however, basal selenium levels in cultured T98G cells are difficult to analyze. Regardless, given that the reduced GPX expression in SeP KD was restored by selenite addition, it is at least conceivable that this was not due to reduced selenoprotein synthesis or selenium metabolism by SeP KD, but rather a reduced selenium supply via SeP. SeP is thought to move dynamically in and out of cells following interaction with ApoER2 [83]. Therefore, SeP forms a dynamic "cycling-selenium storage system" in the brain, which is thought to be responsible for maintaining GPX expression. Further evidence of the role of the SeP-GPX axis and ApoER2 in ferroptosis and chemotherapy resistance are needed.

ApoER2 is involved in SeP uptake into the cell as a receptor for SeP and has a significant impact on cellular selenium metabolism and homeostasis. On the other hand, ApoER2 also binds to many other ligands[84]. ApoER2 as a low-density lipoprotein receptor related protein， which downstream impacts many pathways. For example, Reelin binds to its receptor ApoER2 to activate a phosphorylation cascade through Dab-2, PI3K, Akt and importantly NF-κB[84,85]. Neuroinflammation and paralysis were essentially eliminated in ApoER2 KO mice. ApoER2 deficiency suppresses neuroinflammatory signaling[86]. Although ApoER2 is highly expressed in the brain, its role in GBM is still little is known. It has been reported that ApoER2 regulates cellular mitosis through PP2A and CDC20 pathway [54], thus SeP may be involved in cell proliferation via this signaling pathway.

Although the expression of ApoER2 was reduced by the inhibition of SeP expression, it is unclear why this phenomenon was observed. At least in part, it is likely that low SeP expression promotes ApoER2 degradation, since the reduction in ApoER2 expression upon inhibition of SeP expression was canceled by bafilomycin A1, an inhibitor of lysosomal degradation (data not shown). Further details should be verified in the future.

This study not only reveals a unique selenium utilization and metabolism pathway, but also defines SeP/ApoER2 as a promising therapeutic target for GBM treatment to enhance sensitivity against anti-cancer drugs and cancer cell proliferation. However, it is unclear how the expression of SeP is regulated in GBM. Therefore, we focused on CCDC152, a regulator of SeP expression, in next chapter.

Results 2. Involvement of CCDC152, a regulator of the expression of SeP, in drug-resistance and proliferation of GBM

2.1 CCDC152 is highly expressed in GBM patients and is associated with prognosis

Figure 17A shows the motif of SeP, where the highlight is the exonic portion. Interestingly, on the antisense side of SeP, another gene named CCDC152 is encoded. We previously found that in hepatocytes, SeP expression is not only transcriptionally regulated, but also that CCDC152, which is a long noncoding RNA, is important for the regulation of SeP expression. RNA sequence data from glioma patients in TCGA were analyzed using U-MAP, which maps the similarity of gene expression, and showed that the gene expression patterns of GBM and other gliomas differed, and that CCDC152 was highly expressed in the glioblastoma population (Fig. 17B).

In addition, high expression of CCDC152 was observed in astrocytes with gene expression similar to that of glioblastomas, which are pre-glioblasticized astrocytomas (Fig. 17B). PrognoScan was used for the detection of genes associated with prognosis in gliomas, and in glioblastomas, high expression of CCDC152 was associated with reduced survival, but not significantly (Fig. 17C). However, we found that CCDC152 had a more significant effect on prognosis in low-grade gliomas and astrocytomas. Combined with the previous TCGA results above, it is possible that gliomas with high CCDC152 expression are involved in deterioration and higher grading, i.e., malignant transformation, at the time of recurrence, leading to a worse prognosis. Therefore, we set out to verify whether CCDC152 is involved in this deterioration by modulating SeP expression.

2.2 CCDC152 positively regulates the expression of SeP and its downstream GPX, thereby affecting ferroptosis resistance.

Data analysis in silico revealed a positive correlation between CCDC152 expression and SeP expression in patients (Figure S4). To in validate the effect of CCDC152 on SeP expression, the respective CCDC152 expression in GBM cell lines was examined at first. As a result, the highest CCDC152 expression was observed in SeP high-expressing T98G (Fig. 18A). Therefore, it was decided to use this cell line as a model for SeP-CCDC152 high-expressing GBM. On the contrary, since YKG1 had low expression of both SeP and CCDC152 it was used as a model for low SeP-CCDC152 expression (Fig. 18A). Then, we started from these two GBMs and observed how the SeP expression of these two GBMs changed after knockdown of CCDC152 in T98G and overexpression of CCDC152 in YKG1 (Fig. 18B, D). As a result, when the expression of CCDC152 was inhibited in T98G, a significant suppression of SeP mRNA expression was observed, and this suppression was also observed at the protein level as well (Fig. 18C). On the other hand, when CCDC152 was highly expressed in YKG1, the expression of SeP was observed to be induced, also at the protein level (Fig. 18E). This suggests that CCDC152 is a positive regulator of SeP in GBM.

Next, the expression of various selenoproteins involved in drug resistance downstream of the preceding SeP/ApoER2 was examined. The results showed that knockdown of CCDC152 decreased the expression of selenoproteins (TrxR1, GPX1 and GPX4), those are involved in vulnerability against oxidative stresses (Fig. 19A). This was similar to the results observed when SeP expression was inhibited. On the other hand, overexpression of CCDC152 in YKG1 increased the expression of selenoproteins (Fig. 19B). The above results suggest that the expression of SeP and selenoproteins may be

positively regulated by CCDC152 expression. Therefore, we hypothesized that CCDC152 is involved in ferroptosis resistance by regulating the expression of SeP and GPx. Therefore, we used the ferroptosis inducers RSL3 and Erastin to test the sensitivity. There was no significant change in cell activity in the control group using low concentrations of inducers, whereas in knockdown CCDC152 cells, the same concentration of inducers caused a significant reduction in cell viability (Fig 19 C,D). This effect was canceled by the ferroptosis inhibitor deferoxamine (Fig. 19 C, D). These results suggest that, like SeP KD, down-regulation of CCDC152 increases sensitivity to ferroptosis.

2.3 CCDC152 positively regulates the expression of SeP and its downstream ApoER2, thereby affecting cell proliferation.

We then tested the possibility that the SeP receptor ApoER2 could also be regulated by CCDC152 through SeP. The results showed that inhibition of CCDC152 expression partially decreased the mRNA expression of ApoER2 (Fig 20A), as well as significantly decreased the expression of ApoER2 protein (Fig 20B). Although it had no significant effect on the mRNA of ApoER2 (Fig 20C), high expression of CCDC152 on YKG1 increased ApoER2 protein expression (Fig 20D). The above results suggest that CCDC152 regulates ApoER2 expression, so we hypothesized that CCDC152 expression also affects cell proliferation. The results were consistent with the speculation that when CCDC152 expression was inhibited in T98G cells, cell proliferation activated by the ApoER2 pathway was also reduced (Fig 21A). On the other hand, making high expression of CCDC152 in YKG1 cells increased cell proliferation (Fig 21B). In the previous study in our laboratory, the downstream effect of ApoER2 was to inhibit cell

proliferation through M-phase arrest of cells. Therefore, we similarly investigated the effect of CCDC152 KD on the cell cycle. We found that, similar to the results observed with ApoER2 KD, more binucleated cells appeared in the CCDC152 KD cells (Fig. 22AB). These results suggest that CCDC152 is involved in GBM cell proliferation by regulating the upstream of the SeP/ApoER2 pathway.

2.4 CCDC152 regulates ApoER2 protein level through lysosomal catabolism

Next, we investigate how CCDC152 affects the amount of ApoER2 protein. ApoER2 is known to be degraded in lysosomes, so lysosomal acidity was measured using lysotracker. As shown, knockdown of CCDC152 increased lysosomal acidity (Fig 23A). Subsequently, bafilomycin was used to inhibit lysosomal protein hydrolysis. We found that knockdown of CCDC152 decreased ApoER2 protein expression, but inhibition of lysosomal acidification restored ApoER2 protein levels (Fig 23B). This indicates CCDC152 inhibits lysosomal function.

2.4 CCDC152 affects GBM processes as a non-coding RNA

In our previous study CCDC152 acted as a non-coding RNA in the liver to regulate SeP translation. However, CCDC152 has open reading frame, and it has the potential to be translated into peptide chains or proteins. It may have a different role in GBM cells than in the liver. To confirm whether CCDC152 is translated into protein in T98G cells, we added HA-tagged CCDC152 plasmid to T98G cells and then detected the presence of HA-tagged protein by WB. The HA-tagged iNOS plasmid was added as a positive control, and high expression of the corresponding mRNA was detected after transfection of both plasmids (Fig. 24A). Using anti-HA antibody to detect the

HA-tagged protein by WB, a band for the positive control iNOS at 130k molecular weight was detected. However, no bands were detected in cell lysates after CCDC152 plasmid treatment (Fig. 24B). This suggests that CCDC152 affected SeP and ApoER2 levels as a non-coding RNA in GBM cells.

2.5 The sequence on which CCDC152 acts is the part that is complementary to SeP

We considered CCDC152 as a long noncoding RNA and investigated its site of action on GBM cell proliferation. The sequence of CCDC152 is partially complementary to SeP and is shown in pink (Fig. 25A). We adapted the plasmid by trimming out parts of the sequence to obtain four partially defective CCDC152 plasmids (Fig. 25A). These plasmids were introduced into YKG1, which has low CCDC152 expression, to study its proliferation effect. The results were shown that both 5' and 3' defective plasmids promoted the proliferation of YKG1 cells (Fig 25B), and the effect of promoting proliferation was also observed for the plasmid containing the sequence complementary to SeP, whereas the plasmid defective in the sequence complementary to SeP could not affect the cell proliferation efficiency (Fig 25C). This suggests that the sequence is important for GBM proliferation.

Discussion 2.

The results of this chapter indicates that CCDC152, a regulator of SeP, is involved in ferroptosis resistance and cell proliferation of GBM. This support that the conclusion of chapter 1 and CCDC152-SeP-ApoER2 axis would be a promising target for treatment of GBM. Although there are still some evidence are needed, the mechanism of action of CCDC152 is dependent on sequences that are complementary to SeP, and increases the expression of ApoER2 by inhibiting the degradation of ApoER2 by lysosomes, thus jointly promoting cell proliferation.

Although much remains unknown about long non-coding RNA, and many discoveries have been made in recent years as a hot spot for cancer research. A lncRNA, PVT1 plays a role in promoting breast cancer cell growth, metastasis, and invasion, making it an attractive target for the treatment of breast cancer as well as a diagnostic indicator for breast cancer[87]. Studies of GBM have shown that dysregulated lncRNA can mediate the progression of glioblastoma multiforme [88]. As a lncRNA, CCDC152 has been little studied and its role for GBM is even more unknown. In our study, we found that CCDC152, which is present in the antisense strand of SeP, has a role in the positive regulation of SeP mRNA and protein. However, the mechanism of how CCDC152 affects the amount of mRNA and protein of SeP remains unknown. We speculate that it may be that CCDC152 and the complementary parts of the SeP sequence bind to each other and serve to stabilize SeP mRNA, to prevent SeP mRNA from being disassembled. In future experiments, we anticipate performing RNA-pull down to verify whether they bind.

Inhibition of CCDC152 expression was able to cause an increase in lysosomal acidity, resulting in a decrease in ApoER2 protein amounts. However, the mechanism of how CCDC152 affects lysosomal activity is unknown, and to elucidate this mechanism the pathway regulating lysosomal acidity should be tested. At least, lysosomal acidity is known to regulated by master regulator of lysosome TFEB and the proton pump are responsible for acidification of lysosome[89]. Thus check the effect of CCDC152 on TFEB and proton pump would help to understanding of the underlying mechanism.

In future studies, we would like to investigate the regulatory mechanism of CCDC152 and investigate the regulators of CCDC152 transcription. This will lead to the development of new therapeutic targets for GBM in order to further find GBM treatments with better specificity and fewer side effects.

Result 3. New therapeutic for GBM, which target SeP/ApoER2 axis

3.1 Drug screening for SeP suppressor in GBM

Our laboratory, supported by Basis for Supporting Innovative Drug Discovery and Life Science Research (BINDS), received about 7,500 compounds from the Tohoku University compound library for screening. We conducted a comprehensive search for compounds capable of modulating SeP transcriptional activity. The results of the screening showed that 18 compounds significantly reduced the promoter activity in HepG2 cells, a liver cancer cell (unpublished observation by Yamashita). Subsequently, we tested the inhibitory effects of these 18 compounds on SeP in T98G cells. The results showed that compounds #4 and #16 reduced the inhibition of SeP mRNA to less than 40% (Fig. 26A).

3.2 Effect of SeP suppressor on the proliferation of GBM

Compound #4 exhibited concentration-dependent inhibition at low concentrations (Fig. 26B). Next, the effects of the above compounds on cell proliferation were tested. The results showed that compound #4 exhibited growth inhibition at a concentration of 2 μM, while compound #16 exhibited cytotoxicity (Fig. 26C). We considered that compound #4 could act as a SeP inhibitor to inhibit the proliferation of GBM.

3.3 Effect of SeP suppressor on the ferroptosis resistance of GBM

Second, the reduction of SeP is expected to decrease GPX protein expression and drug resistance due to the reduced retention capacity of selenium. Therefore, we also tested the compound's effect on reducing GPX. The results showed that compound #4 does not

affect the mRNA levels of GPX (Fig 27A) but decreases its expression at the protein level (Fig 27B), suggesting that selenium utilization is affected. Therefore, we hypothesized that compound #4 may be a resistance eliminator for SeP-highly expressed GBM, thereby reducing resistance and increasing sensitivity to other anticancer drugs. Then, we analyzed the effect of compound 4 in combination with anticancer drugs to induce reinhibition using SynergyFinder (version 3). The results showed that drug sensitivity increased when compound 4 was combined with TMZ and RSL3 at lower concentrations (Figure 28AB).

Discussion 3.

Drugs that inhibit SeP expression have yet to be identified. In the present chapter we found few candidates that suppress SeP expression of GBM. Compound #4 is capable to inhibit cell proliferation and increase sensitivity against ferroptosis. This is a potential new therapeutic drug candidate targeting the ApoER2 SeP pathway that we have discovered, and we believe it is worth further validation, including compound development.

We recently found that sulforaphane and epigallocatechin gallate suppress SeP expression in hepatocytes. Chemical structure of drug #4 is still undisclosed in this dissertation, maybe there are some chemical properties. We would like to verify its efficacy as a drug by comparing it to these known compounds and examining its bioavailability.

SeP expression is known to contribute to the risk of colorectal cancer[69], prostate cancer[90], and pancreatic cancer[91], and may show an important role not only in GBM but also in other cancers. Therapeutics against SeP-ApoER2 axis may contribute treatment of such SeP-associated diseases.

One of the reasons GBM is so difficult to cure is that GBM is a tumor in brain. The blood-brain barrier (BBB) serves as a protection between the cerebral ventricles and the systemic circulation, limiting the entry of circulating toxins, inflammatory cells, and macromolecules into the brain parenchyma[92]. GBM contributes to the dysfunction of the blood-brain barrier through several mechanisms, such as junctional proteins are down-regulated and BBB transporter proteins are up-regulated, leading to increased BBB permeability[93]. The drug efflux pumps are significantly upregulated in GBM, thus

preventing therapeutic compounds from entering the tumor parenchyma [94]. In recent years, local efficacy has been improved due to the development of drug delivery methods, but drug residence time at the therapeutic target and half-life period are often overlooked. The concentration of temozolomide in brain tumor tissues is approximately 20% of plasma levels, and the concentration in cerebrospinal fluid is similar to that in radiotherapy[95].

Concentrations of TMZ in cerebrospinal fluid (CSF) are similar, and combination with radiotherapy may increase CSF levels to up to 35% of plasma levels[96]. It has also been shown that the final concentration of TMZ in the plasma of human patients is 50 μM, while in the cerebrospinal fluid it is only 5 μM. and only 5 μM in cerebrospinal fluid[95-97]. For tumor cells in the marginal zone, their BBB is disrupted, so they may be exposed to the plasma concentration of the drug (50 μM), whereas infiltrating tumor cells in normal brain parenchyma were exposed to only 5 μM of the therapeutic concentration[95]. Although temozolomide is effective against tumors, its relative concentration in the brain is low, and achieving the desired therapeutic effect requires the tumor to be very sensitive to temozolomide. New therapeutic agents are urgently needed to enhance the sensitivity of GBM. Whether the compounds we screened can reach the tumor area through the blood-brain barrier under pathological conditions is a topic we should pursue in the future.

Conclusion

Scheme of the summary of the study was shown as Fig 29.

1. The SeP/ApoER2 pathway contributes to ferroptosis resistance via selenium supply.

2. SeP enhances cell proliferation of GBM via ApoER2 as a ligand

3. CCDC152 is involved in cell proliferation and ferroptosis resistance of GBM via regulation of SeP and ApoER2 expression

4. Inhibitors of SeP expression may be applicable as therapeutic agents by canceling the above

**Acknowledgment**

I would like to express my heartfelt gratitude to my advisor, Prof. Saito, as well as Lecturer Toyama. I would like to thank them for their encouragement and guidance during my studies. Their expertise and consistent support has been invaluable.

I would also like to thank Assistant Kaneko and teaching assistant Arizawa from our research lab who gave me a lot of guidance and help.

I would like to thank Prof. Mita of Doshisha University for providing me with research advice and the CCDC152 plasmid.

Ms. Yamashita from the Division of Neurological Surgery, Graduate School of Medicine, Tohoku University, who helped me with my animal experiments. There are many more people who helped me in my PhD career. Without them, this thesis would not have been possible.

Finally, I would like to thank all those who took the time to read this thesis and provide valuable comments. Your insights will undoubtedly benefit me in my future studies.

**References**


1 Miller, K. D. *et al.* Brain and other central nervous system tumor statistics, 2021. *CA: A Cancer Journal for Clinicians* **71**, 381-406, doi:https://doi.org/10.3322/caac.21693 (2021).

2 Ostrom, Q. T., Francis, S. S. & Barnholtz-Sloan, J. S. Epidemiology of Brain and Other CNS Tumors. *Current Neurology and Neuroscience Reports* **21**, 68, doi:10.1007/s11910-021-01152-9 (2021).

3 Xu, S., Tang, L., Li, X., Fan, F. & Liu, Z. Immunotherapy for glioma: Current management and future application. *Cancer Letters* **476**, 1-12, doi:https://doi.org/10.1016/j.canlet.2020.02.002 (2020).

4 Louis, D. N. *et al.* The 2016 World Health Organization Classification of Tumors of the Central Nervous System: a summary. *Acta Neuropathologica* **131**, 803-820, doi:10.1007/s00401-016-1545-1 (2016).

5 Ohgaki, H. & Kleihues, P. Population-Based Studies on Incidence, Survival Rates, and Genetic Alterations in Astrocytic and Oligodendroglial Gliomas. *Journal of Neuropathology & Experimental Neurology* **64**, 479-489, doi:10.1093/jnen/64.6.479 %J Journal of Neuropathology & Experimental Neurology (2005).

6 Bleeker, F. E., Molenaar, R. J. & Leenstra, S. Recent advances in the molecular understanding of glioblastoma. *Journal of Neuro-Oncology* **108**, 11-27, doi:10.1007/s11060-011-0793-0 (2012).

7 Omuro, A. & DeAngelis, L. M. Glioblastoma and other malignant gliomas: a clinical review. *Jama* **310**, 1842-1850, doi:10.1001/jama.2013.280319 (2013).

8 Pellerino, A., Caccese, M., Padovan, M., Cerretti, G. & Lombardi, G. Epidemiology, risk factors, and prognostic factors of gliomas. *Clinical and Translational Imaging* **10**, 467-475, doi:10.1007/s40336-022-00489-6 (2022).

9 Alexander, B. M. & Cloughesy, T. F. Adult Glioblastoma. *Journal of clinical oncology : official journal of the American Society of Clinical Oncology* **35**, 2402-2409, doi:10.1200/jco.2017.73.0119 (2017).

10 Hombach-Klonisch, S. *et al.* Glioblastoma and chemoresistance to alkylating agents: Involvement of apoptosis, autophagy, and unfolded protein response. *Pharmacology & therapeutics* **184**, 13-41, doi:10.1016/j.pharmthera.2017.10.017 (2018).

11 Stupp, R. *et al.* Radiotherapy plus concomitant and adjuvant temozolomide for glioblastoma. *N Engl J Med* **352**, 987-996, doi:10.1056/NEJMoa043330 (2005).

12 Dixon, S. J. *et al.* Ferroptosis: an iron-dependent form of nonapoptotic cell death. *Cell* **149**, 1060-1072, doi:10.1016/j.cell.2012.03.042 (2012).

13 Fang, X., Ardehali, H., Min, J. & Wang, F. The molecular and metabolic landscape of iron and ferroptosis in cardiovascular disease. *Nature reviews. Cardiology* **20**, 7-23, doi:10.1038/s41569-022-00735-4 (2023).

14 Rajabi, A. *et al.* Non-coding RNAs and glioma: Focus on cancer stem cells. *Molecular therapy oncolytics* **27**, 100-123, doi:10.1016/j.omto.2022.09.005 (2022).

15 Zhang, Y. *et al.* Loss of COPZ1 induces NCOA4 mediated autophagy and ferroptosis in glioblastoma cell lines. *Oncogene* **40**, 1425-1439, doi:10.1038/s41388-020-01622-3 (2021).

16 Song, Q., Peng, S., Sun, Z., Heng, X. & Zhu, X. Temozolomide Drives Ferroptosis via a DMT1-Dependent Pathway in Glioblastoma Cells. *Yonsei medical journal* **62**, 843-849, doi:10.3349/ymj.2021.62.9.843 (2021).

17 Lee, S. Y. Temozolomide resistance in glioblastoma multiforme. *Genes & diseases* **3**, 198-210, doi:10.1016/j.gendis.2016.04.007 (2016).

18 Tomar, M. S., Kumar, A., Srivastava, C. & Shrivastava, A. Elucidating the mechanisms of Temozolomide resistance in gliomas and the strategies to overcome the resistance. *Biochimica et biophysica acta. Reviews on cancer* **1876**, 188616, doi:10.1016/j.bbcan.2021.188616 (2021).

19 Lei, G., Zhuang, L. & Gan, B. Targeting ferroptosis as a vulnerability in cancer. *Nature reviews. Cancer* **22**, 381-396, doi:10.1038/s41568-022-00459-0 (2022).

20 Wiernicki, B. *et al.* Excessive phospholipid peroxidation distinguishes ferroptosis from other cell death modes including pyroptosis. *Cell death & disease* **11**, 922, doi:10.1038/s41419-020-03118-0 (2020).

21 Campos-Sandoval, J. A. *et al.* Antioxidant responses related to temozolomide resistance in glioblastoma. *Neurochemistry international* **149**, 105136, doi:10.1016/j.neuint.2021.105136 (2021).

22 Yao, Y. *et al.* Selenium-GPX4 axis protects follicular helper T cells from ferroptosis. *Nature immunology* **22**, 1127-1139, doi:10.1038/s41590-021-00996-0 (2021).

23 Seibt, T. M., Proneth, B. & Conrad, M. Role of GPX4 in ferroptosis and its pharmacological implication. *Free radical biology & medicine* **133**, 144-152, doi:10.1016/j.freeradbiomed.2018.09.014 (2019).

24 Traverso, N. *et al.* Role of glutathione in cancer progression and chemoresistance. *Oxidative medicine and cellular longevity* **2013**, 972913, doi:10.1155/2013/972913 (2013).

25 Panieri, E. & Santoro, M. M. ROS homeostasis and metabolism: a dangerous liason in cancer cells. *Cell death & disease* **7**, e2253, doi:10.1038/cddis.2016.105 (2016).

26 Aquilano, K., Baldelli, S. & Ciriolo, M. R. Glutathione: new roles in redox signaling for an old antioxidant. **5**, doi:10.3389/fphar.2014.00196 (2014).

27 Koppula, P., Zhang, Y., Zhuang, L. & Gan, B. Amino acid transporter SLC7A11/xCT at the crossroads of regulating redox homeostasis and nutrient dependency of cancer. *Cancer communications (London, England)* **38**, 12, doi:10.1186/s40880-018-0288-x (2018).

28 Koppula, P., Zhuang, L. & Gan, B. Cystine transporter SLC7A11/xCT in cancer: ferroptosis, nutrient dependency, and cancer therapy. *Protein & cell* **12**, 599-620, doi:10.1007/s13238-020-00789-5 (2021).

29 Yakubov, E. *et al.* Therapeutic Potential of Selenium in Glioblastoma. *Frontiers in neuroscience* **15**, 666679, doi:10.3389/fnins.2021.666679 (2021).

30 Cardoso, B. R., Roberts, B. R., Bush, A. I. & Hare, D. J. Selenium, selenoproteins and neurodegenerative diseases. *Metallomics : integrated biometal science* **7**, 1213-1228, doi:10.1039/c5mt00075k (2015).

31 Sherlock, L. G. *et al.* Hepatic-Specific Decrease in the Expression of Selenoenzymes and Factors Essential for Selenium Processing After Endotoxemia. *Frontiers in immunology* **11**, 595282, doi:10.3389/fimmu.2020.595282 (2020).

32 Hoffmann, P. R. & Berry, M. J. Selenoprotein synthesis: a unique translational mechanism used by a diverse family of proteins. *Thyroid : official journal of the American Thyroid Association* **15**, 769-775, doi:10.1089/thy.2005.15.769 (2005).

33 Santesmasses, D., Mariotti, M. & Gladyshev, V. N. Bioinformatics of Selenoproteins. *Antioxidants & redox signaling* **33**, 525-536, doi:10.1089/ars.2020.8044 (2020).

34 Labunskyy, V. M., Hatfield, D. L. & Gladyshev, V. N. Selenoproteins: molecular pathways and physiological roles. *Physiological reviews* **94**, 739-777, doi:10.1152/physrev.00039.2013 (2014).

35 Chen, Y. F. *et al.* A quantitative model for the rate-limiting process of UGA alternative assignments to stop and selenocysteine codons. *PLoS computational biology* **13**, e1005367, doi:10.1371/journal.pcbi.1005367 (2017).

36 Kitabayashi, N. *et al.* Role of selenoprotein P expression in the function of pancreatic β cells: Prevention of ferroptosis-like cell death and stress-induced nascent granule degradation. *Free radical biology & medicine* **183**, 89-103, doi:10.1016/j.freeradbiomed.2022.03.009 (2022).

37 Alborzinia, H. *et al.* LRP8-mediated selenocysteine uptake is a targetable vulnerability in MYCN-amplified neuroblastoma. *EMBO molecular medicine* **15**, e18014, doi:10.15252/emmm.202318014 (2023).

38 Burk, R. F. & Hill, K. E. Regulation of Selenium Metabolism and Transport. *Annual review of nutrition* **35**, 109-134, doi:10.1146/annurev-nutr-071714-034250 (2015).

39 Scharpf, M. *et al.* Neuronal and ependymal expression of selenoprotein P in the human brain. *Journal of neural transmission (Vienna, Austria : 1996)* **114**, 877-884, doi:10.1007/s00702-006-0617-0 (2007).

40 Sasuclark, A. R., Khadka, V. S. & Pitts, M. W. Cell-Type Specific Analysis of Selenium-Related Genes in Brain. *Antioxidants (Basel, Switzerland)* **8**, doi:10.3390/antiox8050120 (2019).

41 Burk, R. F. & Hill, K. E. Selenoprotein P: an extracellular protein with unique physical characteristics and a role in selenium homeostasis. *Annual review of nutrition* **25**, 215-235, doi:10.1146/annurev.nutr.24.012003.132120 (2005).

42 Burk, R. F. & Hill, K. E. Selenoprotein P-expression, functions, and roles in mammals. *Biochimica et biophysica acta* **1790**, 1441-1447, doi:10.1016/j.bbagen.2009.03.026 (2009).

43 Schweizer, U. *et al.* Hepatically derived selenoprotein P is a key factor for kidney but not for brain selenium supply. *The Biochemical journal* **386**, 221-226, doi:10.1042/bj20041973 (2005).

44 Dlugosz, P. & Nimpf, J. The Reelin Receptors Apolipoprotein E receptor 2 (ApoER2) and VLDL Receptor. *International journal of molecular sciences* **19**, doi:10.3390/ijms19103090 (2018).

45 Bock, H. H. & May, P. Canonical and Non-canonical Reelin Signaling. *Frontiers in cellular neuroscience* **10**, 166, doi:10.3389/fncel.2016.00166 (2016).

46 Burk, R. F. *et al.* Deletion of apolipoprotein E receptor-2 in mice lowers brain selenium and causes severe neurological dysfunction and death when a low-selenium diet is fed. *The Journal of neuroscience : the official journal of the Society for Neuroscience* **27**, 6207-6211, doi:10.1523/jneurosci.1153-07.2007 (2007).

47 Kurokawa, S., Hill, K. E., McDonald, W. H. & Burk, R. F. Long isoform mouse selenoprotein P (Sepp1) supplies rat myoblast L8 cells with selenium via endocytosis mediated by heparin binding properties and apolipoprotein E receptor-2 (ApoER2). *The Journal of biological chemistry* **287**, 28717-28726, doi:10.1074/jbc.M112.383521 (2012).

48 Schomburg, L., Schweizer, U. & Köhrle, J. Selenium and selenoproteins in mammals: extraordinary, essential, enigmatic. *Cellular and Molecular Life Sciences CMLS* **61**, 1988-1995, doi:10.1007/s00018-004-4114-z (2004).

49 Burk, R. F. *et al.* Selenoprotein P and apolipoprotein E receptor-2 interact at the blood-brain barrier and also within the brain to maintain an essential selenium pool that protects against neurodegeneration. *FASEB journal : official publication of the Federation of American Societies for Experimental Biology* **28**, 3579-3588, doi:10.1096/fj.14-252874 (2014).

50 Mizuno, A. *et al.* An efficient selenium transport pathway of selenoprotein P utilizing a high-affinity ApoER2 receptor variant and being independent of selenocysteine lyase. *The Journal of biological chemistry* **299**, 105009, doi:10.1016/j.jbc.2023.105009 (2023).

51 Saito, Y. Selenium Transport Mechanism via Selenoprotein P-Its Physiological Role and Related Diseases. *Frontiers in nutrition* **8**, 685517, doi:10.3389/fnut.2021.685517 (2021).

52 Yang, Y. *et al.* A Pan-Cancer Analysis of the Role of Selenoprotein P mRNA in Tumorigenesis. *International journal of general medicine* **14**, 7471-7485, doi:10.2147/ijgm.S332031 (2021).

53 Schomburg, L. Selenoprotein P - Selenium transport protein, enzyme and biomarker of selenium status. *Free radical biology & medicine* **191**, 150-163, doi:10.1016/j.freeradbiomed.2022.08.022 (2022).

54 Komaravolu, R. K., Waltmann, M. D., Konaniah, E., Jaeschke, A. & Hui, D. Y. ApoER2 (Apolipoprotein E Receptor-2) Deficiency Accelerates Smooth Muscle Cell Senescence via Cytokinesis Impairment and Promotes Fibrotic Neointima After Vascular Injury. *Arteriosclerosis, thrombosis, and vascular biology* **39**, 2132-2144, doi:10.1161/atvbaha.119.313194 (2019).

55 Huang, T., Alvarez, A., Hu, B. & Cheng, S. Y. Noncoding RNAs in cancer and cancer stem cells. *Chinese Journal of Cancer* **32**, 582-593, doi:10.5732/cjc.013.10170 (2013).

56 Djebali, S. *et al.* Landscape of transcription in human cells. *Nature* **489**, 101-108, doi:10.1038/nature11233 (2012).

57 Heery, R., Finn, S. P., Cuffe, S. & Gray, S. G. Long Non-Coding RNAs: Key Regulators of Epithelial-Mesenchymal Transition, Tumour Drug Resistance and Cancer Stem Cells. *Cancers* **9** (2017).

58 Ji, Z., Song, R., Regev, A. & Struhl, K. Many lncRNAs, 5'UTRs, and pseudogenes are translated and some are likely to express functional proteins. *eLife* **4**, e08890, doi:10.7554/eLife.08890 (2015).

59 Tan, Y. T. *et al.* LncRNA-mediated posttranslational modifications and reprogramming of energy metabolism in cancer. *Cancer communications (London, England)* **41**, 109-120, doi:10.1002/cac2.12108 (2021).

60 Ransohoff, J. D., Wei, Y. & Khavari, P. A. The functions and unique features of long intergenic non-coding RNA. *Nature reviews. Molecular cell biology* **19**, 143-157, doi:10.1038/nrm.2017.104 (2018).

61 Luo, J., Langer, L. F. & Liu, J. A novel role of LncRNA in regulating tumor metabolism and angiogenesis under hypoxia. *Cancer communications (London, England)* **39**, 2, doi:10.1186/s40880-019-0348-x (2019).

62 Mita, Y. *et al.* Identification of a novel endogenous long non-coding RNA that inhibits selenoprotein P translation. *Nucleic acids research* **49**, 6893-6907, doi:10.1093/nar/gkab498 (2021).

63 Li, R. *et al.* Identification of 6 gene markers for survival prediction in osteosarcoma cases based on multi-omics analysis. *Experimental biology and medicine (Maywood, N.J.)* **246**, 1512-1523, doi:10.1177/1535370221992015 (2021).

64 Talebi, A., Rokni, P. & Kerachian, M. A. Transcriptome analysis of colorectal cancer liver metastasis: The importance of long non-coding RNAs and fusion transcripts in the disease pathogenesis. *Molecular and cellular probes* **63**, 101816, doi:10.1016/j.mcp.2022.101816 (2022).

65 Mita, Y. *et al.* Selenoprotein P-neutralizing antibodies improve insulin secretion and glucose sensitivity in type 2 diabetes mouse models. *Nature communications* **8**, 1658, doi:10.1038/s41467-017-01863-z (2017).

66 de Souza, I. *et al.* High levels of NRF2 sensitize temozolomide-resistant glioblastoma cells to ferroptosis via ABCC1/MRP1 upregulation. *Cell death & disease* **13**, 591, doi:10.1038/s41419-022-05044-9 (2022).

67 Moslemizadeh, A. *et al.* Combination therapy with interferon-gamma as a potential therapeutic medicine in rat's glioblastoma: A multi-mechanism evaluation. *Life sciences* **305**, 120744, doi:10.1016/j.lfs.2022.120744 (2022).

68 Behnisch-Cornwell, S., Wolff, L. & Bednarski, P. J. The Effect of Glutathione Peroxidase-1 Knockout on Anticancer Drug Sensitivities and Reactive Oxygen Species in Haploid HAP-1 Cells. *Antioxidants (Basel, Switzerland)* **9**, doi:10.3390/antiox9121300 (2020).

69 Pilat, J. M. *et al.* SELENOP modifies sporadic colorectal carcinogenesis and WNT signaling activity through LRP5/6 interactions. *The Journal of clinical investigation* **133**, doi:10.1172/jci165988 (2023).

70 Zhao, L. *et al.* Ferroptosis in cancer and cancer immunotherapy. *Cancer communications (London, England)* **42**, 88-116, doi:10.1002/cac2.12250 (2022).

71 Kram, H. *et al.* Glioblastoma Relapses Show Increased Markers of Vulnerability to Ferroptosis. *Frontiers in oncology* **12**, 841418, doi:10.3389/fonc.2022.841418 (2022).

72 Liu, H. J. *et al.* Ferroptosis-Related Gene Signature Predicts Glioma Cell Death and Glioma Patient Progression. *Frontiers in cell and developmental biology* **8**, 538, doi:10.3389/fcell.2020.00538 (2020).

73 Tong, S. *et al.* TFR2 regulates ferroptosis and enhances temozolomide chemo-sensitization in gliomas. *Experimental cell research* **424**, 113474, doi:10.1016/j.yexcr.2023.113474 (2023).

74 Vlachostergios, P. J., Hatzidaki, E., Stathakis, N. E., Koukoulis, G. K. & Papandreou, C. N. Bortezomib downregulates MGMT expression in T98G glioblastoma cells. *Cellular and molecular neurobiology* **33**, 313-318, doi:10.1007/s10571-013-9910-2 (2013).

75 Witte, K. E. *et al.* PLEKHG5 regulates autophagy, survival and MGMT expression in U251-MG glioblastoma cells. *Scientific reports* **10**, 21858, doi:10.1038/s41598-020-77958-3 (2020).

76 Banerjee, S., Yang, S. & Foster, C. B. A luciferase reporter assay to investigate the differential selenium-dependent stability of selenoprotein mRNAs. *The Journal of nutritional biochemistry* **23**, 1294-1301, doi:10.1016/j.jnutbio.2011.07.010 (2012).

77 Seyedali, A. & Berry, M. J. Nonsense-mediated decay factors are involved in the regulation of selenoprotein mRNA levels during selenium deficiency. *RNA (New York, N.Y.)* **20**, 1248-1256, doi:10.1261/rna.043463.113 (2014).

78 Arnér, E. S. J. Common modifications of selenocysteine in selenoproteins. *Essays in biochemistry* **64**, 45-53, doi:10.1042/ebc20190051 (2020).

79 Chen, X., Li, J., Kang, R., Klionsky, D. J. & Tang, D. Ferroptosis: machinery and regulation. *Autophagy* **17**, 2054-2081, doi:10.1080/15548627.2020.1810918 (2021).

80 Brigelius-Flohé, R. & Flohé, L. Regulatory Phenomena in the Glutathione Peroxidase Superfamily. *Antioxidants & redox signaling* **33**, 498-516, doi:10.1089/ars.2019.7905 (2020).

81 Jablonska, E. *et al.* Lipid peroxidation and glutathione peroxidase activity relationship in breast cancer depends on functional polymorphism of GPX1. *BMC cancer* **15**, 657, doi:10.1186/s12885-015-1680-4 (2015).

82 Han, C. *et al.* Berbamine Suppresses the Progression of Bladder Cancer by Modulating the ROS/NF-κB Axis. *Oxidative medicine and cellular longevity* **2021**, 8851763, doi:10.1155/2021/8851763 (2021).

83 Kurokawa, S., Bellinger, F. P., Hill, K. E., Burk, R. F. & Berry, M. J. Isoform-specific binding of selenoprotein P to the β-propeller domain of apolipoprotein E receptor 2 mediates selenium supply. *The Journal of biological chemistry* **289**, 9195-9207, doi:10.1074/jbc.M114.549014 (2014).

84 Alexander, A., Herz, J. & Calvier, L. Reelin through the years: From brain development to inflammation. *Cell reports* **42**, 112669, doi:10.1016/j.celrep.2023.112669 (2023).

85 Calvier, L. *et al.* Reelin Depletion Protects Against Atherosclerosis by Decreasing Vascular Adhesion of Leukocytes. *Arteriosclerosis, thrombosis, and vascular biology* **41**, 1309-1318, doi:10.1161/atvbaha.121.316000 (2021).

86 Calvier, L. *et al.* Apolipoprotein E receptor 2 deficiency decreases endothelial adhesion of monocytes and protects against autoimmune encephalomyelitis. *Science immunology* **6**, doi:10.1126/sciimmunol.abd0931 (2021).

87 Baljon, K. J. *et al.* LncRNA PVT1: as a therapeutic target for breast cancer. *Pathology, research and practice* **248**, 154675, doi:10.1016/j.prp.2023.154675 (2023).

88 Mukherjee, S., Kundu, U., Desai, D. & Pillai, P. P. Particulate Matters Affecting lncRNA Dysregulation and Glioblastoma Invasiveness: In Silico Applications and Current Insights. *Journal of molecular neuroscience : MN* **72**, 2188-2206, doi:10.1007/s12031-022-02069-9 (2022).

89 Franco-Juárez, B. *et al.* TFEB; Beyond Its Role as an Autophagy and Lysosomes Regulator. *Cells* **11**, doi:10.3390/cells11193153 (2022).

90 Diamond, A. M. Selenoproteins of the Human Prostate: Unusual Properties and Role in Cancer Etiology. *Biological trace element research* **192**, 51-59, doi:10.1007/s12011-019-01809-0 (2019).

91 Maehara, S. *et al.* Selenoprotein P, as a predictor for evaluating gemcitabine resistance in human pancreatic cancer cells. *International journal of cancer* **112**, 184-189, doi:10.1002/ijc.20304 (2004).

92 Sweeney, M. D., Ayyadurai, S. & Zlokovic, B. V. Pericytes of the neurovascular unit: key functions and signaling pathways. *Nature neuroscience* **19**, 771-783, doi:10.1038/nn.4288 (2016).

93 Wolburg, H. *et al.* Localization of claudin-3 in tight junctions of the blood-brain barrier is selectively lost during experimental autoimmune encephalomyelitis and human glioblastoma multiforme. *Acta neuropathologica* **105**, 586-592, doi:10.1007/s00401-003-0688-z (2003).

94 Mason, W. P. Blood-brain barrier-associated efflux transporters: a significant but underappreciated obstacle to drug development in glioblastoma. *Neuro-oncology* **17**, 1181-1182, doi:10.1093/neuonc/nov122 (2015).

95 Portnow, J. *et al.* The neuropharmacokinetics of temozolomide in patients with resectable brain tumors: potential implications for the current approach to chemoradiation. *Clinical cancer research : an official journal of the American Association for Cancer Research* **15**, 7092-7098, doi:10.1158/1078-0432.Ccr-09-1349 (2009).

96 Ostermann, S. *et al.* Plasma and cerebrospinal fluid population pharmacokinetics of temozolomide in malignant glioma patients. *Clinical cancer research : an official journal of the American Association for Cancer Research* **10**, 3728-3736, doi:10.1158/1078-0432.Ccr-03-0807 (2004).

97 Brada, M. *et al.* Phase I dose-escalation and pharmacokinetic study of temozolomide (SCH 52365) for refractory or relapsing malignancies. *British journal of cancer* **81**, 1022-1030, doi:10.1038/sj.bjc.6690802 (1999).

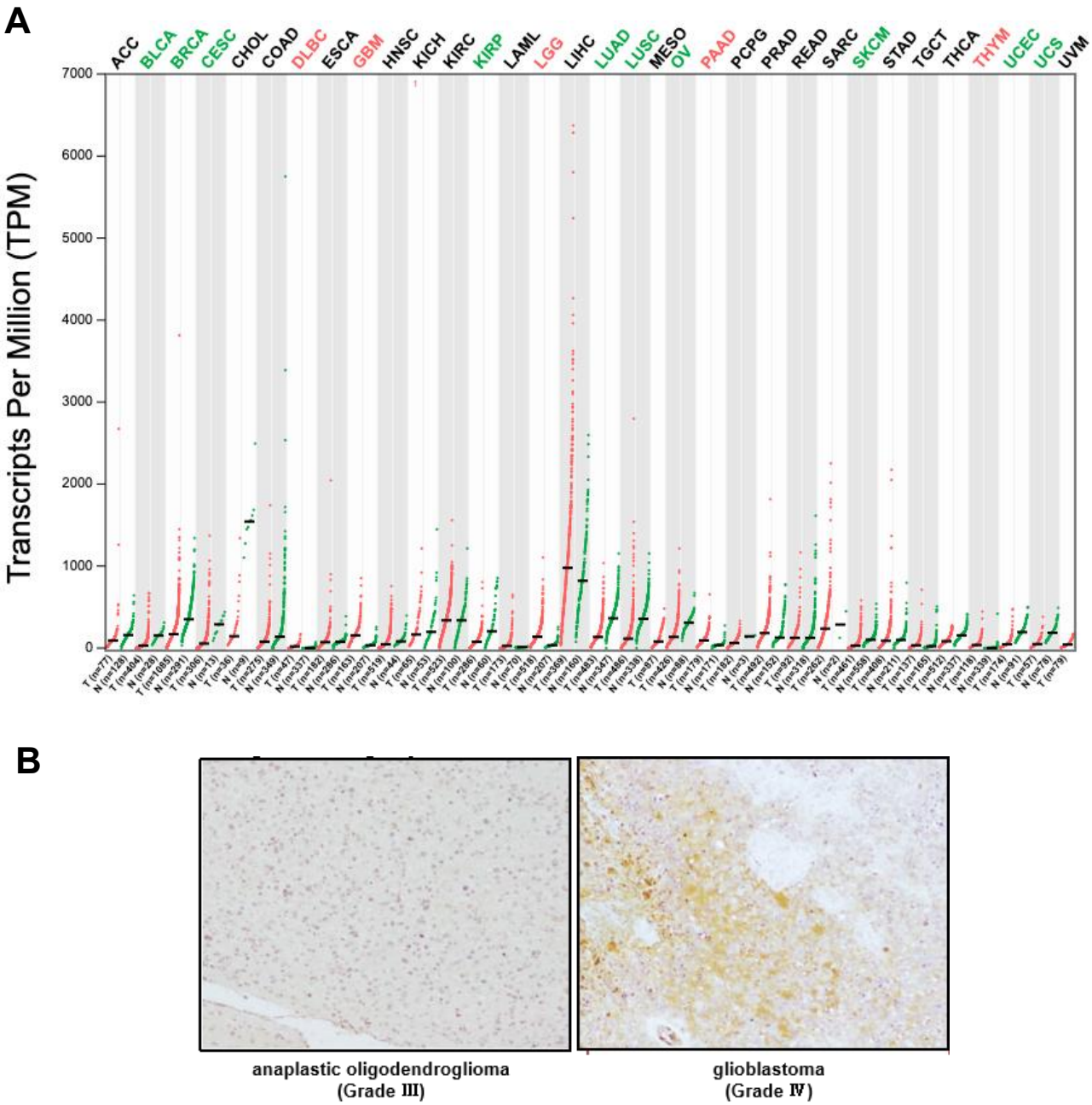


**Figure 1. SeP is highly expressed in GBM patients.** Comparison of tumor and normal tissue mRNA level obtained from the TCGA database by GEPIA2 (A). Red plots indicates cancer patients, and Green plots indicates healthy subjects. If the title of the cancer are colored, it means there is significant change. ACCA (drenocortical carcinoma), BLCA (Bladder Urothelial Carcinoma), BRCA (Breast invasive carcinoma), CESC (Cervical squamous cell carcinoma and endocervical adenocarcinomaCHOLCholangio carcinomaCOADColon adenocarcinoma), DLBC (Lymphoid Neoplasm Diffuse Large B-cell Lymphoma), ESCA (Esophageal carcinoma), GBM (Glioblastoma multiforme), HNSC (Head and Neck squamous cell carcinoma), KICH (Kidney Chromophobe), KIRC (Kidney renal clear cell carcinoma), KIRP (Kidney renal papillary cell carcinoma), LAML (Acute Myeloid Leukemia), LGG (Brain Lower Grade Glioma), LIHC (Liver hepatocellular carcinoma), LUAD (Lung adenocarcinoma), LUSC (Lung squamous cell carcinoma), MESO (MesotheliomaOVOvarian serous cystadenocarcinoma), PAAD (Pancreatic adenocarcinoma), PCPG (Pheochromocytoma and Paraganglioma), PRAD (Prostate adenocarcinoma), READ (Rectum adenocarcinoma), SARC (Sarcoma), SKCM (Skin Cutaneous Melanoma), STAD (Stomach adenocarcinoma), TGCT (Testicular Germ Cell Tumors), THCA (Thyroid carcinoma), THYM (Thymoma), UCEC (Uterine Corpus Endometrial Carcinoma), UCS (Uterine Carcinosarcoma), UVM (Uveal Melanoma). Immunostaining of patient tissue sections using anti-SeP monoclonal antibody (B).

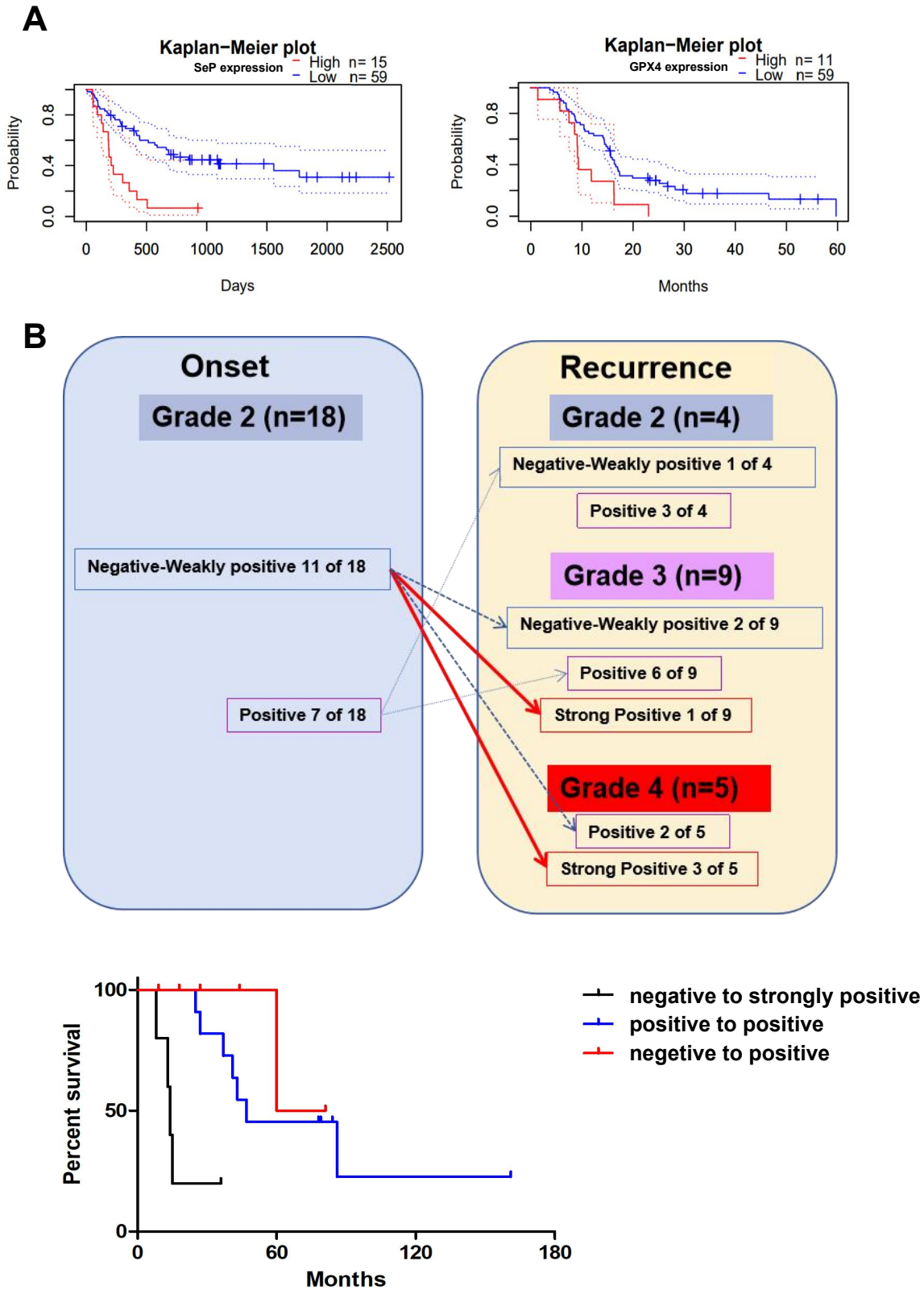


**Figure 2. SeP was associated with patient prognosis.** the association between patient gene expression and prognosis was obtained from the prognoscan database (A), Tissue sections of patients were immunostained using anti-SeP monoclonal antibody, and the association between the amount of SeP protein and prognosis was analyzed after patients were classified according to the intensity of staining (B).

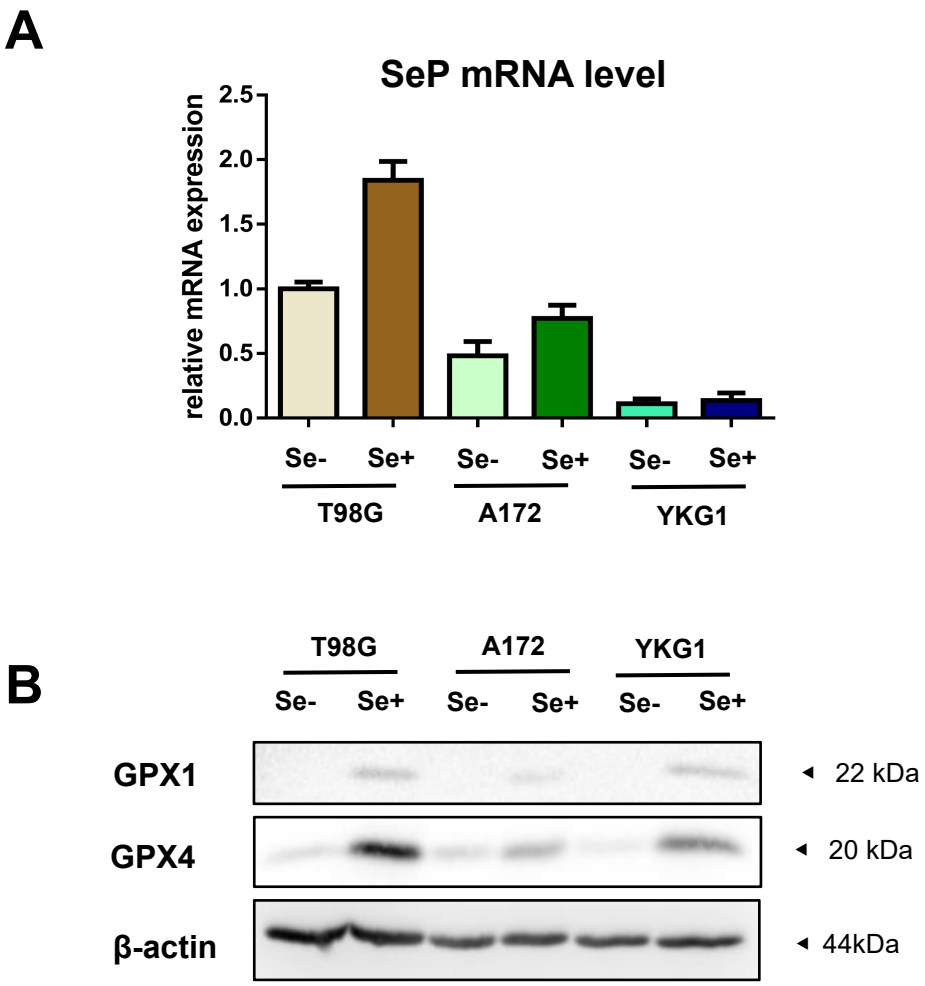


**Figure 3. SeP expression in three GBM cell lines.** Three types of GBM cell line were cultured with or without of selenite (100 nM, continuously), and mRNA expression of SeP was detected by RT-qPCR (A), GPX protein expression was detected by WB (B). Data are shown as mean±S.D.; n=3 .

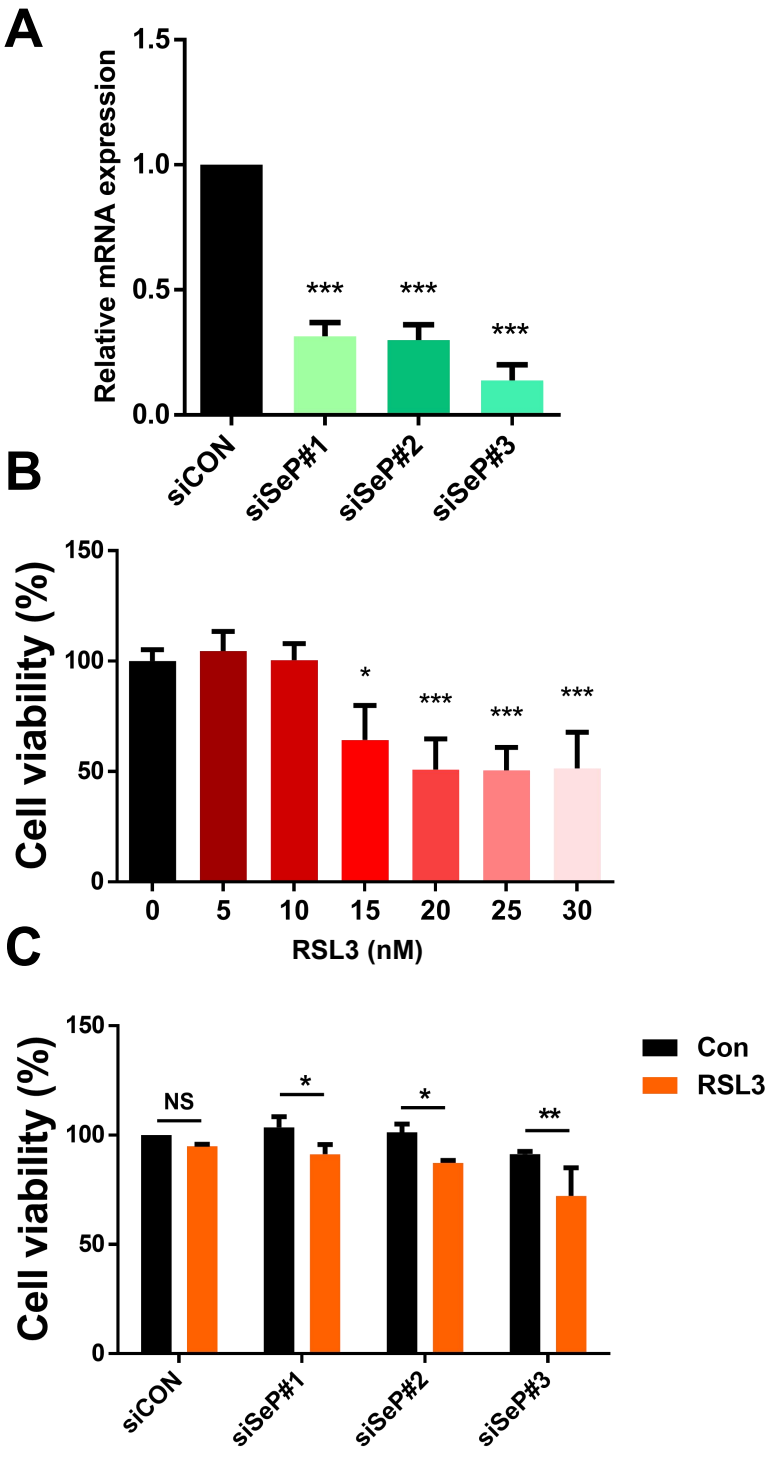


**Figure 4. SeP inhibits cell death induced by RSL3, a ferroptosis inducer, in T98G.** T98G cells were transfected with three different SeP siRNAs and 48 hours post-treatment, SeP mRNA levels were measured by RT-qPCR (A). T98G cells were treated with control siRNA (siCON), and RSL3 was added at the indicated concentrations. After 24 hours, cell viability was measured (B) Cells were pre-treated with three different siRNAs against SeP for 24 hours, then treated with 10 nM RSL3 for an additional 24 hours, and cell viability was measured (C). Data are presented as the mean ± S.D; n=3.Statistical significance was assessed by Dunnett's test (AB) and Tukey's HSD (C). *$p < 0.05$, **$p < 0.01$, ***$p < 0.001$ vs control.

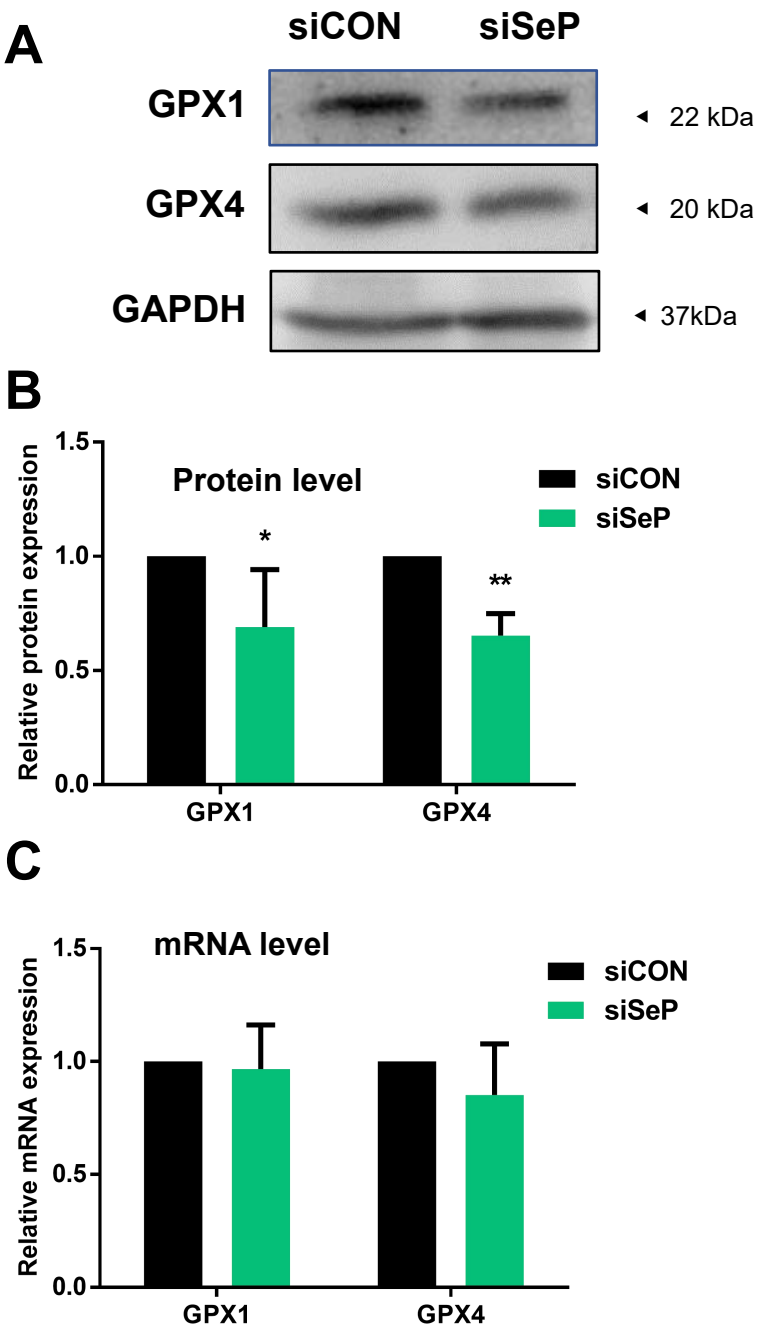


**Figure 5. SeP is required for maintaining of glutathione peroxidase expression in T98G.** Cells were transfected with SeP siRNA (#3 siRNA was used as the representative) for 48 hours. Protein expression of selenoproteins (GPx1 and GPx4) were measured by Western blotting (A). Protein content of each selenoprotein was normalized using GAPDH, and relative expression levels are shown with the control as 1 (B), Under the same conditions, mRNA levels of each selenoprotein were measured by RT-qPCR (C) data are shown as mean±S.D.; n=3 . Statistical significance was assessed by the *t*-test. **p* < 0.05, ***p* < 0.01 vs control.

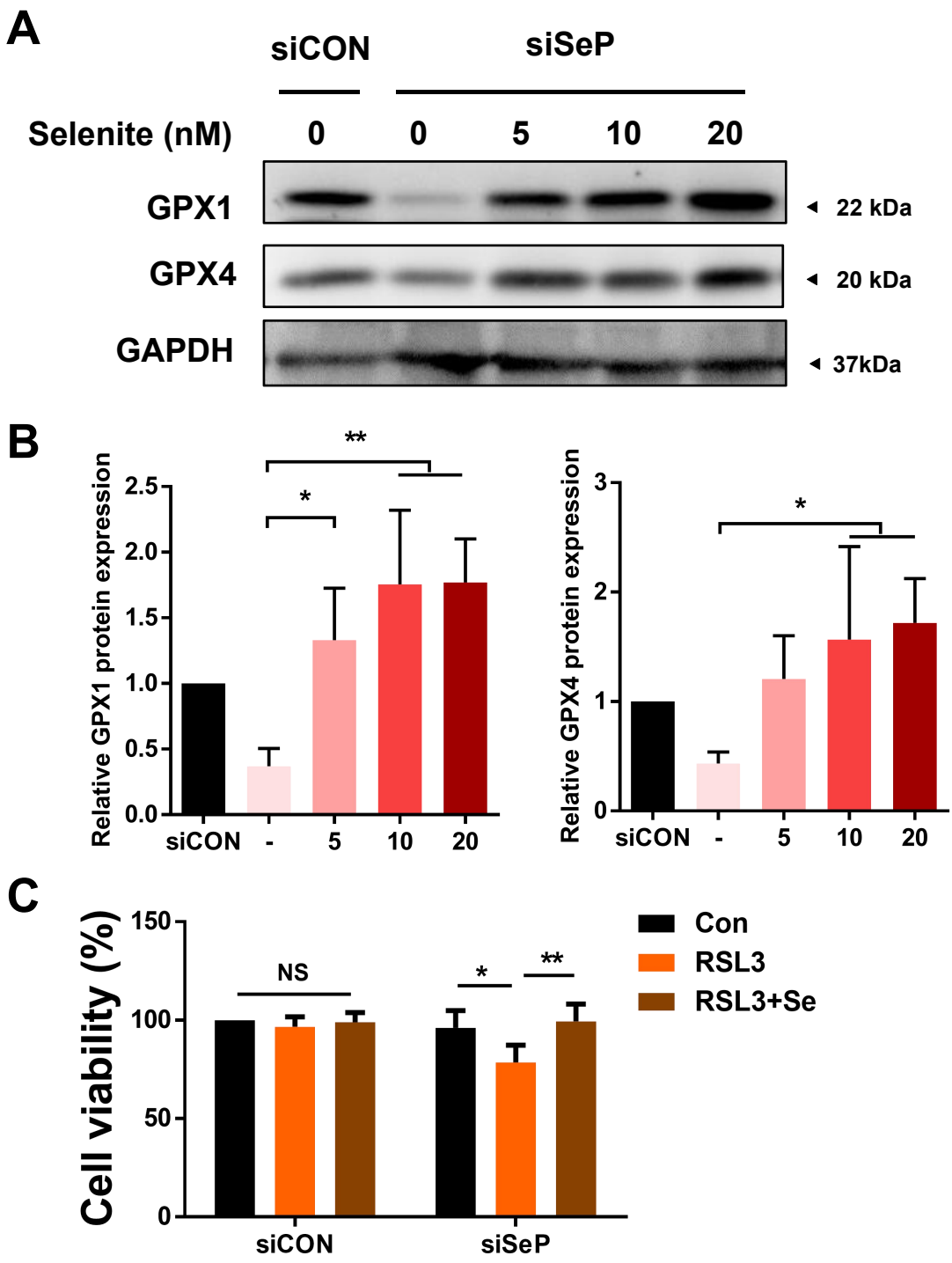


**Figure 6**. **Selenium supplementation rescues sensitivity against RSL3 in SeP siRNA transfected cells.** T98G cells were transfected with siRNA for 24 hours and incubated with the indicated concentration of selenite for an additional 24 hours. The protein was extracted, and GPx levels were detected by Western blot (A). Protein content of each selenoprotein was normalized using GAPDH, and relative expression levels are shown with the control as 1 (B). After SeP was knocked down, RSL3 or selenite 10 nM was added and incubated for 24 hours before cell viability was measured (C). Data are presented as the mean ± S.D. ; n=3. Statistical significance was assessed by Dunnett's test (B)Tukey's HSD(C). *$p < 0.05$, **$p < 0.01$ vs control.

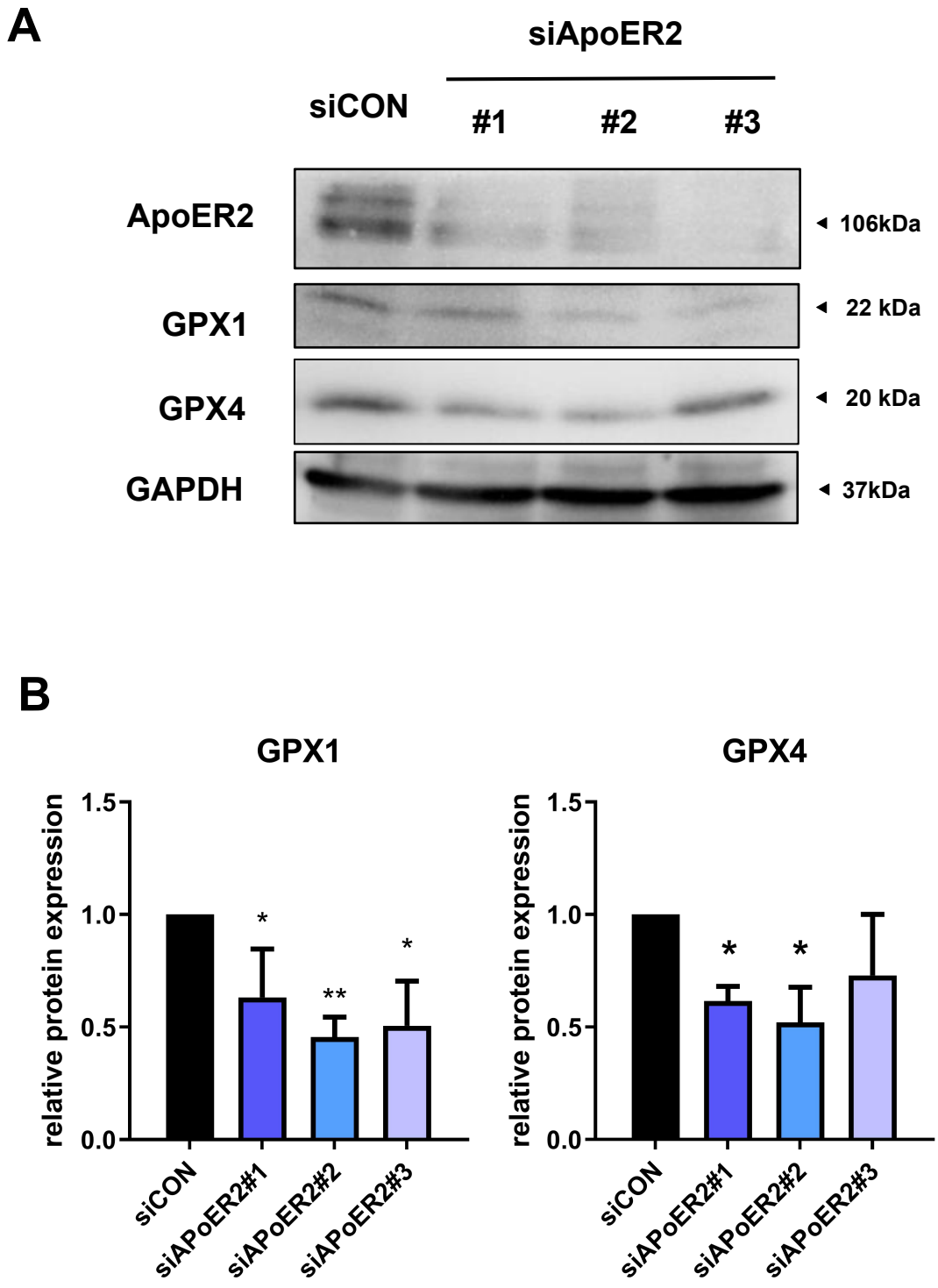


**Figure 7. Inhibition of ApoER2 resulted in a reduced GPX protein.** Cells were transfected with ApoER2 siRNA for 48 hours. Protein expression of selenoproteins (GPx1 and GPx4) were measured by Western blotting (A). Protein content of each selenoprotein was normalized using GAPDH, and relative expression levels are shown with the control as 1 (B), data are shown as mean±S.D.; n=3 . Statistical significance was assessed by the Dunnet's test. *$p < 0.05$, **$p < 0.01$ vs control.

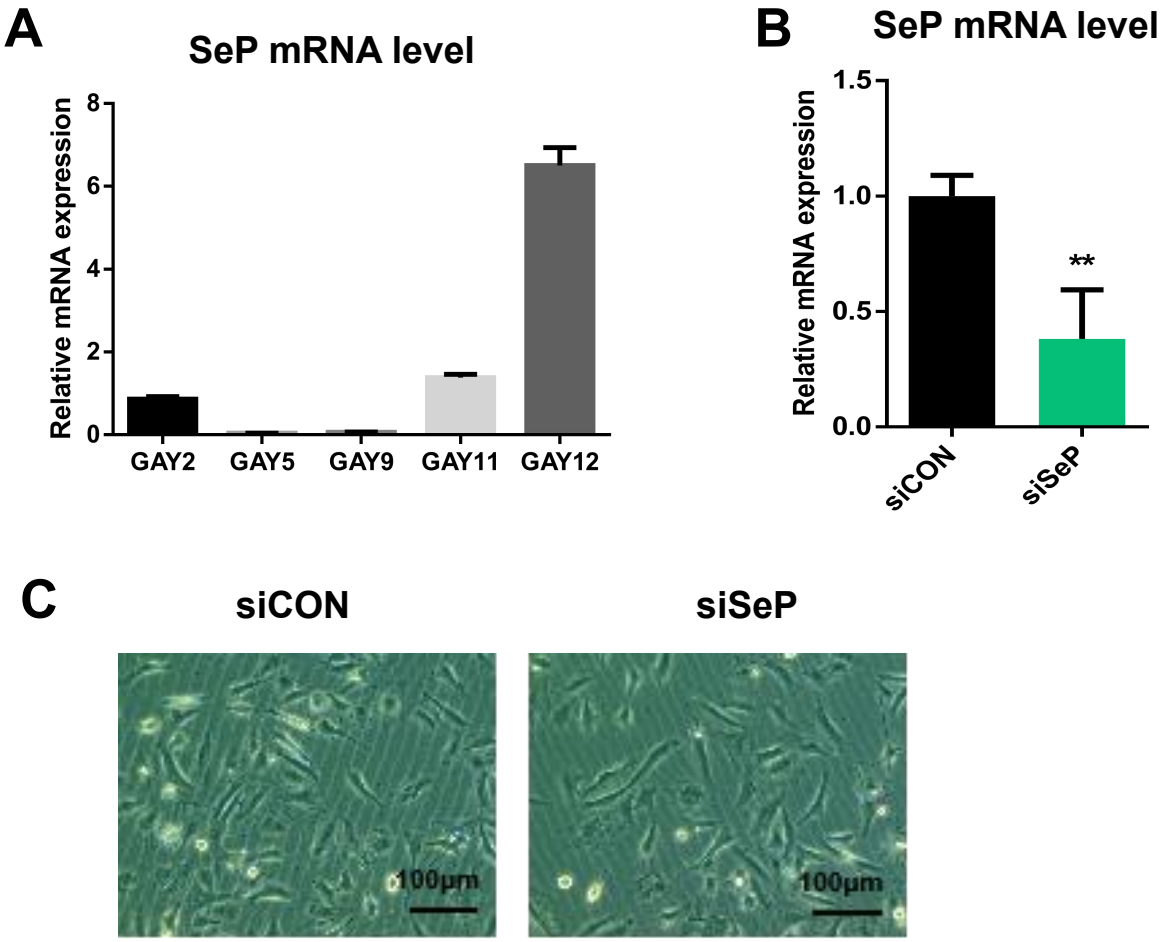


**Figure 8**. **Patient-derived GBM express SeP .** SeP mRNA levels of Patient-derived GBM cells were determined by RT-qPCR(A), GAY12 was transfected with SeP siRNA for 48 hours, and SeP mRNA levels were determined by RT-qPCR (B), and cellular morphology were shown in (C). Data are shown as mean±S.D.; n=3. Statistical significance was assessed by *t*-test (B), $^{**}p < 0.01$ vs control.

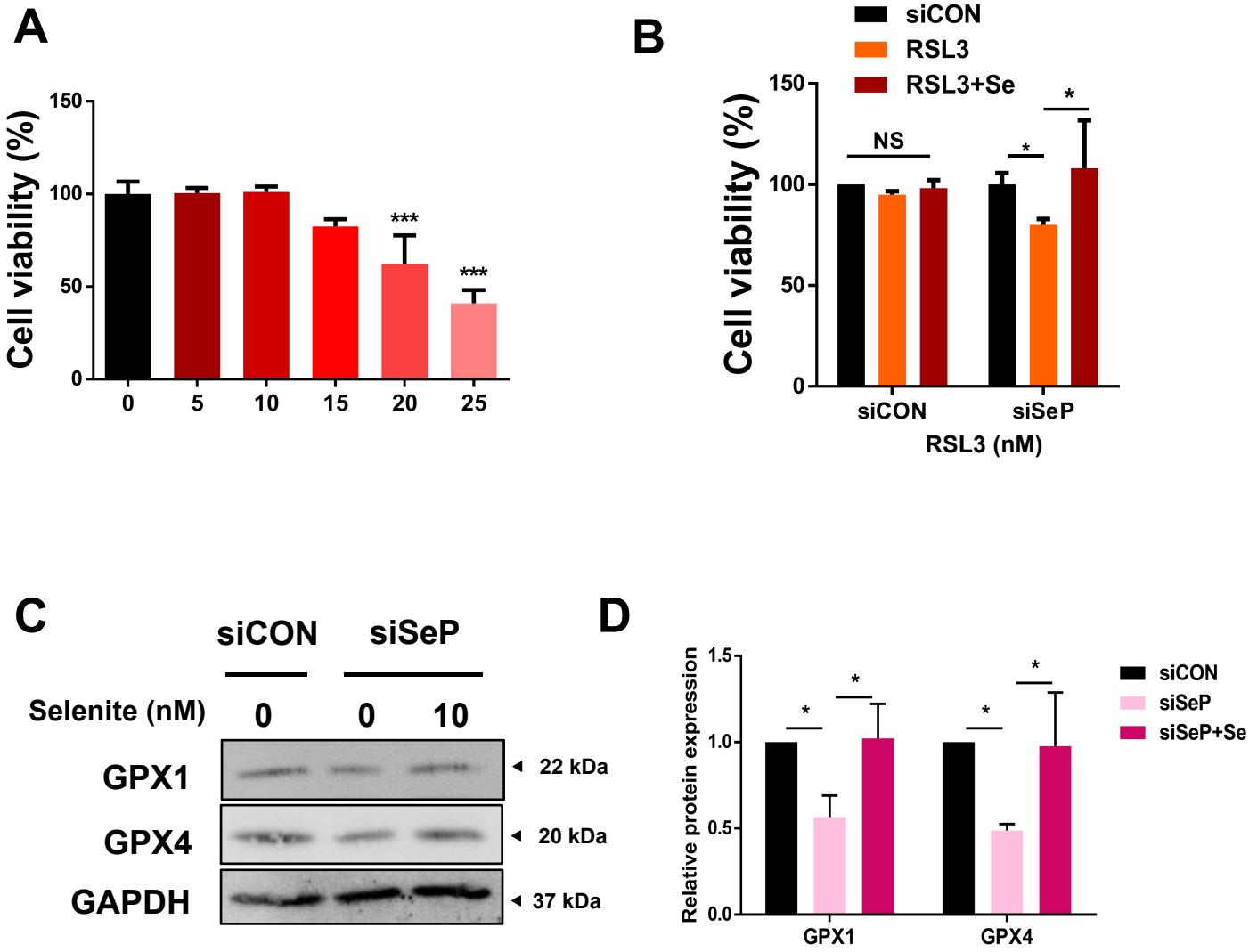


**Figure 9. Patient-derived GBM express SeP and its inhibition enhances RSL3-induced cell death.** The cells were treated with the indicated concentration of RSL3 for 24 hours, and cell viability was determined by alamarBlue assay (A). Cells were transfected with siRNAs against SeP for 24 hours, then treated with 15 nM RSL3 for an additional 24 hours, and cell viability was measured (B). Cells were transfected with SeP siRNA for 48 hours. Protein expression of selenoproteins (GPx1 and GPx4) were measured by Western blotting (C). Protein content of each selenoprotein was normalized using GAPDH, and relative expression levels are shown with the control as 1 (D). Data are shown as mean±S.D.; n=3. Statistical significance was assessed by Dunnet's test (A, D), Tukey's HSD (B). *$p < 0.05$, ***$p < 0.001$ vs control.

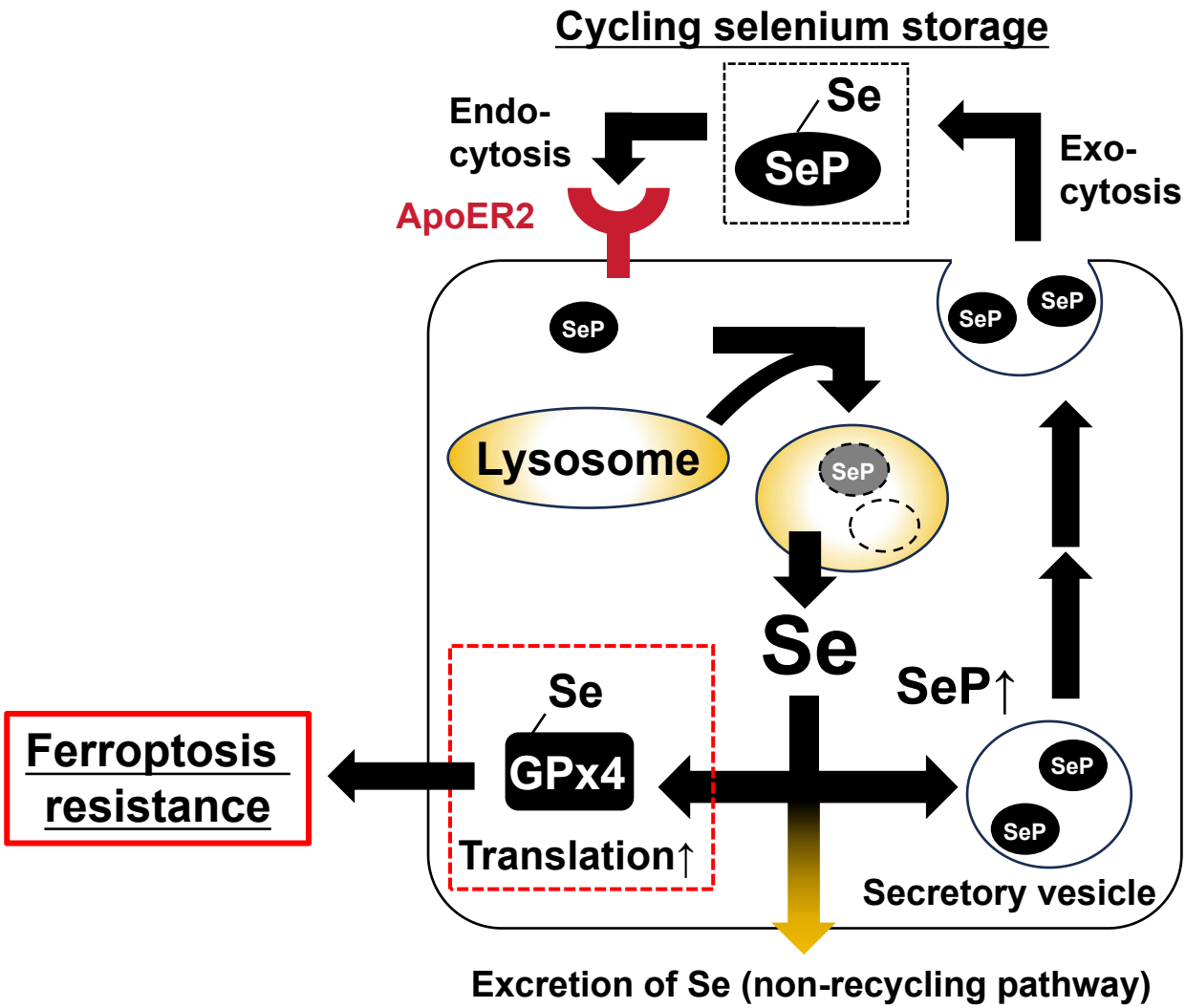


**Figure 10. Scheme of SeP-mediated cycling storage of selenium.**

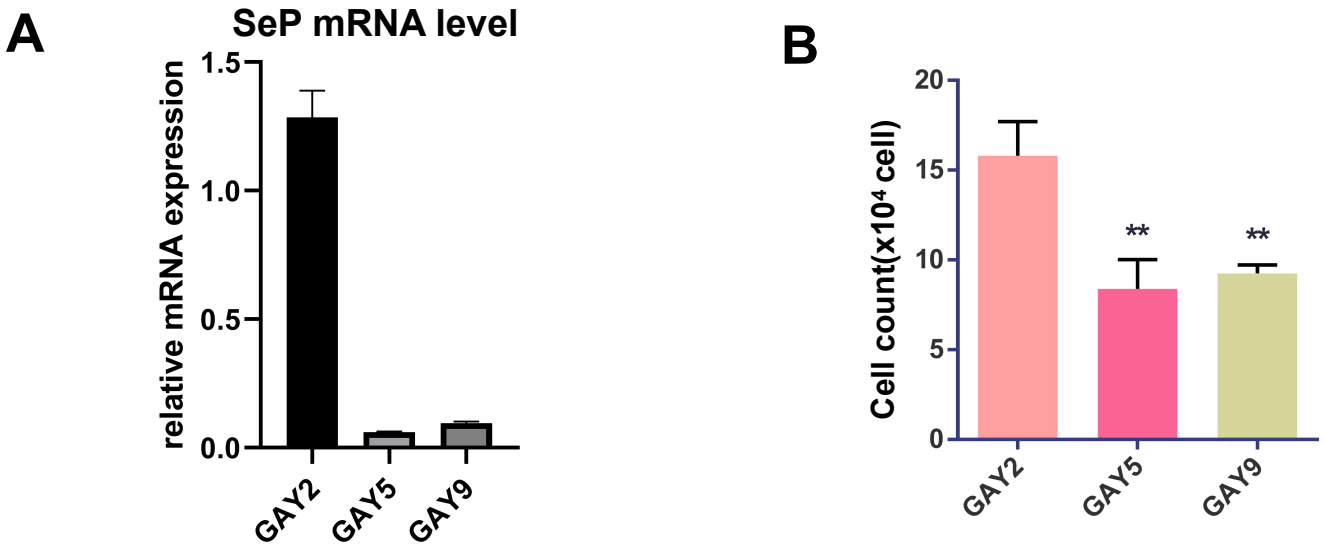


**Figure 11. SeP expression and proliferation rate are correlated.** RT-qPCR was used to detect SeP mRNA in cells(A). .Cells were cultured for 72 hrs and cell counting was performed (B). data are shown as mean±S.D.; n=3 . Statistical significance was assessed by the Dunnet's test. *$p < 0.05$, **$p < 0.01$ vs control.

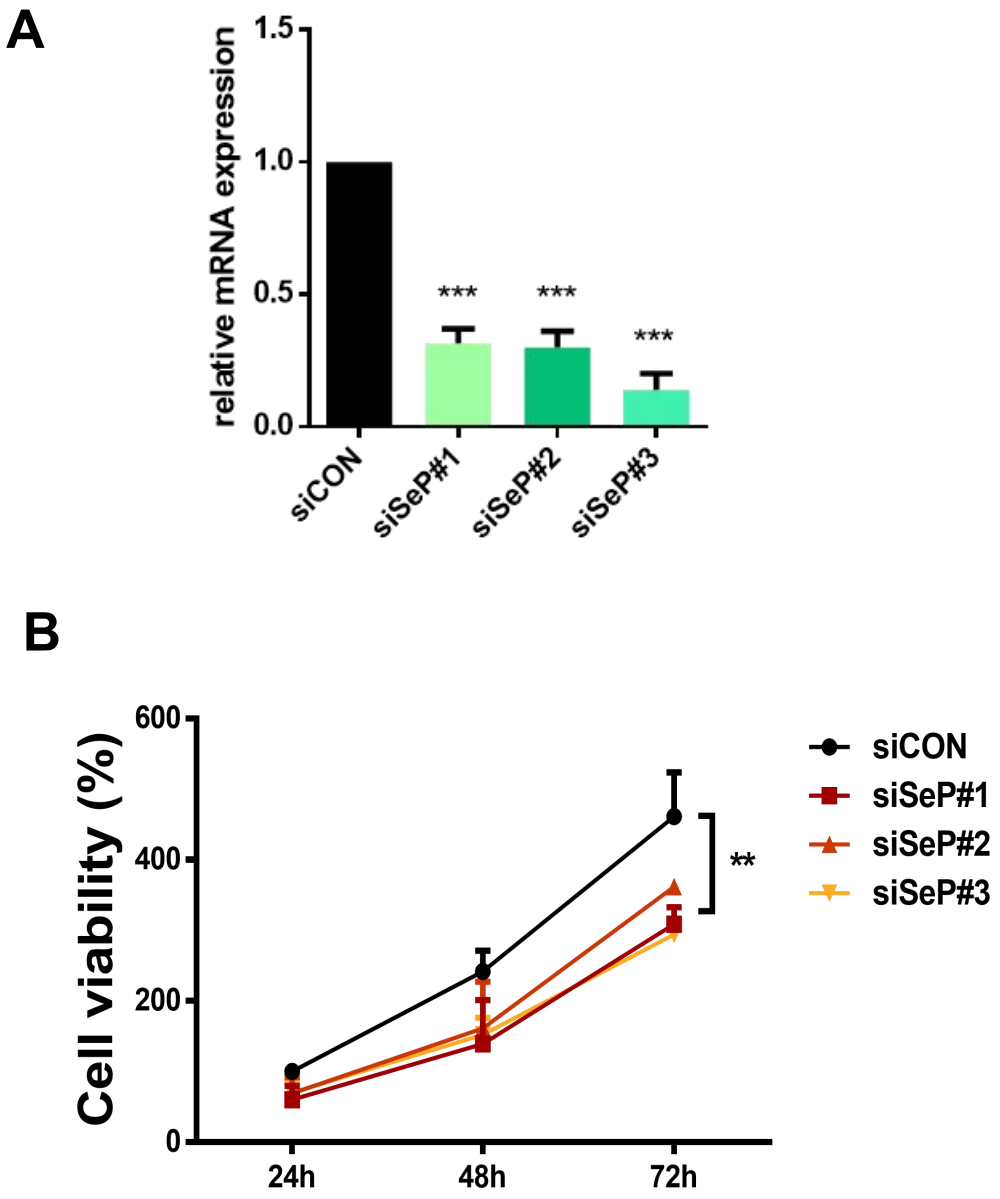


**Figure 12**. **SeP KD Decreased T98G cell proliferation.** The cells were treated with SeP siRNA for 48 hours, SeP mRNA levels of each selenoprotein were measured by RT-qPCR (A). Cells were transfected with SeP siRNA for 24 hours, cultured for 72 hrs and cell viability was determined by alamarBlue assay (B). Data are shown as mean±S.D.; n=3. Statistical significance was assessed by Dunnet's test (A), Tukey's HSD (B). $^{**}p < 0.01$, $^{***}p < 0.001$ vs control.

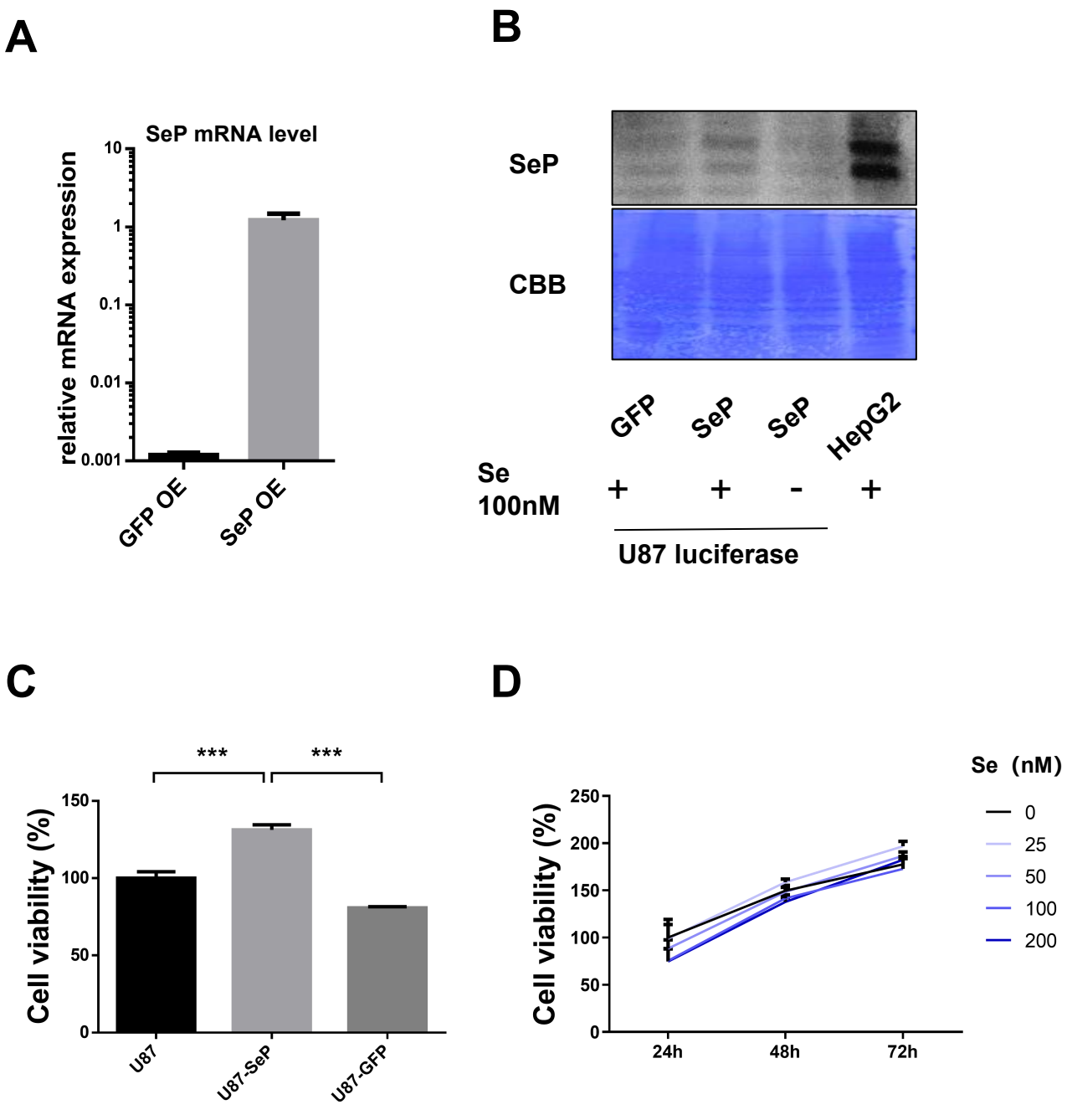


**Figure 13**. **SeP OE increased U87 proliferation.** Viral transfection was used on U87 cells to overexpression of SeP, SeP mRNA levels were measured by RT-qPCR (A) and protein level was measured by WB (B). then cultured for 72 hrs and perform cell count(C). After adding the indicated concentration of selenite to A172 cells, they were cultured for 72 hours, and cell viability was measured using alamarblue(D). Data are shown as mean±S.D.; n=3. Statistical significance was assessed by Dunnet's test (C), ***$p < 0.001$ vs control.

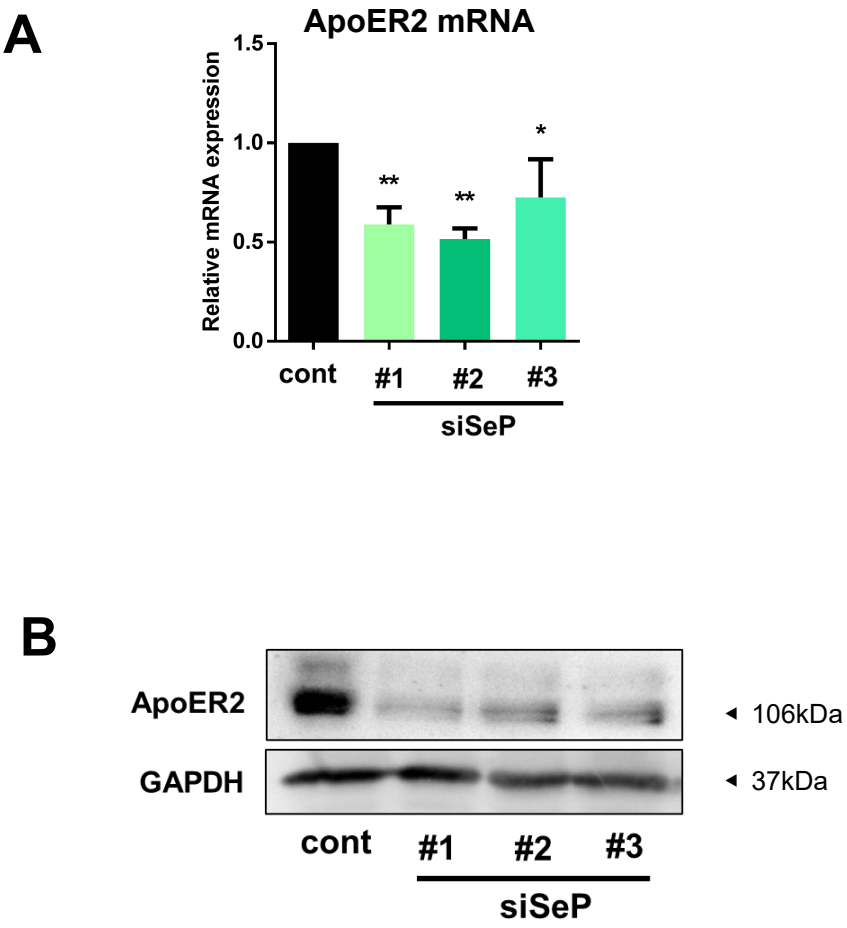


**Figure 14**. **SeP KD resulted in a reduced ApoER2.** T98G cells were transfected with SeP siRNA for 48 hours, ApoER2 mRNA levels were measured by RT-qPCR (A) and protein level was measured by WB (B). Data are shown as mean±S.D. n=3. Statistical significance was assessed by Dunnet's test (A). *$p < 0.05$, **$p < 0.01$ vs control.

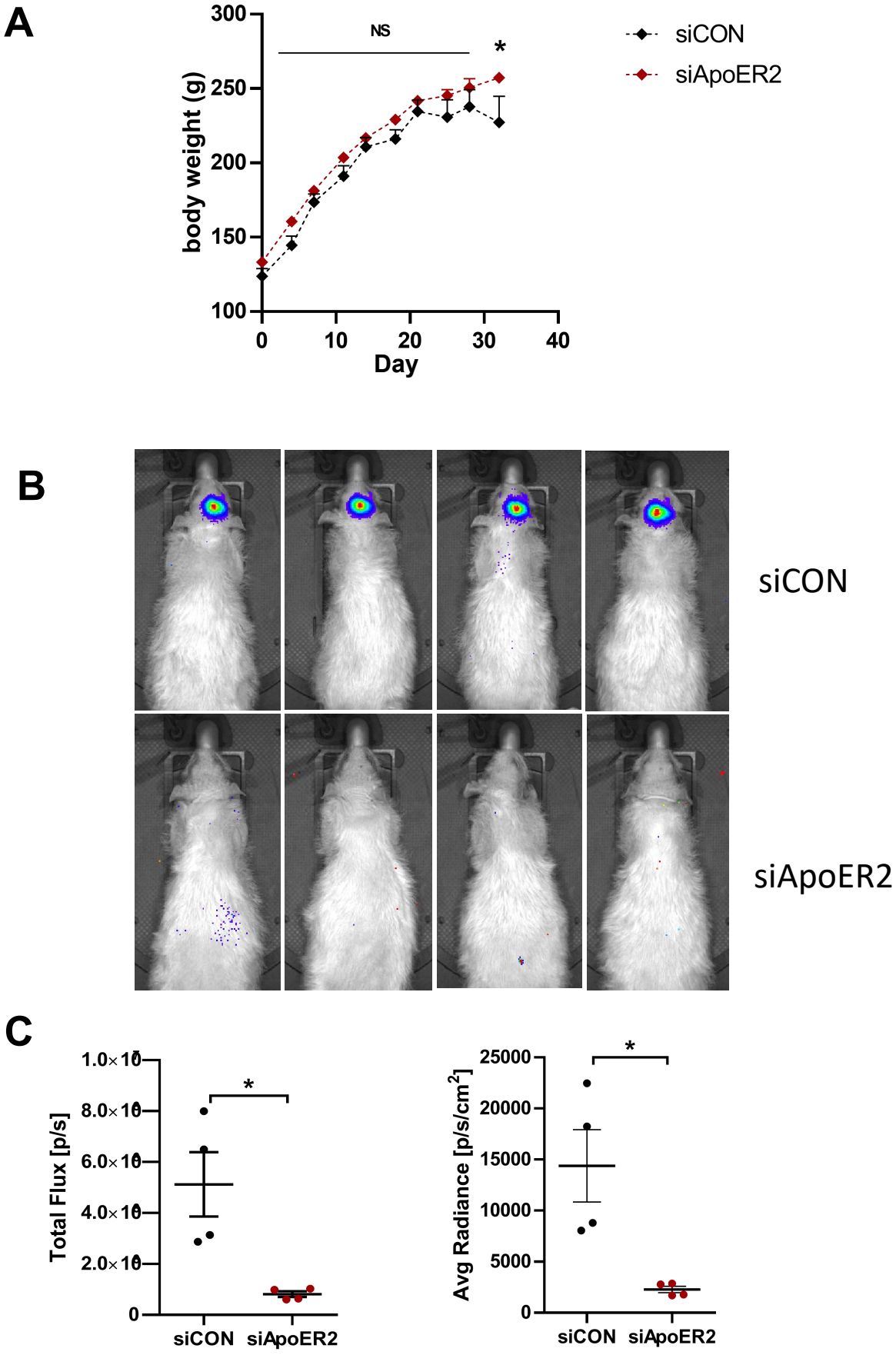


**Figure 15. ApoER2 affects GBM proliferation in vivo**

Ten nude rats were randomly divided into two groups, 1.siCON and 2.siApoER2. U87 luciferase cell siRNA treatment 48h. 200000 cells injected into rat ventricles. After 32 days, Cycluc1 1.4 mg/kg was injected intraperitoneally, and fluorescence intensity was measured.

Representative graph of fluorescence intensity in rats(A) . Body weight after orthotopic Transplant (B). Total and mean fluorescence intensity in rat brain(C).Data are shown as mean±SEM.; n=4. Statistical significance was assessed by *t*-test (C), $*p < 0.05$ vs control.

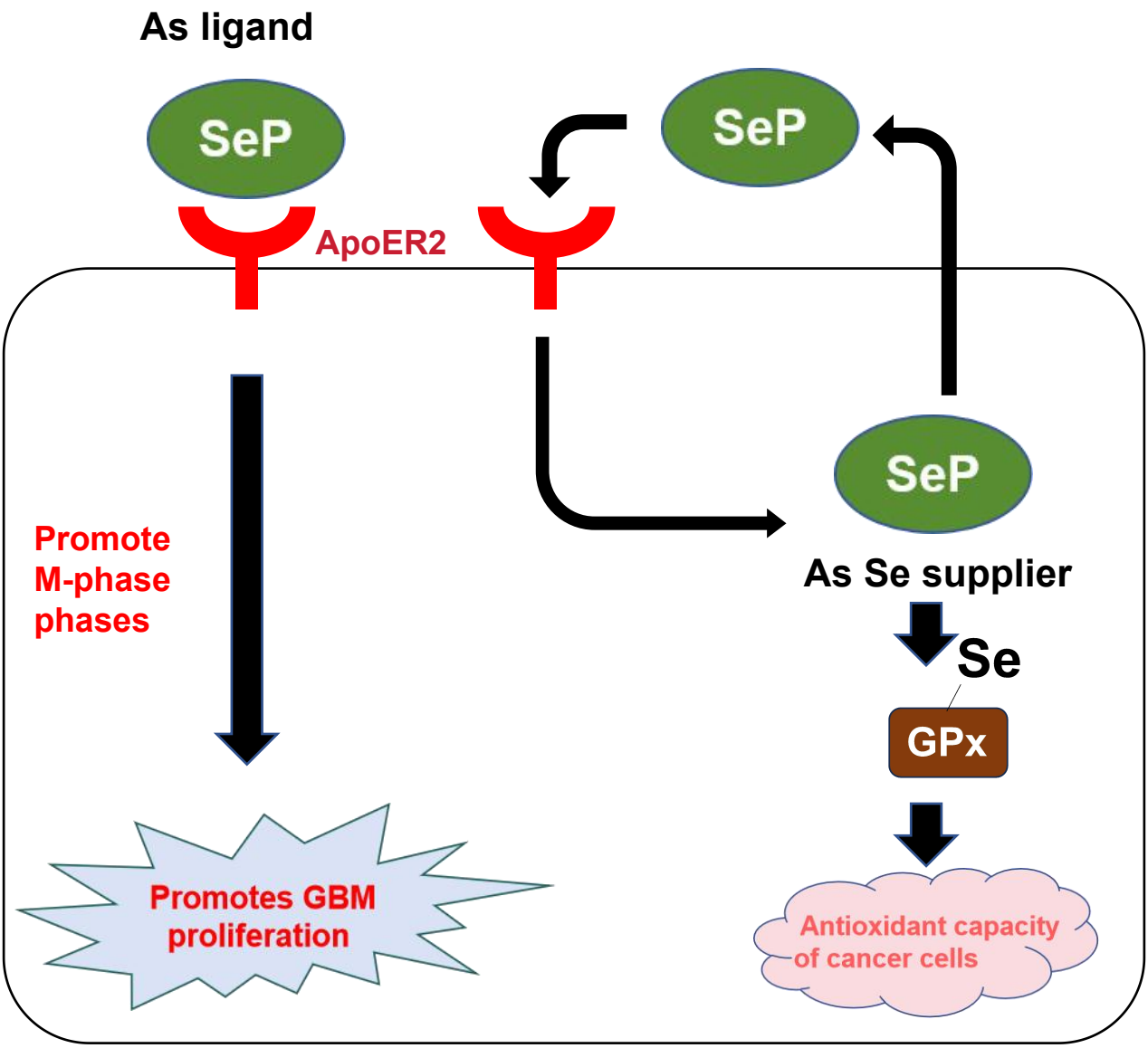


**Figure 16. SeP improves GBM resistance by regulating GPX expression and promotes GBM proliferation through ApoER2.**

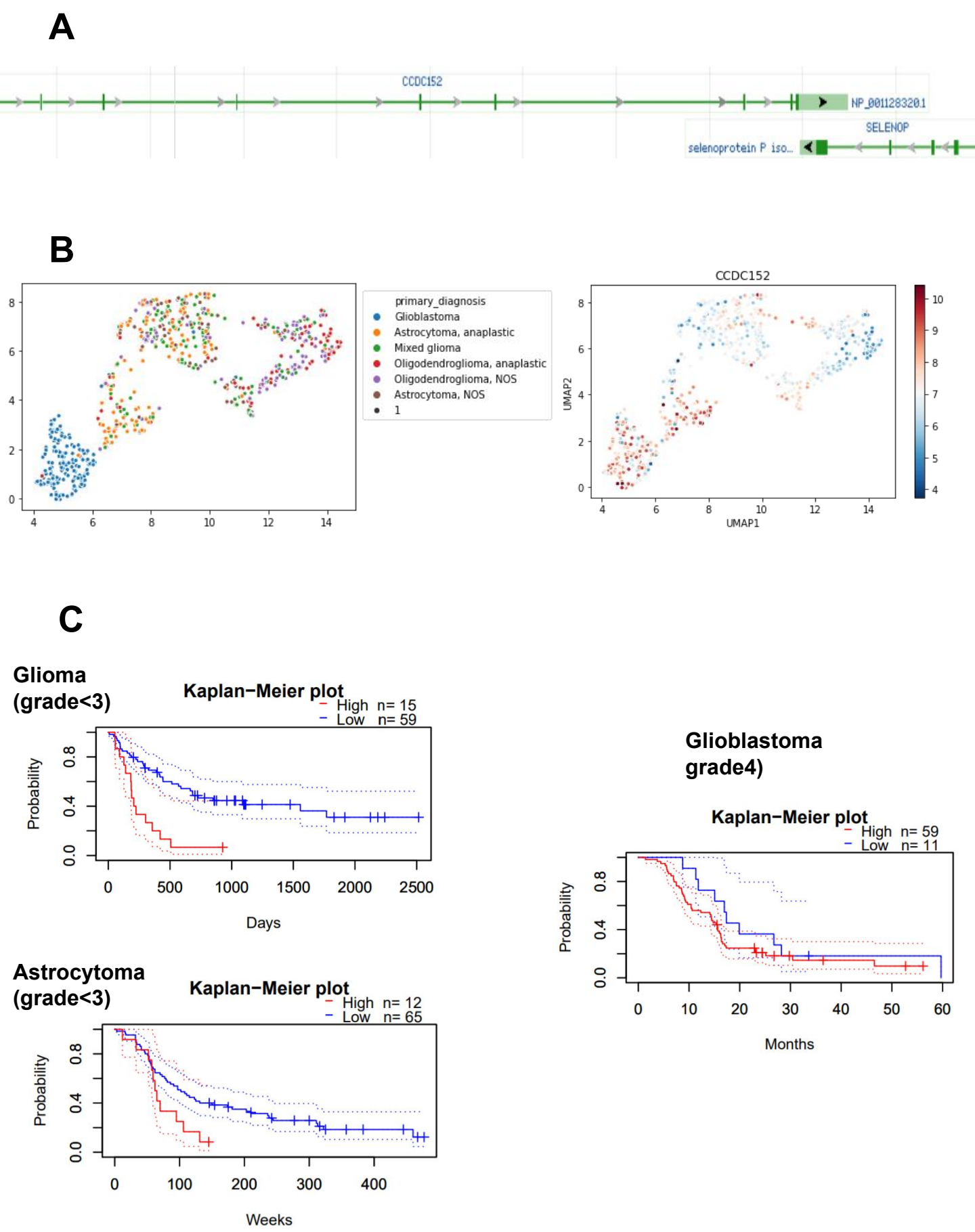


**Figure 17. CCDC152 was associated with patient prognosis.** Schematic diagram of the sequence of SELENOP and the CCDC152 gene. The exons of each gene are shown in bold(A). TCGA database retrieval of gene expression patterns of various gliomas and their CCDC152 expression.(B). the association between patient CCDC152 expression and prognosis was obtained from the prognoscan database (C),

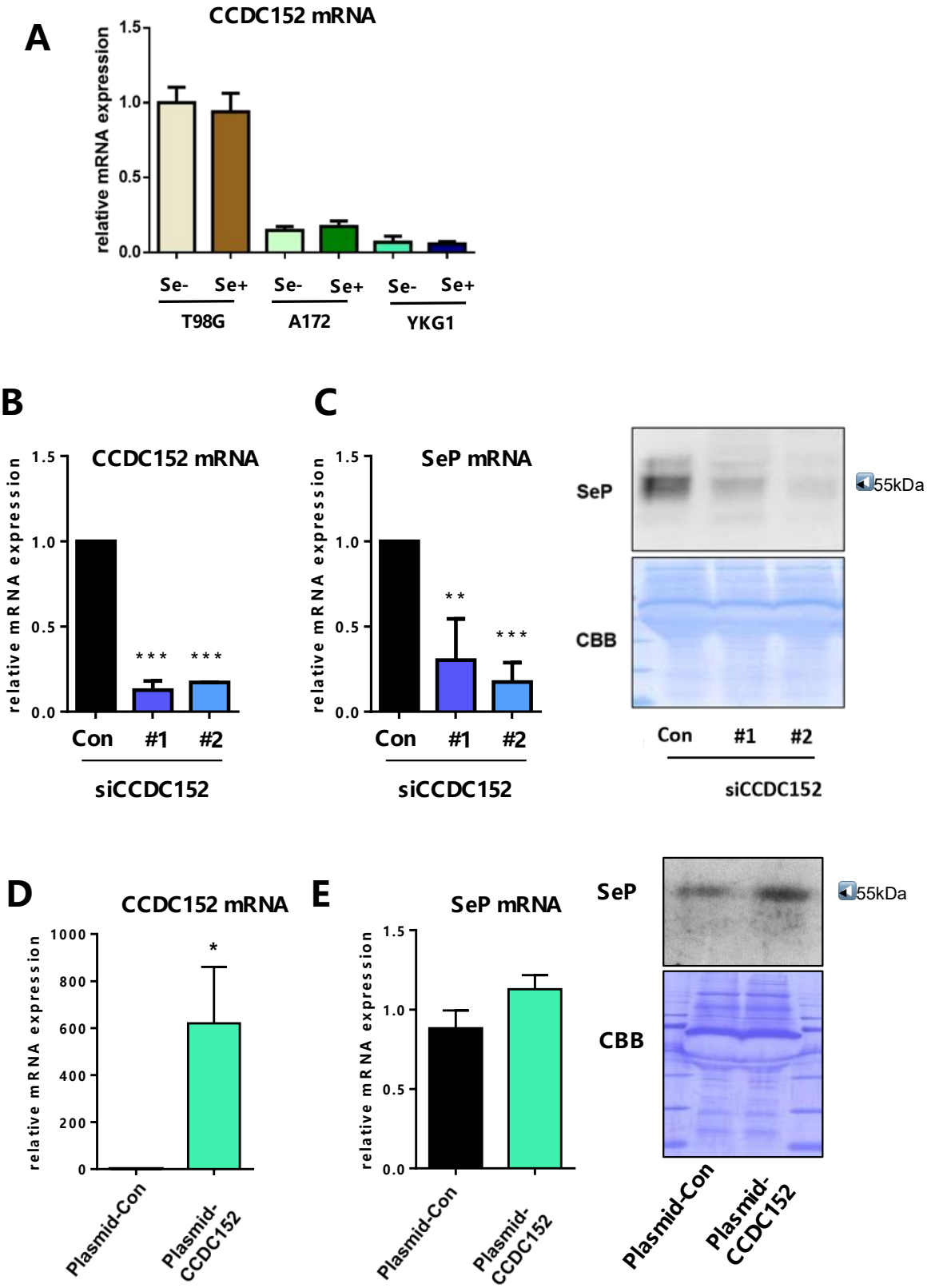


**Figure 18. CCDC152 regulates SeP expression in T98G cells.** mRNA expression of CCDC152 was detected by RT-qPCR (A), T98G cells were transfected with CCDC152 siRNA for 48 hours, CCDC152 mRNA levels were measured by RT-qPCR (B), SeP mRNA levels were measured by RT-qPCR and protein level was measured by WB (C). YKG1 cells were transfected with CCDC152 plasmid for 24 hours, CCDC152 mRNA levels were measured by RT-qPCR (D), SeP mRNA levels were measured by RT-qPCR and protein level was measured by WB (E). Data are shown as mean ± S.D.; n=3. Statistical significance was assessed by Dunnet's test (BC), *t*-test (D). *$p < 0.05$, **$p < 0.01$, ***$p < 0.001$ vs control.

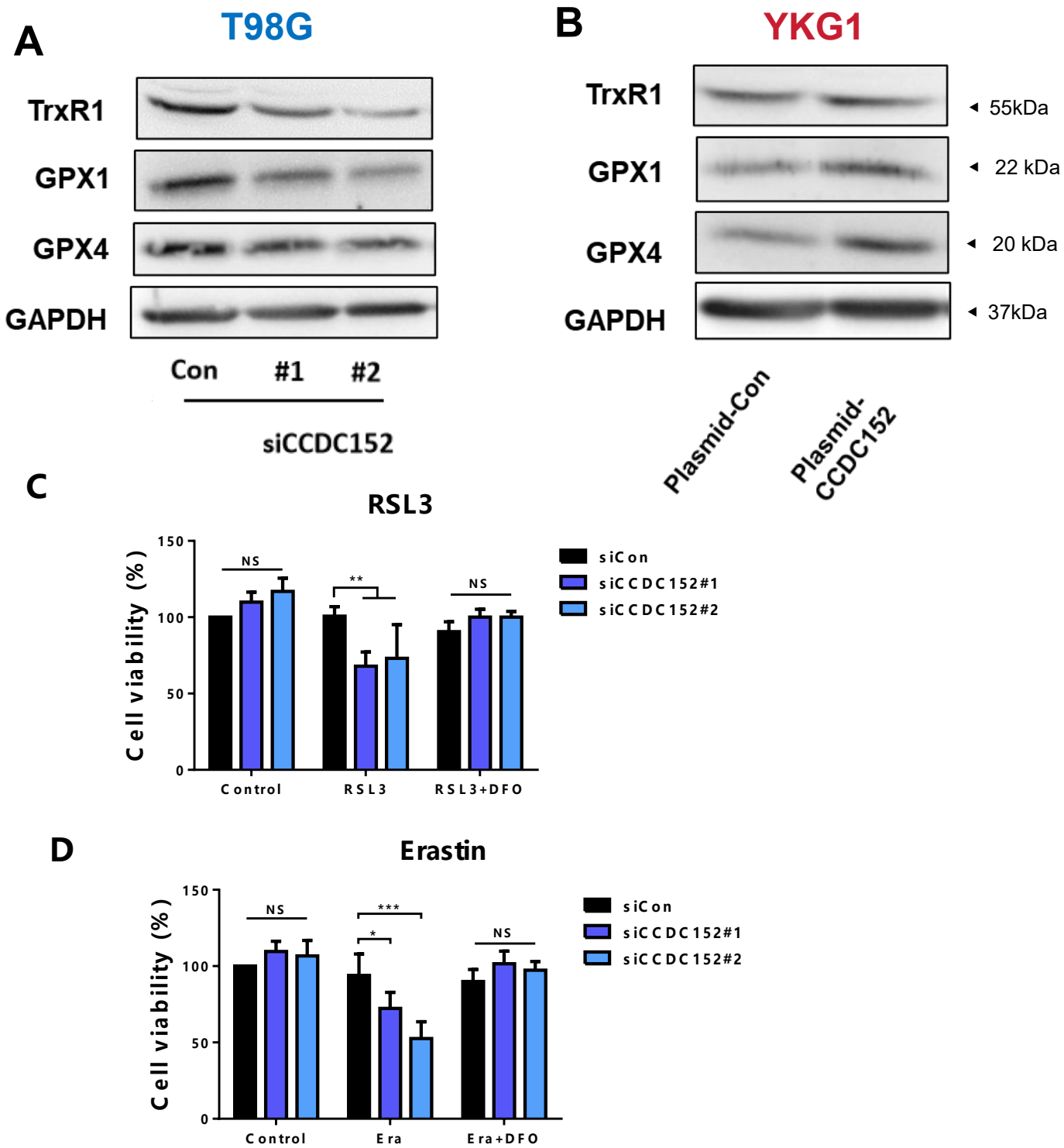


**Figure 19. CCDC152 KD reduce GPX expression and enhances sensitivity against ferroptosis in T98G cells.** T98G cells were transfected with CCDC152 siRNA for 48 hours, selenoprotein level was measured by WB (A). Cells were transfected with siRNAs against SeP for 24 hours, the ferroptosis inducers RSL3 (10 nM) and Erastin (1 μM) and the ferroptosis inhibitor Deferoxamin (50 μM) were administered to them, and cell activity was detected after 24 h(CD), Data are shown as mean±S.D.; n=3. Statistical significance was assessed by Tukey's HSD (CD),*$p < 0.05$, **$p < 0.01$, ***$p < 0.001$ vs control.

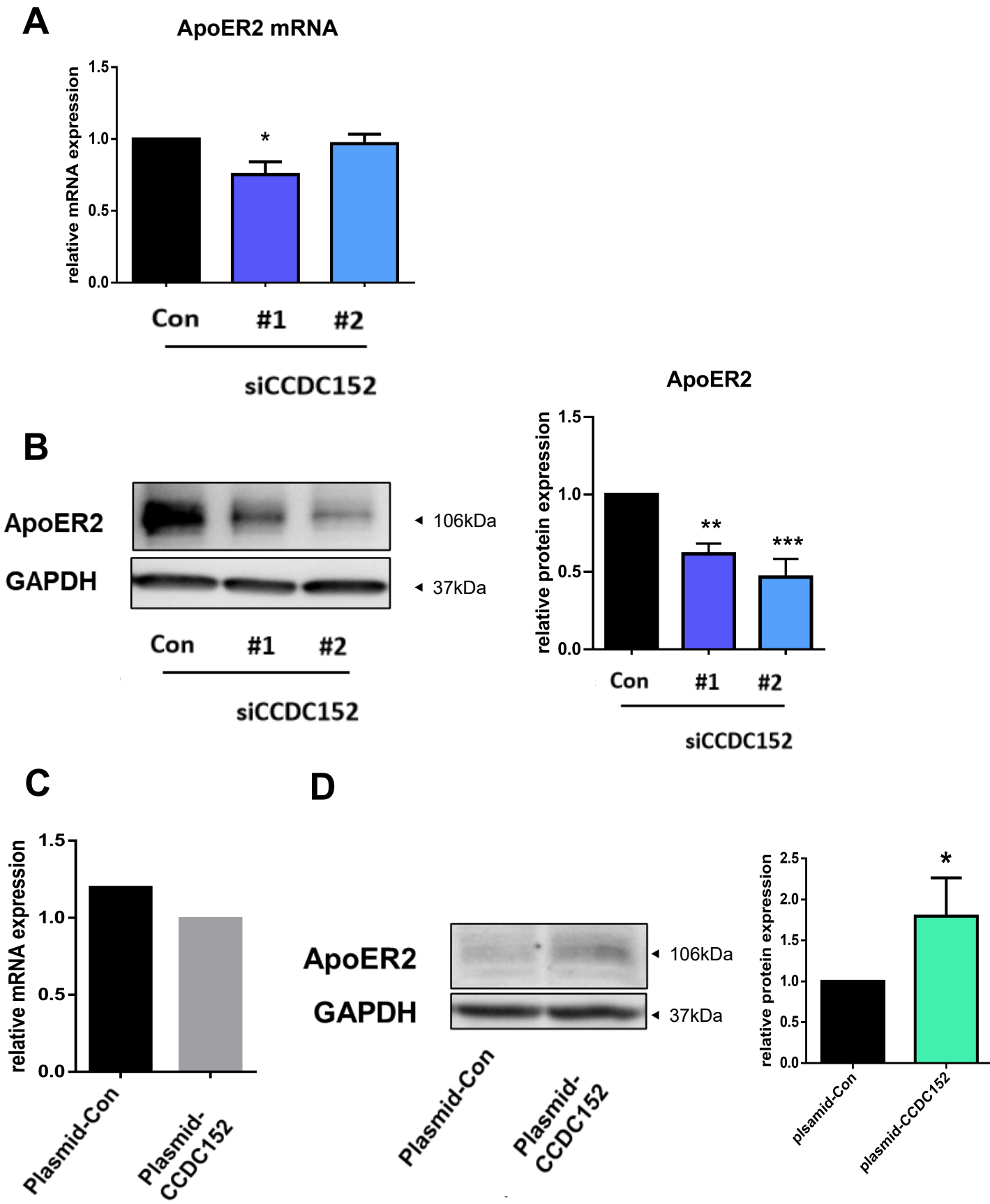


**Figure 20**. **CCDC152 maintain ApoER2.** T98G cells were transfected with CCDC152 siRNA for 48 hours, ApoER2 mRNA levels were measured by RT-qPCR (A) and protein level was measured by WB (B). YKG1 cells were transfected with CCDC152 plasmid for 24 hours, ApoER2 mRNA levels were measured by RT-qPCR (C) and protein level was measured by WB (D). Data are shown as mean±S.D.; n=3. Statistical significance was assessed by Dunnet's test (AB), *t*-test (CD). *$p < 0.05$, **$p < 0.01$, ***$p < 0.001$ vs control.

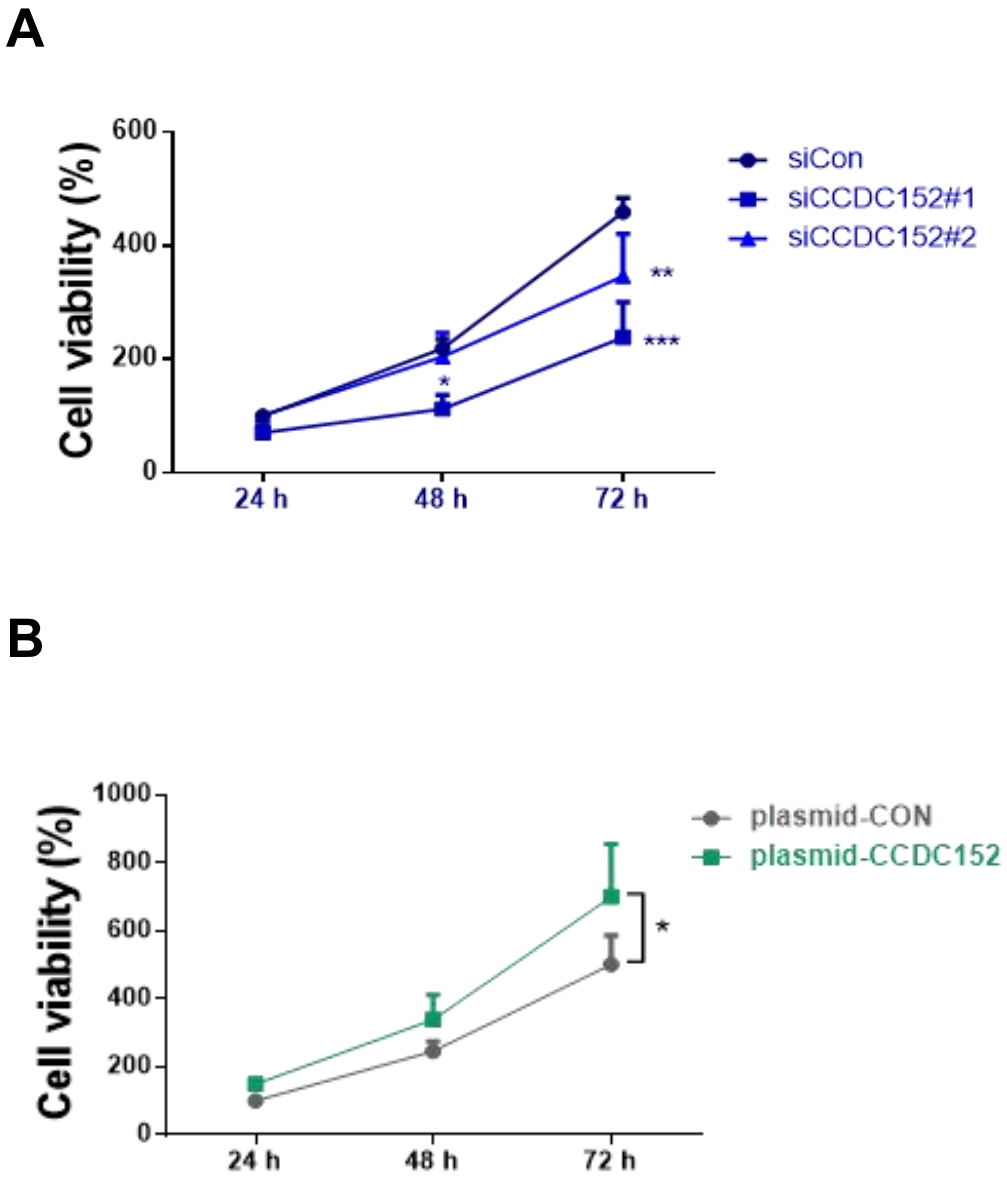


**Figure 21**. **CCDC152 promote proliferation.** The T98G cells were transfected with CCDC152 siRNA for 48 hours, then cultured for 72 hrs and cell viability was determined by alamarBlue assay (A). YJG1 cells were transfected with CCDC152 plasmid for 24 hours, cultured for 72 hrs and cell viability was determined by alamarBlue assay (B). Data are shown as mean±S.D.; n=3. Statistical significance was assessed by Dunnet's test (A), Tukey's HSD (B). *$p < 0.05$,**$p < 0.01$, ***$p < 0.001$ vs control.

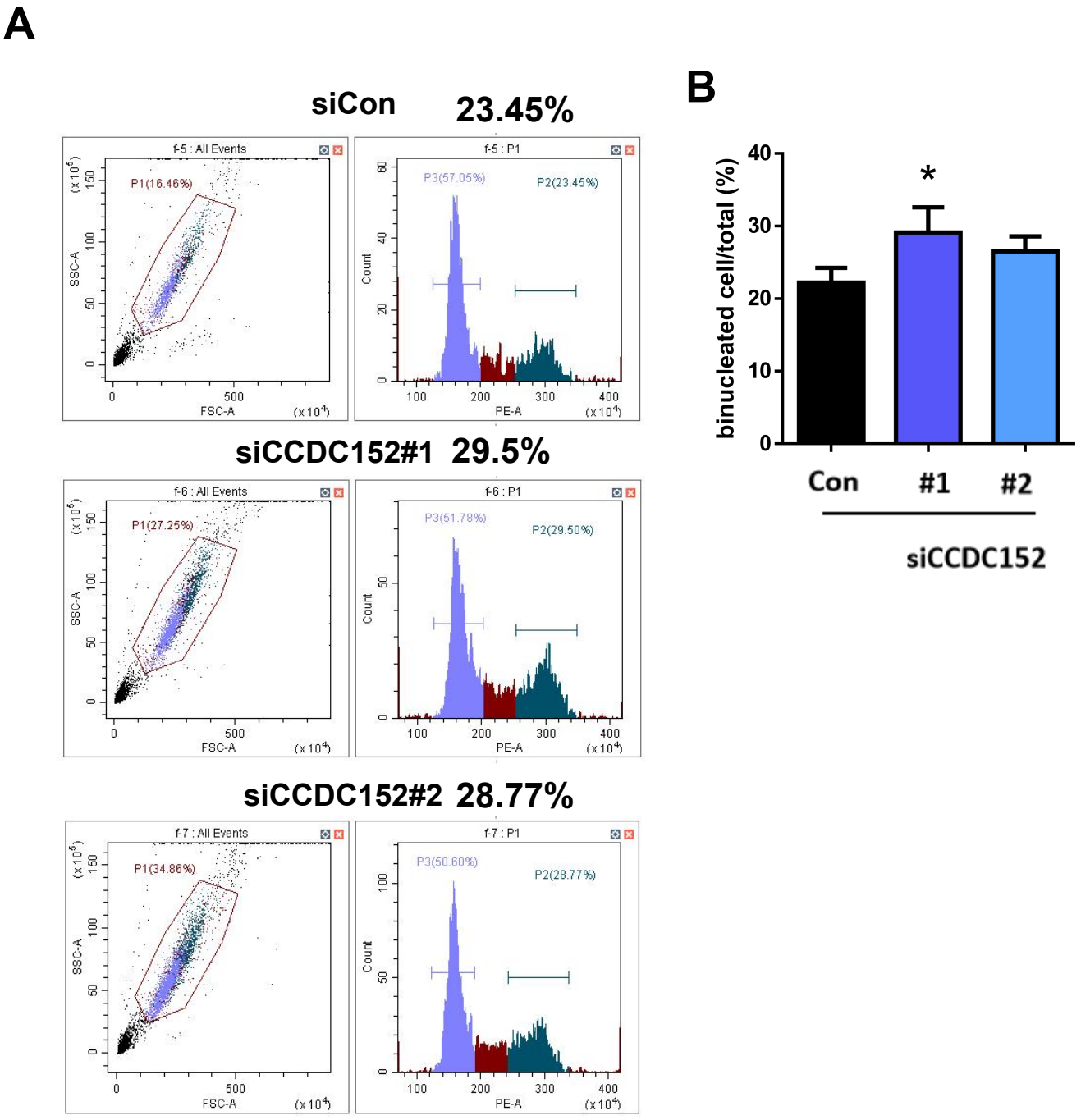


**Figure 22**. **CCDC152 regulates GBM proliferation through the cell cycle.** The T98G cells were transfected with CCDC152 siRNA for 48 hours, After knockdown of CCDC152(AB), flow cytometry was used to detect the cell cycle. Data are shown as mean±S.D.; n=3. Statistical significance was assessed by Dunnet's test (B). *$p < 0.05$ vs control.

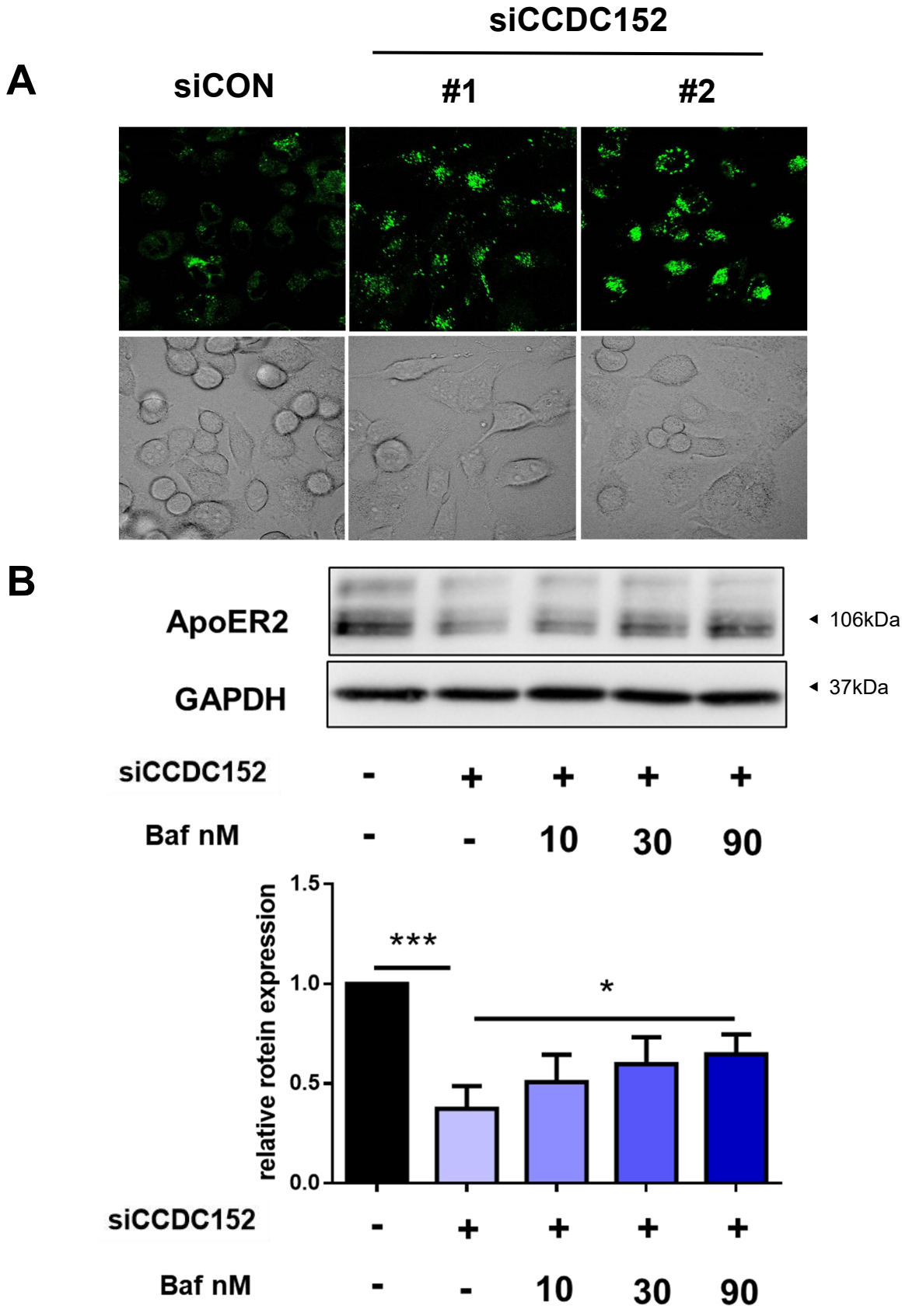


**Figure 23**. **Regulation of ApoER2 protein level by lysosomal catabolism** T98G cells were transfected with CCDC152 siRNA for 48 hours, fluorescence intensity was observed after thirty minutes of treatment with lysotracker 75 nM.(A), T98G cells were transfected with CCDC152 siRNA for 24 hours, The indicated concentrations of bafilomycin were then added and treated for 24h, ApoER2 protein were measured by WB (B). Data are shown as mean±S.D.; n=3. Statistical significance was assessed by Dunnet's test (B), *$p < 0.05$, ***$p < 0.001$ vs control.

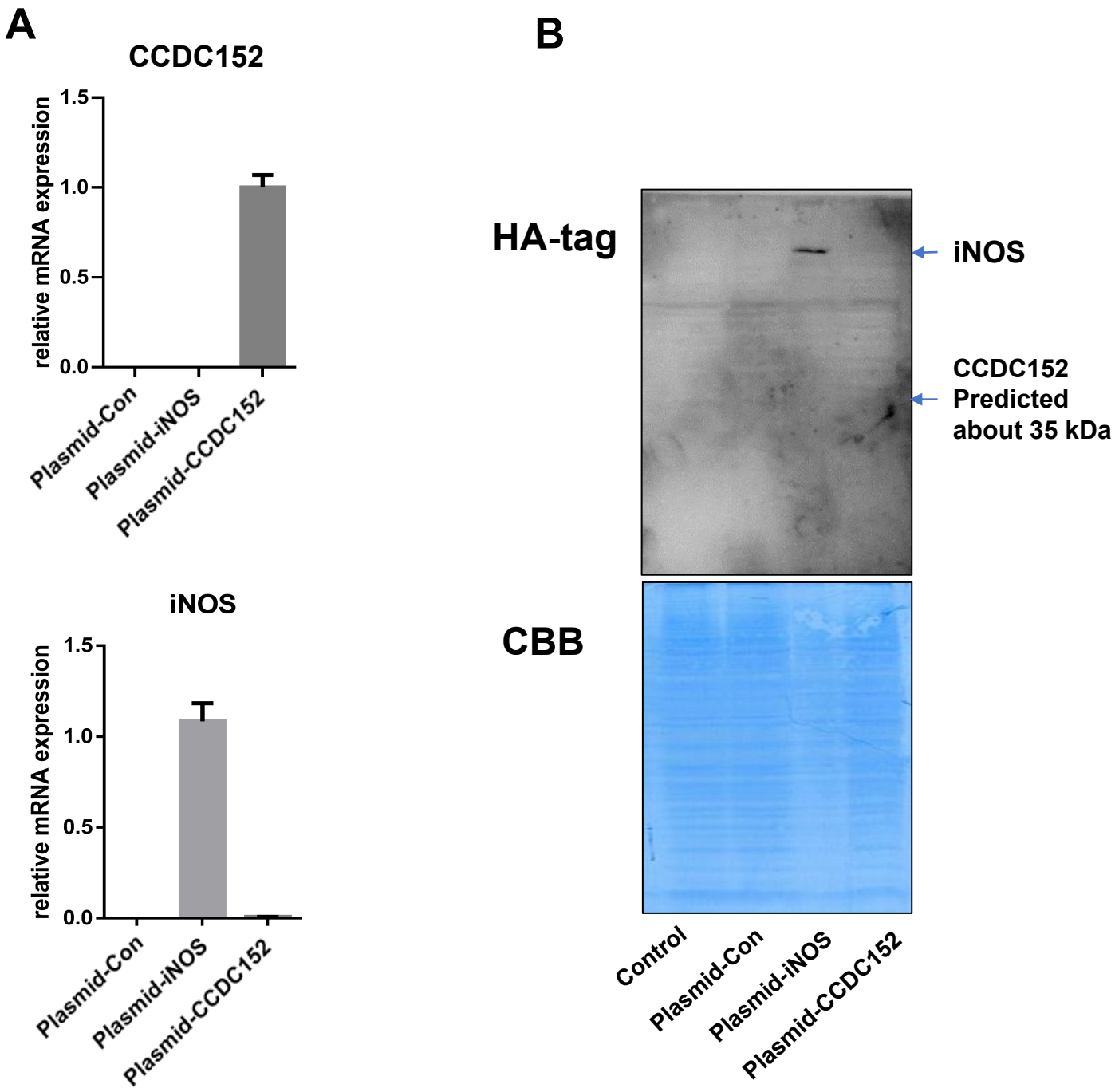


**Figure 24. CCDC152 affects GBM processes as a non-coding RNA.** T98G cells were transfected with HA-tag plasmid for 24 hours, CCDC152 and iNOS mRNA levels were measured by RT-qPCR (A) and HA-tag protein level was measured by WB (B). Data are shown as mean±S.D.

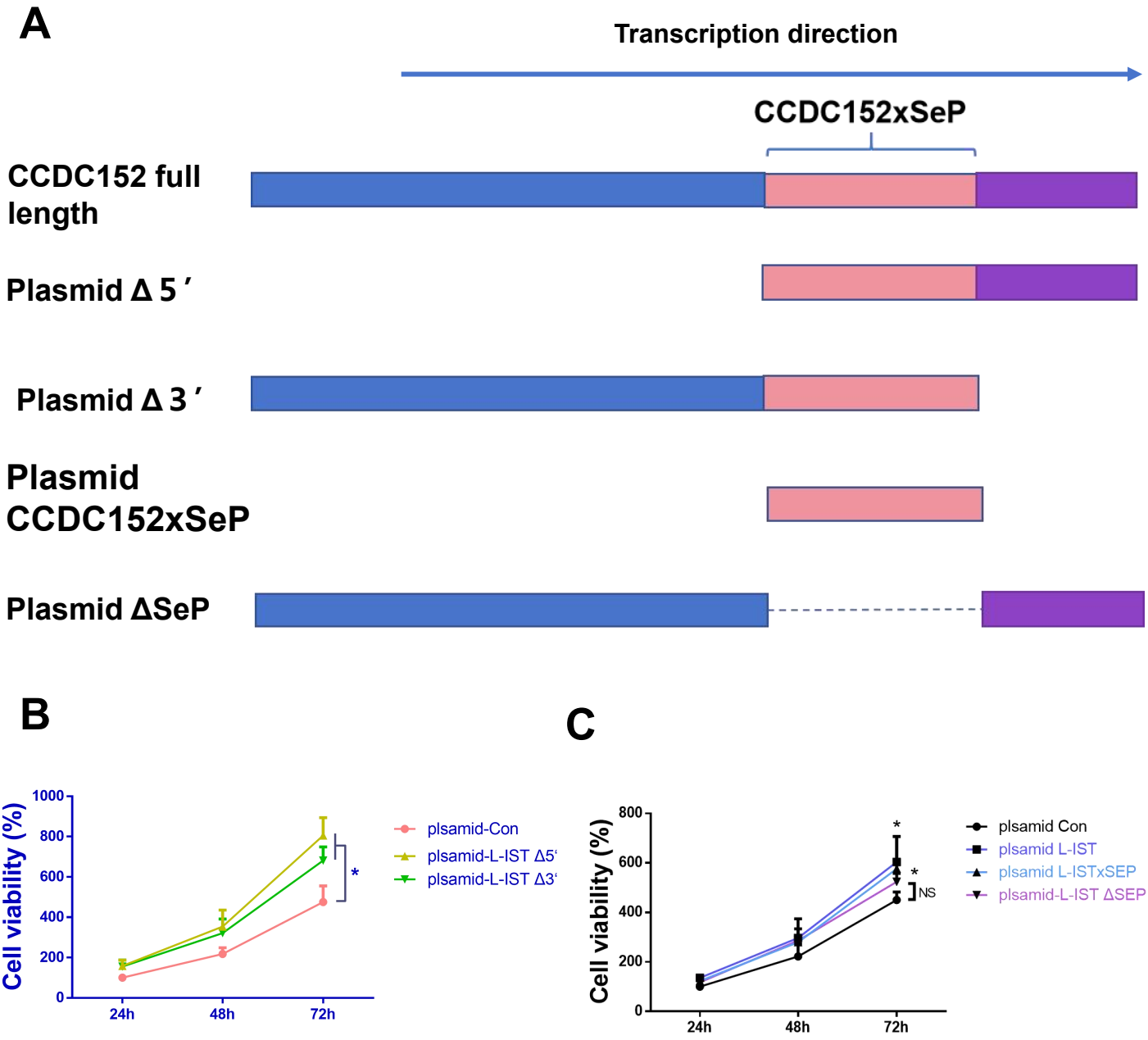


**Figure 25. The sequence on which CCDC152 acts is the part that is complementary to SeP.** Trimming out parts of the CCDC152 plasmid sequence to obtain four partially defective CCDC152 plasmids (A). YKG1 cells were transfected with indicated CCDC152 plasmid for 24 hours, cultured for 72 hrs and cell viability was determined by alamarBlue assay (BC). Data are shown as mean±S.D.; n=3. Statistical significance was assessed by , Tukey's HSD (BC). *$p < 0.05$ vs control.

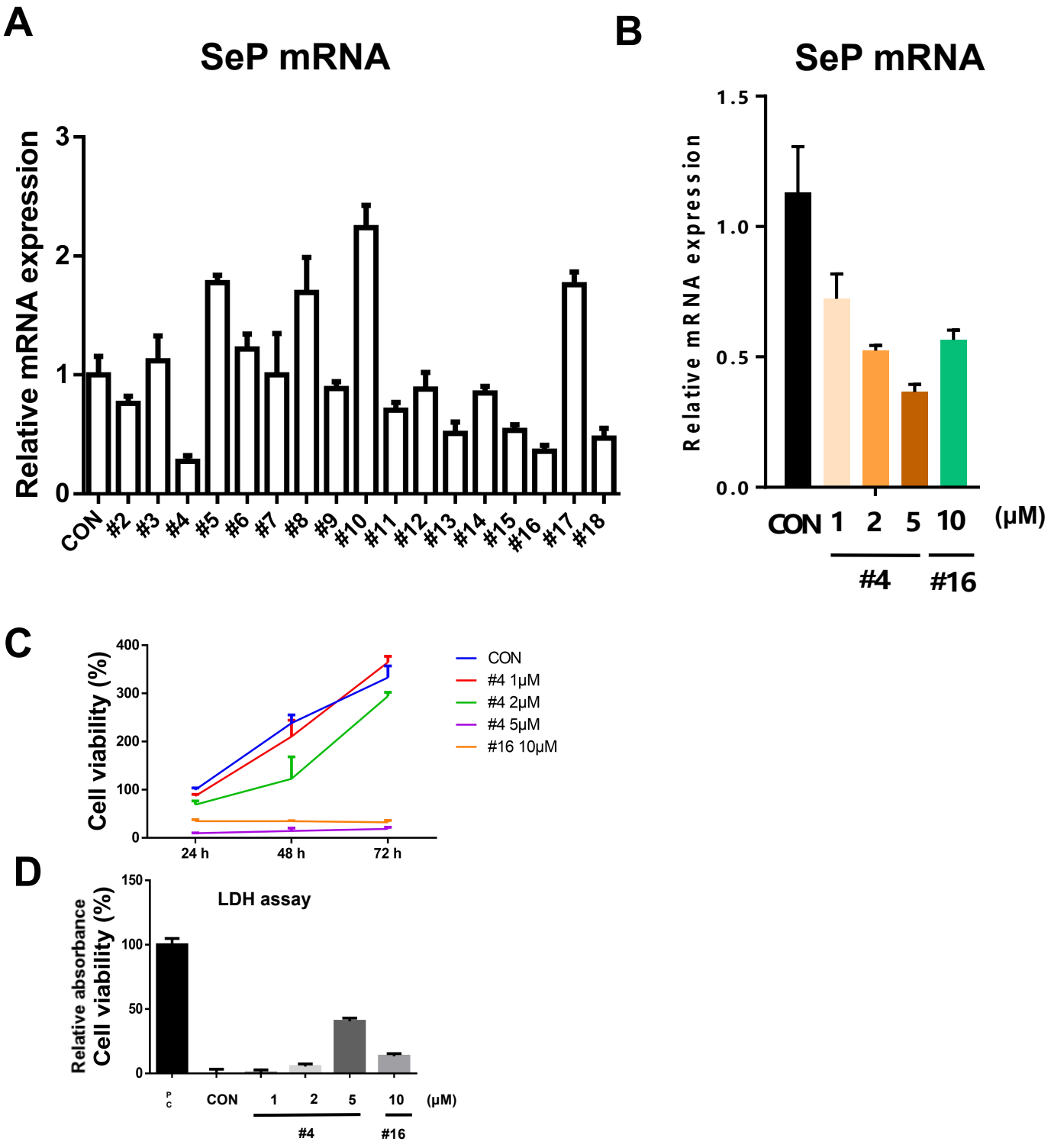


**Figure 26. Candidate compounds that inhibit SeP inhibit T98G proliferation.** T98G cells were treated with indicated compounds 10 μM for 24 hours, SeP mRNA levels were measured by RT-qPCR (A) T98G cells were treated with compounds in indicated concentration for 24 hours, SeP mRNA levels were measured by RT-qPCR (B)，then cultured for 72 hrs and cell viability was determined by alamarBlue assay (C), then cultured for 24 hrs cell death was detected by LDH assay(D). Data are shown as mean±S.D.

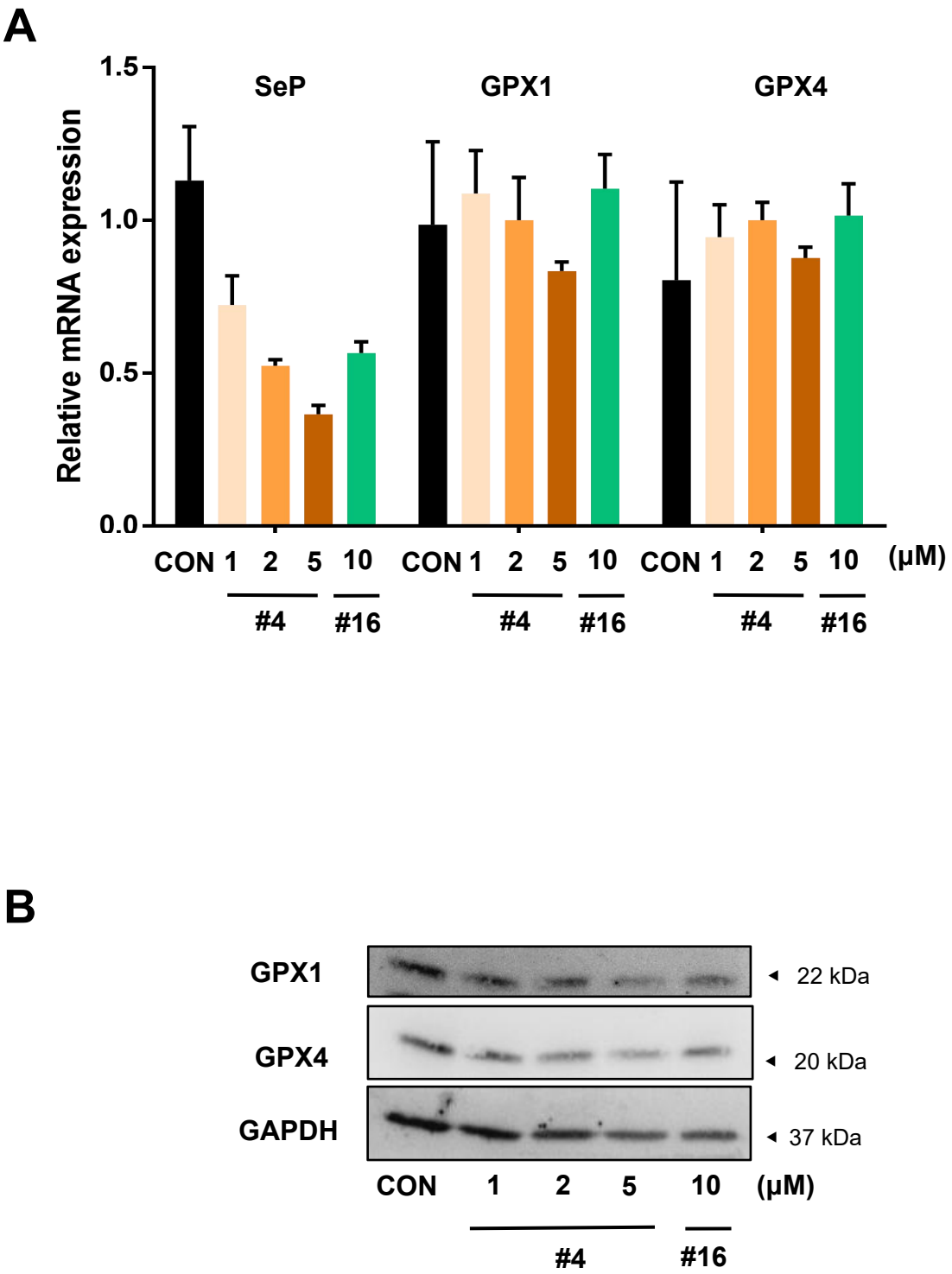


**Figure 27. Candidate compounds that inhibit SeP reduce the GPX protein of T98G.** T98G cells were treated with compounds in indicated concentration for 24 hours, SeP mRNA levels were measured by RT-qPCR (A) GPX protein level was measured by WB (B). Data are shown as mean±S.D.

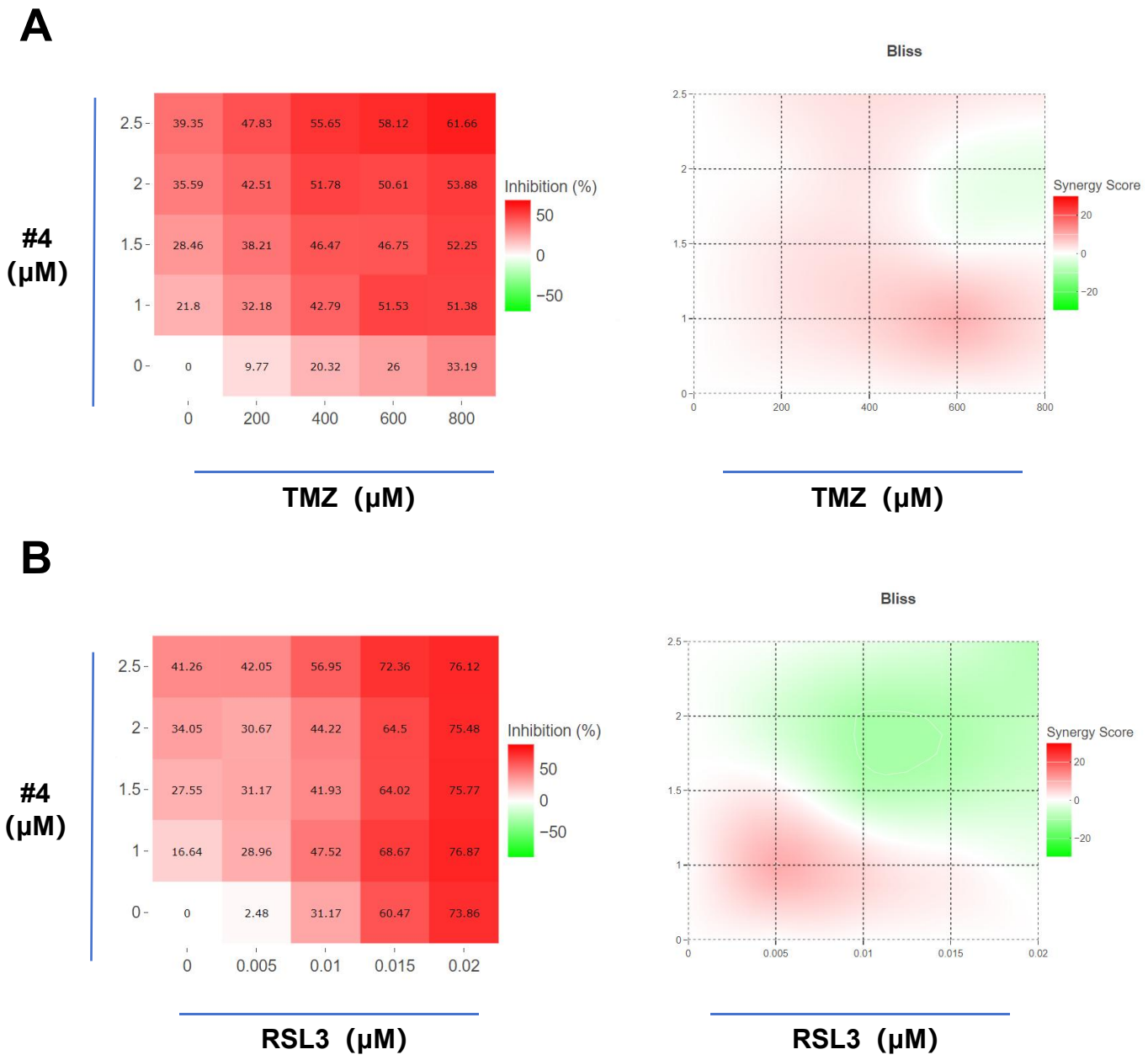


**Figure 28. Candidate compounds that inhibit SeP increase drug sensitivity of T98G.** T98G cells were treated with compound #4 and drugs in indicated concentration for 24 hours, cell viability was determined by alamarBlue assay. Synchronization and antagonism between compound #4 and the drug was analyzed using SynergyFinder (version 3) (AB) .

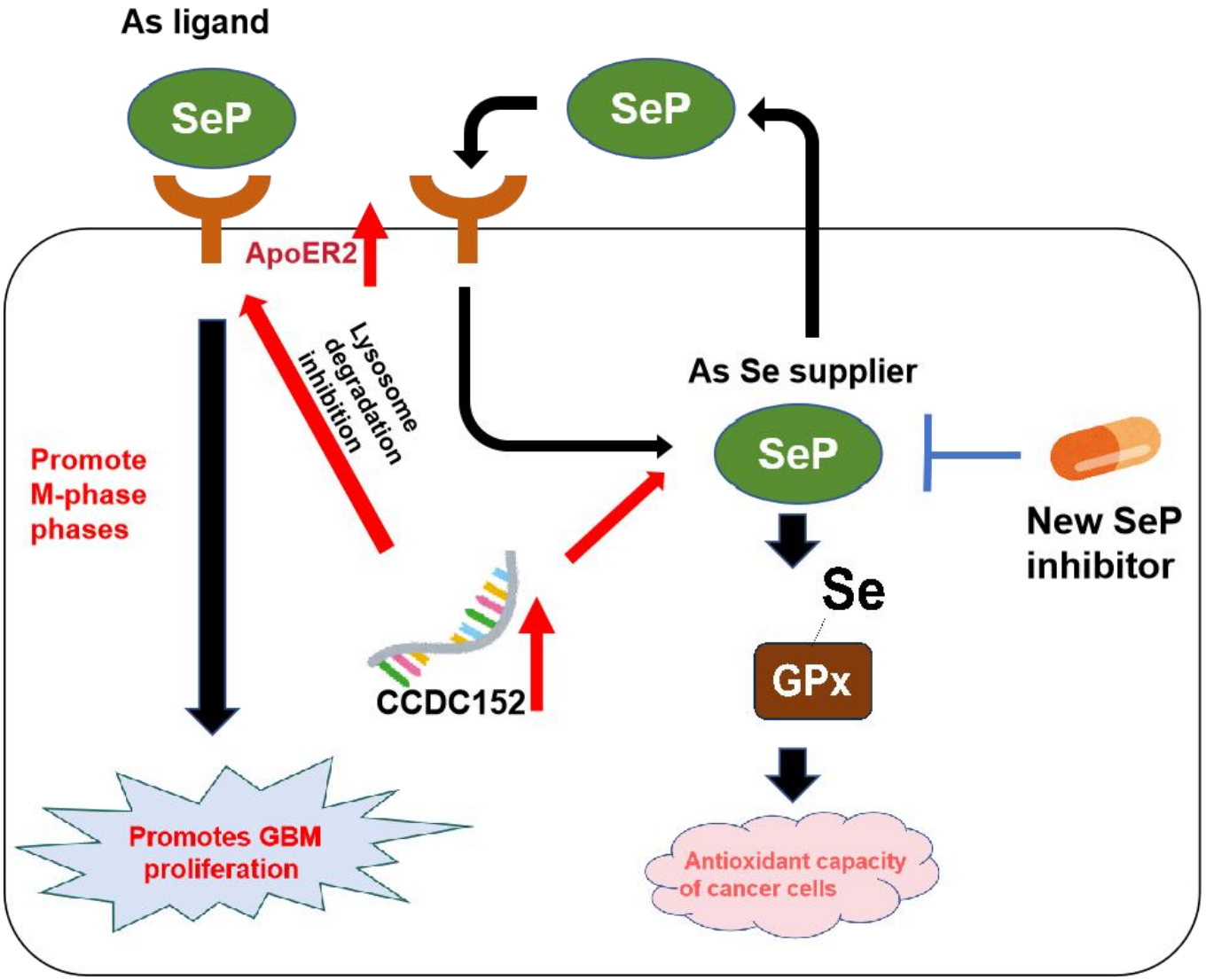


**Figure 29. CCDC152 promotes drug resistance and proliferation of GBM by modulating the SeP/ApoER2 pathway.**

Supplemental Fig. 1

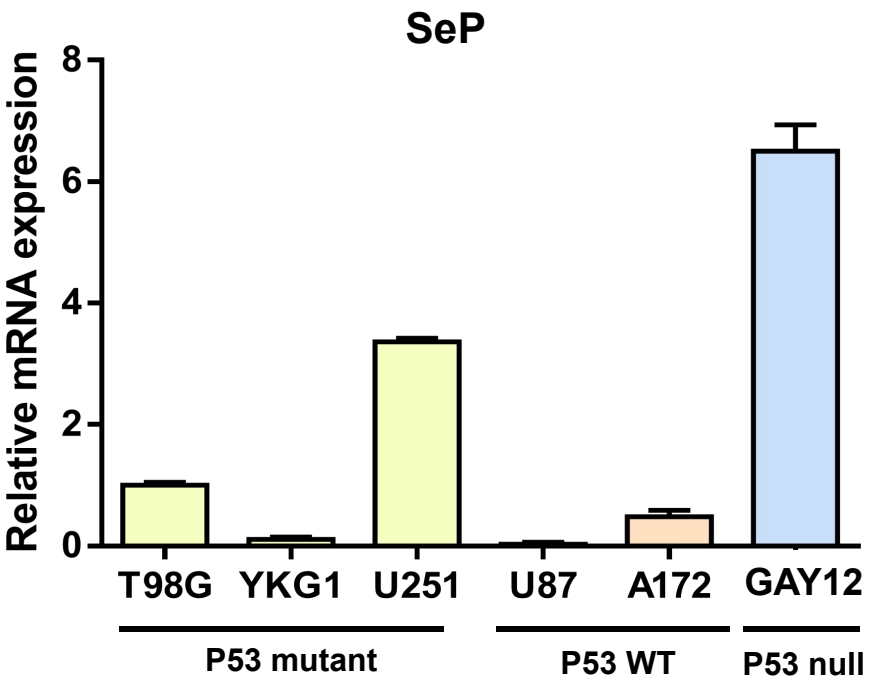


**Figure S1, qPCR detection of SeP expression in GBM cell lines and GBM cells from patients.**

Supplemental Fig. 2

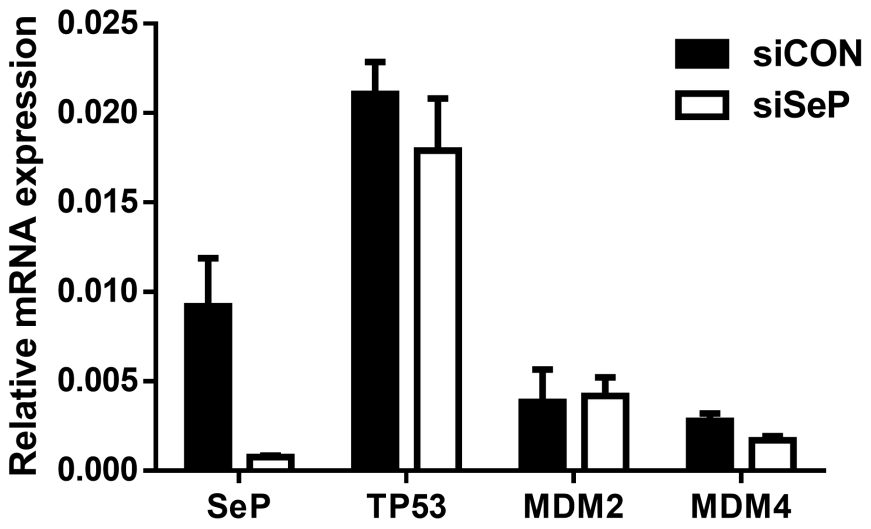


**Figure S2, Effect of SeP on the regulation of TP53.** After knockdown of SeP of T98G cell, mRNA expression of TP53, MDM2,MDM4 genes was detected by qPCR.

# Supplemental Fig. 3

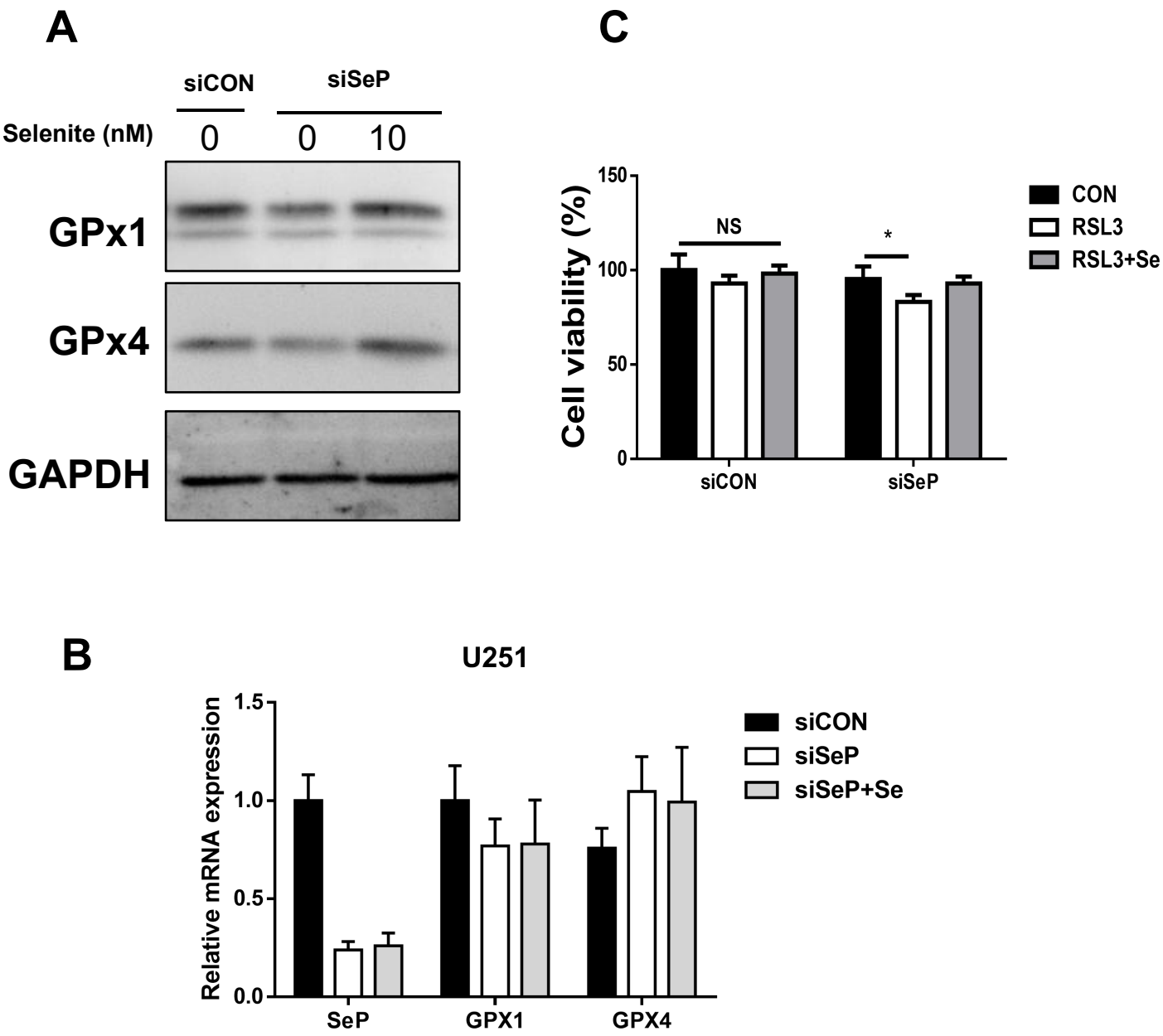


**Figure S3**. **Effect of SeP on selenium utilization and ferroptosis resistance of U251 cells.** U251 cells were transfected with siRNA for 24 hours and incubated with the indicated concentration of selenite for an additional 24 hours. The protein was extracted, and GPx protein levels were detected by Western blot (A) and mRNA level was detected by qPCR(B). After SeP was knocked down, RSL3 or selenite 10 nM was added and incubated for 24 hours before cell viability was measured (C). Data are presented as the mean ± S.D. ; n=3. Statistical significance was assessed by Tukey's HSD(C). *$p < 0.05$ vs control.

# Supplemental Fig. 4

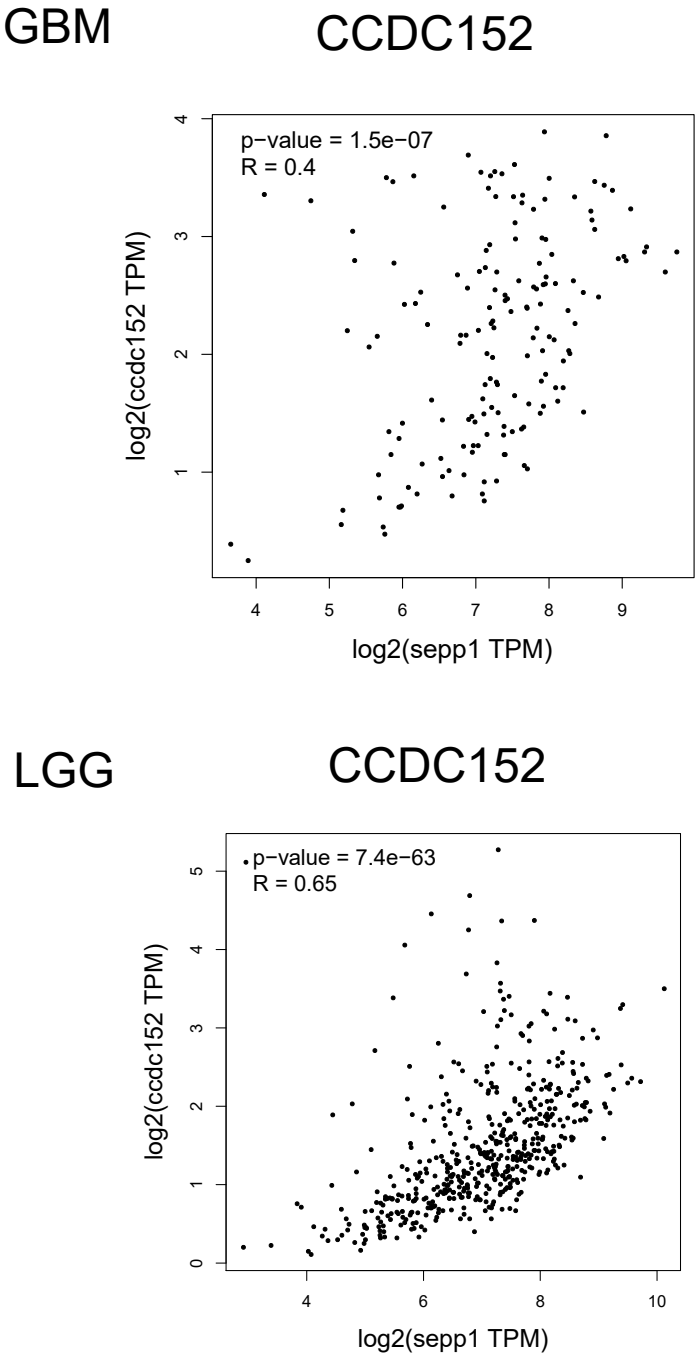


**Figure S4. CCDC152 expression and SeP expression in patients were positively correlated.**